SYNTHESIS OF CATIONIC STAR POLYMERS VIA RAFT POLYMERIZATION

A Thesis Submitted to
the Graduate School of Engineering and Sciences of
İzmir Institute of Technology
in Partial Fulfillments of the Requirements for the Degree of
MASTER OF SCIENCE
in Biotechnology

by
Gürbüz DURSUN

July 2018

İZMİR

We approve the thesis of **Gürbüz DURSUN**

Examining Committee Members:

Prof. Dr. Volga BULMUŞ
Department of Bioengineering, İzmir Institute of Technology

Assist. Prof. Dr. Ayben TOP
Department of Chemical Engineering, İzmir Institute of Technology

Assist. Prof. Dr. Ahmet AYKAÇ
Department of Engineering Sciences, İzmir Katip Çelebi University

02 July 2018

Prof. Dr. Volga BULMUŞ
Supervisor, Department of Bioengineering
İzmir Institute of Technology

Assoc. Prof. Dr. Engin ÖZÇİVİCİ
Head of the Department of Biotechnology and Bioengineering

Prof. Dr. Aysun SOFUOĞLU
Dean of the Graduate School of Engineering and Sciences

ACKNOWLEDGMENTS

Foremost, I would like to express my indebtedness to my advisor Prof. Dr. Volga BULMUŞ for her continuous support, guidance, motivation and suggestions in all the time of research and writing of this thesis. It has been an honor to me to be the member of her team.

I would like to gratefully thank The Scientific and Technological Research Council of Turkey (TÜBİTAK, the grant #115R301) for their financial support throughout my M.Sc. study.

I would like to thank staff of Biotechnology and Bioengineering Applications and Research Centre (BİYOMER) for their contributions; especially Yekta GÜNAY OĞUZ for Dynamic Light Scattering experiments and Dane RUSÇUKLU for Gel Electrophoresis experiments.

I am also thankful to Aykut ZELÇAK, Fazilet GÜRER, Aytaç GÜL, Aysel TOMAK and other colleagues for their supports during my experiments.

I warmly thank my dear friends Çağlar ERSANLI, Damla TAYKOZ, Seda DUMAN, Özge KALENDER and Şule Zeynep ÖZER. They have supported me in all difficult and stressful times with their patience and friendship. Thank you for making my life easier.

Most importantly, I strongly thank my father Zafer DURSUN, my mother Nuray DURSUN and my sister Gözde DURSUN for their understanding, never ending support and unconditional love. They make me feel like the luckiest person in the world.

ABSTRACT

SYNTHESIS OF CATIONIC STAR POLYMERS VIA RAFT POLYMERIZATION

The aim of this master thesis is to synthesize cleavable, core-crosslinked, cationic, new star polymers as potential siRNA carrier systems. The core-crosslinked star polymers of aminoethyl aminoethyl methacrylate (AEAEMA) monomer were synthesized for the first time in the literature. A crosslinker, potentially cleavable in cell cytosol, bis(2-methacryloyl) oxyethyl disulfide, and AEAEMA monomer with Boc-protection groups (BocAEAEMA) were polymerized using P(OEGMA) macroRAFT agents (5 kDa or 10 kDa). The polymerization kinetics revealed a linear increase in ($[M]_0/[M]$) with increasing polymerization time, indicating the RAFT-controlled polymerization mechanism. The incorporation of arms into star structure completed between 2 and 8 hours of polymerization, leading to star formation yields of approx. 55%. Star polymers with narrow PDI values (between 1.52 and 1.80) and controllable molecular weights (between 116 kDa and 620 kDa) were synthesized using a P(OEGMA) macroRAFT agent of 10 kDa. Increasing crosslinker to macroRAFT agent ratio led to increase in crosslinker conversion and decrease in BocAEAEMA conversion. Increasing BocAEAEMA to macroRAFT agent ratio had the exact opposite effect. The use of a macroRAFT agent of 5 kDa led to a dramatic increase in molecular weight (up to 3370 kDa).

The hydrodynamic sizes (D_h) of water soluble, cationic star polymers, obtained after deprotection of amino groups, dropped from 2-36 nm to 1-18 nm after treatment with a reducing agent in water, indicating the cleavable nature of the star structures. Among the star polymers tested, the polymer having 7 arms of POEGMA (10 kDa) and a degree of polymerization of AEAEMA (DP_{AEAEMA}) of 70 efficiently complexed with siRNA at a nitrogen/phosphate ratio of 1. While this polymer showed higher cytotoxicity, when compared with other star polymers tested, all polymers were significantly less toxic, compared to branched PEI, a golden standard cationic polymer for siRNA delivery.

ÖZET

KATYONİK YILDIZ POLİMERLERİN RAFT POLİMERİZASYONU İLE SENTEZİ

Bu tez çalışmasının amacı, RAFT polimerizasyona tekniği ile çapraz bağlanmış, katyonik yıldız polimerlerin, potansiyel siRNA taşıyıcı sistemleri olarak sentezlenmesidir. Polimerizasyonlar, katyonik (2-((tert-butoksikarbonil) (2-((tert-butoksikarbonil) amino) etil) amino) etil metakrilat (BocAEAEMA) monomeri ve çift fonksiyonlu biyobozunur bis(2-metakriloil) oksietildisülfit çapraz bağlayıcı monomeri varlığında gerçekleştirilmiştir. BocAEAEMA varlığı ile yıldız polimer sentezi literatürde ilk kez rapor edilmektedir. Polimerizasyon mekanizmasının iyi anlaşılması için değişen polimerleşme zamanlarıyla (2, 8, 16 ve 24 saat) kinetik çalışmaları yapılmıştır. ($[M]_0/[M]$) oranının zamana bağlı olarak doğrusal değişimi polimerlerin kontrollü RAFT polimerizasyon mekanizmasıyla başarıyla sentezlendiğini kanıtlamıştır. Kol katılımının 2 ve 8 saat arasında tamamlandığı ve polimer verimliliğinin 8 saat sonrası %55 değerlerinde sabitlendiği görülmüştür. Dar PDI aralığında (1.52-1.80) ve molekül ağırlığı kontrollü olarak değişen (116 kDa- 620 kDa) yıldız polimerler başarıyla sentezlenmiştir. Bunun yanı sıra, BocAEAEMA/çapraz bağlayıcı oranları ve kol uzunlukları (5 kDa ve 10 kDa) değiştirilerek bu parametrelerin yıldız tipli yapı oluşumdaki etkisi incelenmiştir. Kısa kollu yapıların daha yüksek molekül ağırlıklarına sahip oldukları gözlenmiştir (3370 kDa).

Boc gruplarının uzaklaştırılmasıyla suda çözünebilir olan polimerler (2-36 nm), suda çözünebilir bir indirgeyici olan TCEP eklendikten sonra bozunma profilleri incelenmiş ve hidrodinamik boyutlarında (D_h) küçülme gözlenmiştir (1-18 nm). Test edilen polimerler arasında, kol sayısının 7 ve katyonik blok molekül ağırlığının 14 kDa olduğu yıldız polimerinin düşük polimer/siRNA (N/P=1) oranlarında bile kompleks oluşturabildiği görülmüştür. Ayrıca, test edilen tüm yıldız polimerlerin, siRNA taşınımı için altın standart olarak kullanılan PEI'den daha az toksit olduğu ve kendi içlerinde ise katyonik blok uzunluğuna ve hidrofilik P(OEGMA) kol sayısına bağlı olarak hücre canlılığı etkilediği gözlenmiştir.

TABLE OF CONTENT

LIST OF FIGURES

Figure **Page**

LIST OF TABLES

Table **Page**

CHAPTER 1

INTRODUCTION

Star polymers are a typical type of hyperbranced polymers with more than three linear arm chains emanating from central moiety (core). They offer a favorable three-dimensional architecture as potential vehicles for site specific drug and/or oligonucleic acid delivery (Cosson et al., 2017; Hild et al., 2016). Star polymers have received considerable attention due to their compact and complex structural properties. Since they have a number of linear chains radiating from central branching point, they can transport more therapeutics than their linear counterparts (Pan et al., 2016; Azuma et al., 2017).

Living/controlled radical polymerization techniques (LRPs) such as reversible addition fragmentation chain transfer (RAFT) polymerization enable the production of well-defined complex architectures such as star polymers with a good control over molecular weight (MW) and polydispersity (PDI). Star polymers can usually be synthesized by using two common approaches: The “core-first” approach in which arms are grown out from a multifunctional initiator with a limited number of arms and the “arm-first” approach where pre-formed polymeric arm chains are linked together with di-functional crosslinkers (Barner-Kowollik et al., 2006).

Star polymers can also be tailored to have functionalized arm and core structures. For instance, stimuli-responsive nanoparticles can be produced with chemically modified chains responding to changes in temperature, chemical composition and/or pH of the environment (Gao and Matyjaszewski, 2008). The incorporation of cationic monomers can lead to star polymers with cationic charge density higher than linear polymers made of the same cationic monomers. Such structures display potential as carriers for nucleic acids such as siRNAs. Polyamines which have the combination of primary, secondary and/or tertiary amines in their structures can be synthesized in star architectures, providing a high density of cationic groups over a wide pH range covering endocytic pathway pH range. Gradual protonation of amino groups can lead to endosomal rupturing with reinforcing the probability of releasing condensed anionic therapeutics to the target. Since polyamines have positive charge on their structure, they can be easily electrostatically attracted to negative charged oligonucleic acids such as pDNA or siRNA.

Vectors that are formed through the electrostatic interactions between a polymer and a nucleic acid are named as polyplexes (Kanayama et al., 2006). These vectors, depending on the ability of the used polymer can have high transfection ability. Also, biocompatible functionalities can be inserted in order to prolong blood circulation time of such polyplex vectors. Hydrophilic poly(oligo(ethylene glycol) methyl ether methacrylate (POEGMA) or polyethylene glycol (PEG) modified star polymers which confers stealth-like attributes cause nanoparticles such as polyplexes to circulate for broaden periods of time (Matsumura and Maeda, 1986).

Star-shaped polymers can be also chemically fabricated to be biodegradable inside the body. For instance, in the presence of reducing environment such as cell cytosol, disulfide groups can be cleaved to disintegrate star-shaped structure into unimers. This reduction characteristic can also be beneficial for release of delivered cargos in the presence of glutathione (GSH) which is a natural reducing agent found within the cytosol of cells (Kamada et al., 2010).

The purpose of this master thesis is to synthesize new, core-crosslinked star (CCS) polymers, which have cationic and biodegradable core structure with P(OEGMA) arms scattering from the core, by using RAFT polymerization technique, as potential new siRNA carriers. To do that, cationic star polymers were synthesized via arm-first approach using a monomer, 2- ((tert-butoxycarbonyl) (2-((tert-butoxycarbonyl) amino) ethyl) amino) ethyl methacrylate (BocAEAEMA) which have protected primary and secondary amines. Several star polymers were synthesized using P(OEGMA) macroRAFT agents with varying molecular weights as pre-arm chains in the presence of a biodegradable crosslinker, (bis(2-methacryloyl) oxyethyl disulfide) and BocAEAEMA co-monomer by changing crosslinker and monomer ratios in the polymerization feed solution. In order to characterize synthesized polymers, Gel Permeation Chromatography (GPC), Nuclear Magnetic Resonance (NMR) Spectroscopy and UV-Visible (UV-vis) Spectroscopy were used. Core-crosslinked star polymers having varying molecular weights and arm numbers were synthesized as potential siRNA delivery vectors. After the deprotection of amine groups, star polymers were characterized with Dynamic Light Scattering (DLS) in order to determine hydrodynamic size characteristics and degradation profiles. Finally, *in vitro* cytotoxicity assays and complexation experiments of selected polymers with siRNA were performed as preliminary experiments to determine the potential of the new star polymers as siRNA carrier systems. Throughout Chapter 2, 3 and 4, the literature review, experimental procedures and results along with discussions are presented, respectively.

CHAPTER 2

LITERATURE REVIEW

2.1. Carrier Systems for Nucleic Acid Therapeutics

In the last 20 years, short interfering ribonucleic acids (siRNA) has been received increased attention for the efficient post-transcriptional gene silencing in eukaryotic cells. Severe diseases including cancer, heart disease, obesity and diabetes are because of inappropriate expression of disease related genes. When compared to conventional treatments, siRNA has powerful advantages for specific silencing activity without causing any associated pathogenic effects (Chen et al., 2017).

In Figure 2.1, siRNA silencing activity path has been presented. In brief, when siRNA enters into cell, it is incorporated into protein complex which is called as RNA-induced Silencing Complex (RISC). Afterwards, RISC complex unwinds the siRNA and the sense strand of siRNA is cleaved. The activated RISC contains only anti-sense strand scan and find complementary mRNA (target mRNA). The single stranded siRNA then binds to target mRNA and cleave it. This finally leads to the degradation of mRNA. In this pathway, siRNA must first pass through cell membrane, reach cytoplasm and incorporated into RISC (Cavallaro et al., 2017). siRNA molecules have relatively small size, but their high hydrophilicity and negative charge prevent their passage through cell membrane (Wang et al., 2010).

Even though, siRNAs have effective gene silencing activity *in vitro*, there is no comparable effectiveness *in vivo*. Since they have some weakness such as fast renal passage and enzymatic blood corruption (Rafael et al., 2017). Therefore, there is a huge need for novel, advanced delivery systems in order to give good specificity for cell targeting, to prolong blood circulation time and to optimize intracellular uptake of siRNA. Obtaining an ideal carrier for siRNA is a key challenge (Cavallaro et al., 2017).

Viral and non-viral systems are the most commonly used for delivery of siRNAs. Viral systems which are modified from adenovirus, herpes virus, vaccinia virus etc. can be highly efficient for siRNA delivery but they are difficult to produce, toxic and can

interfere with the host genome. Non-viral vectors show promising potential to cure acquired and inherited disorders and include lipids, dendrimers, gold nanoparticles and polymers (Cho et al., 2011). Among them the most powerful materials to package and deliver siRNA are polymers which enable physical entrapment, covalent bonding or electrostatic self-assembly of siRNAs (Cooper and Putnam, 2016). Especially, cationic polymeric systems can be utilized to make complexation with siRNA electrostatically, masking their negative charge (Cavallaro et al., 2017).

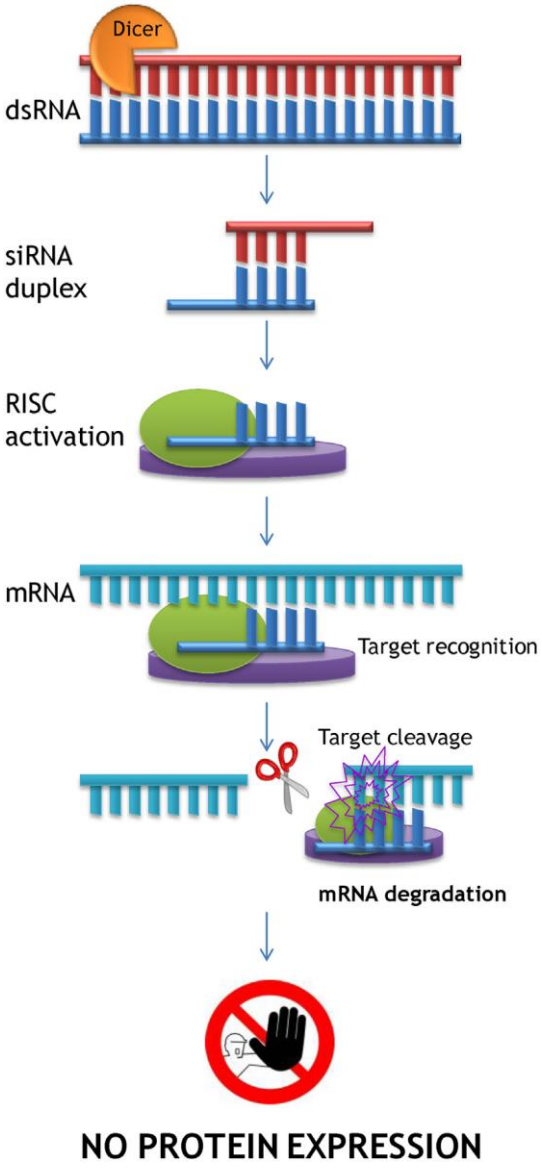

Figure 2.1. Illustration of siRNA mediated gene silencing path
(Source: Cavallaro et al., 2017)

Cationic polymers as non-viral carrier systems have advantages to condense polyanionic oligonucleic acids into nano-sized particulates. Cationic polymers can form compact polyplex structures with nucleic acids such as siRNA or pDNA through

electrostatic interactions. In spite of the fact that polycations are potential vectors for polyanionic nucleic acids, they can fail to fulfill its full potential as carrier systems because of their toxicity problem. Additionally, their *in-vivo* transfection efficiency is limited. Furthermore, while polyplex vectors can protect siRNA from enzymatic degradation and facilitate cellular uptake, they tend to aggregate through non-specific interactions with serum components. (Monnery et al. 2017; Behr, 2012; Dai et al., 2011; Yue et al., 2011).

Hence, in the last decades, there has been a huge effort to develop cationic polymer-based vectors with enhanced transfection efficiency, low toxicity and aggregation behavior. Polyamines such as poly-L-lysine (PLL), polyethyleneimine (PEI) and chitosan have been used as cationic non-viral vectors for siRNA and pDNA delivery. Due to the presence of primary, secondary and tertiary amines in their structure, PEI has high cationic charge capacity. However, in order to utilize this property, architecture (linear or branched), molecular mass (which can vary from 400 Da to 750 kDa) of synthesized PEI polymers is highly important. As molecular weight increases, high transfection activity can be observed but with high toxicity. As molecular weight decreases, less toxicity can be observed but with low transfection activity.

Generally, branched-PEI (bPEI) (25 kDa) is a commercial polymer that is used as a gold standard to compare transfection efficacy of newly emerged cationic polymers (Junquera and Aicart 2016; Bansal et al. 2016). Branched form of PEI display higher transfection efficiency than linear PEIs. Oskuee and colleagues reported that bPEI (25 kDa) formed smaller polyplexes than linear PEI (250 kDa) which led to high transfection efficacy. Also, they showed that bPEI (25 kDa) had higher condensation ability when compared to linear PEI (250 kDa) since branched form of PEI possessed higher amount of primary amines. However, higher dose-associated cytotoxicity of 25 kDa bPEI was still a key issue (Oskuee et al., 2018).

In chronologic order, the first published mono-cationic lipid was Lipofectin as a transfection agent. Meanwhile, polyamines were commenced to be used as transfection agents utilizing “proton sponge” mechanism through endosome buffering. All these have led to improved transfection systems such as commercial lipid agents (e.g. Transfectam, Lipofectamine) and polymers (PEI).

In Figure 2.2, transmission electron microscope image of 3T3 fibroblast cell transfected with polycationic linear polyethyleneimine-siRNA polyplexes can be observed. Red string represents negatively charged oligonucleic acids and green string

represents polycationic linear polyethyleneimine. Thanks to endosome-buffering and proton-sponge effect of PEI, large amounts of ions enter into vacuoles while pH is decreasing. Afterwards, osmotic swelling occurs due to the entry of water and then vacuoles become spherical and break (Behr, 2012).

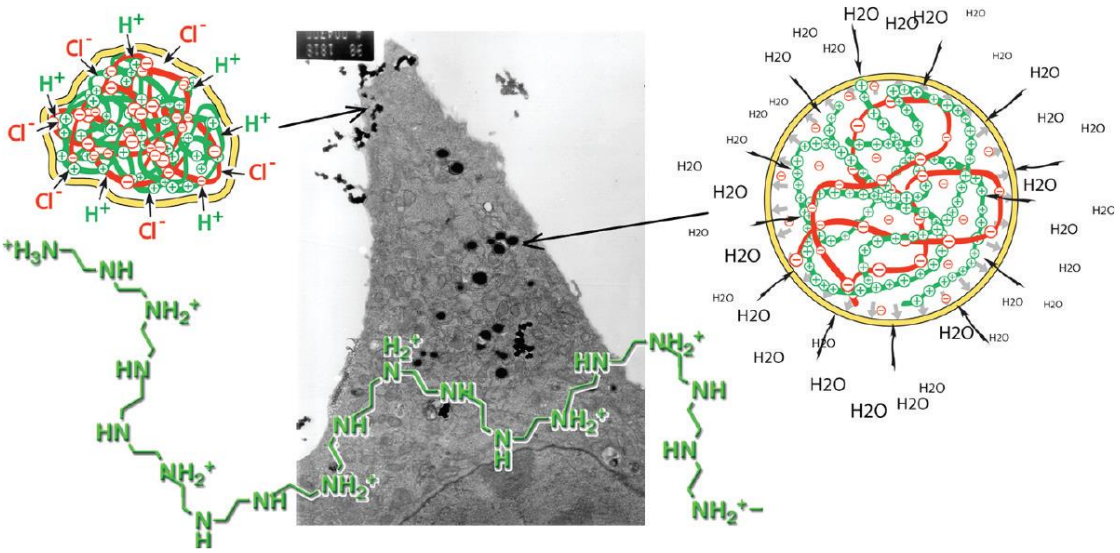

Figure 2.2. Proton sponge paradigm
(Source: Behr, 2012)

Although buffering effect (proton-sponge) of cationic PEI is widely postulated endosomal escape mechanism, it still remains controversial hypothesis. Accordingly, Benjaminsen and colleagues have been discussed the true dominant mechanism of PEI for endosomal escape. They showed that high amount of PEI was internalized to lysosome but there was no significant change in the pH of lysosomes which was confirmed by used nanoparticle pH sensor. This finding made proton sponge theory uncertain. Authors have suggested that this can be because of ATPase proton pumps which can neutralize and stabilize the pH of lysosome in spite of buffering activity of PEI. Also, they have suggested that the dominant mechanism for endosomal escape can be pore-formation on the lysosomal membrane which can be result of enhanced membrane tension due to interaction of cationic PEI and negatively charged membrane (Benjaminsen et al., 2013).

Moreover, high dose-dependent cytotoxicity is another essential problem of PEIs. PEI can induce two kinds of toxicity problem which are immediate and delayed toxicity. Immediate toxicity can occur because of free PEI which can cause disorganizing of cell membrane before transfection while delayed toxicity can occur after the entry of polyplexes due to activation of mitochondrial apoptosis. It was found that both linear and

branched form of PEI can cause membrane damaging and bring major cytotoxicity problem (Parhamifar et al., 2010; Kunath et al., 2003; Oskuee et al., 2018). Kurtulus et al. in 2014 has synthesized a new cationic 2- ((tert-butoxycarbonyl) (2-((tert-butoxycarbonyl) amino) ethyl) amino) ethyl methacrylate (BocAEAEMA) monomer which bears diaminoethane motifs including in repeating units, similar to PEI chemical structure. This new monomer carries primary and secondary amines. After polymerization and deprotection of BocAEAEMA, the synthesized P(AEAEMA) polymers showed good proton sponge capacity when compared with golden standard bPEI (25 kDa) without causing a major toxicity problem (Kurtulus et al., 2014).

One of the effective approach to reduce cytotoxicity and aggregation tendency of cationic polymer complexes with nucleic acids is the modification of cationic polymers with polyethylene glycol (PEG). PEG is a hydrophilic molecule that has flexible, non-ionic and non-immunogenic nature. Hence, it is one of the most widely used polymers in drug delivery. Hydrophilic PEG segments made up the shell of PEG-covered cationic polyplexes. This can increase colloidal solubility, improve circulation, reduce toxicity and protein binding. Thus polyplexes which are “invisible” for phagocytic cells can be produced (Harris and Chess, 2003; Li, 2016).

2.2. Branched Polymers as Carrier Systems

Branched polymers have three-dimensional architectures with their highly branched side chains. This feature provides particular properties such as multiple end-functional groups, relatively lower viscosity compared to linear polymers due to lower chain entanglement, high solubility in various organic and inorganic solvents, structures with cavities that make them suitable for carrying molecules such as therapeutically active molecules (Sigen et al., 2017; Bansal et al., 2016).

Additionally, PEG modified branched polymers proved enhanced blood-circulation times with high transfection efficiency and low toxicity. Accordingly, time dependent bio-distribution experiments carried out by Chen and colleagues has shown that PEG-modified star polymers cannot be eliminated easily from the body. While linear PEG (50 kDa) showed blood circulation time of approximately 17 hours, PEGylated star polymers having molecular mass ranging from 30 kDa to 100 kDa showed increasing

circulation times from 25 hours to 37 hours, respectively (Chen et al., 2011). In a different study, Fox et al. also reported that a library of PEGylated polyester "bow-tie" dendrimers with changing branch numbers showed relationship between branching degree and blood circulation times. Accordingly, bow-tie polymers with similar MW (around 40 kDa) showed increasing blood circulation times with increasing number of arms. It was found that for two-arm dendrimers which are almost linear, circulation time was approximately 1.5 hours, while for four-arm and eight-arm dendrimers, the circulation time increased to about 25 hours and 30 hours, respectively. The bio-distribution studies showed that increasing number of arms led to lower excretion of polymer in the urine of mice (Fox et al., 2009).

Moreover, Bowen et al. suggested that PEGylated proteins with branched PEG also provided increased blood circulation time compared to PEGylated proteins with a single PEG chain. When PEGylated dendrimers were compared to linear PEG with similar MW, the linear PEG showed shorter blood circulation time (Bowen et al., 1999). Branched polymers have smaller radii than linear equivalent polymers, branching decreases flexibility of polymeric chains. Hence, they can be filtered less by glomerulus and circulate in blood with longer times. In order to pass through the pores, first the one or more arm of branched polymers must enter the pore and the rest of polymer must distort backward. As the number of arms increases, this requirement that means energy barrier for entry becomes more and more difficult (Fox et al., 2009).

In Figure 2.3, different polymer architectures and their passage behavior through a pore can be seen. These polymers have approximately the same radius. Accordingly, linear random polymers (Figure 2.3a) readily enter the pore and pass through easily. Globular and rigid polymers (Figure 2.3b) must deform first in order to pass and after certain MW this process can be difficult. Cyclic polymers (Figure 2.3c) which lacks a chain end in order to enter pore first, deform and pass more easily than globular polymers. Tubular polymers (Figure 2.3d) readily penetrates and pass through. Branched polymers (Figure 2.3e) can have at least two different scenarios. First (asymmetric distribution) is the initial entry of one arm rapidly and remainder of polymer passage can be sterically hindered because other arms must deform. Second (symmetric distribution) is the entry of several arms (which is less likely), and easy passage of remainder polymer (Fox et al., 2009).

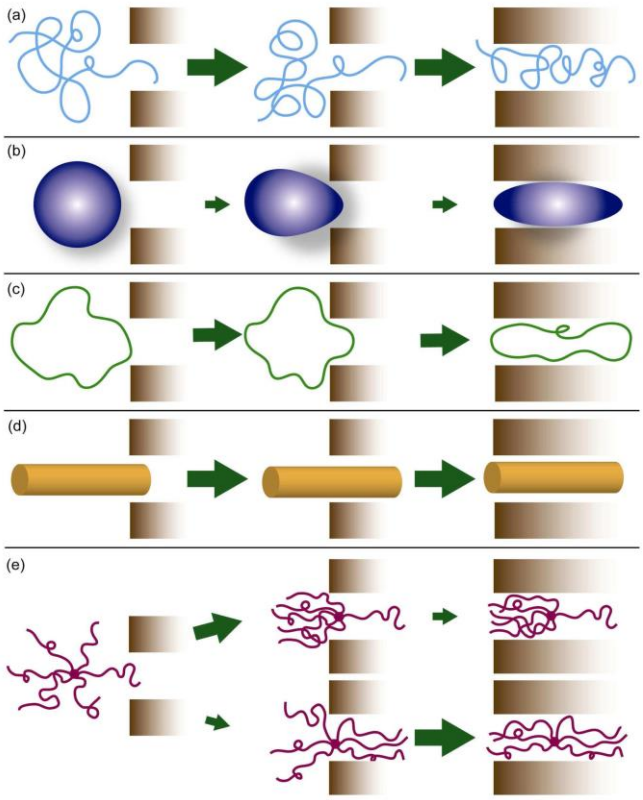

Figure 2.3. Different polymer architectures and their passage behavior through a pore (Source: Fox et al. 2009)

2.3. Cationic Star Polymers as Nucleic Acid Carrier Systems

One class of hyperbranched macromolecular architectures is star polymers which have linear chains radiating from a branching point at center. In a star-shaped macromolecule architecture, there must be at least three polymeric arms connected to a central core. Star polymers can be classified according to sequence distribution and composition of linear arms (Figure 2.4a), variation in types of linear arms (Figure 2.4b), core structure (Figure 2.4c) and functional position (Figure 2.4d) (Ren et al., 2016).

Star polymers that have same arm structure and chain length are considered to be homogeneous. Otherwise, they can be classified as heterogeneous (mikto-arm). Star polymers can be designed with functionalizable arms giving additional properties to star-shaped polymers. For instance, the linear branching chains (arms) or central moiety (core) can be chemically modified to obtain stimuli-responsive materials. Owing to this manipulation, polymers can have ability to response chemical changes from external

environment, which is an ideal property for drug/gene delivery applications in which site-specific or controlled release of therapeutics is crucial. Some typical external stimuli can be electrical, optical, mechanical, thermal, redox, chemical, pH and biological signals. Star polymers can have not only stimuli-responsive moieties but also specific biomarkers to target polymers to the desired physiological zones such as tumor cells. Star polymers which have functionalizable branches can be chemically tailored to take control over biodegradation rates inside the body. Moreover, star polymers with lots of linear arms can carry more therapeutics than their linear counterparts (Yang et al., 2017).

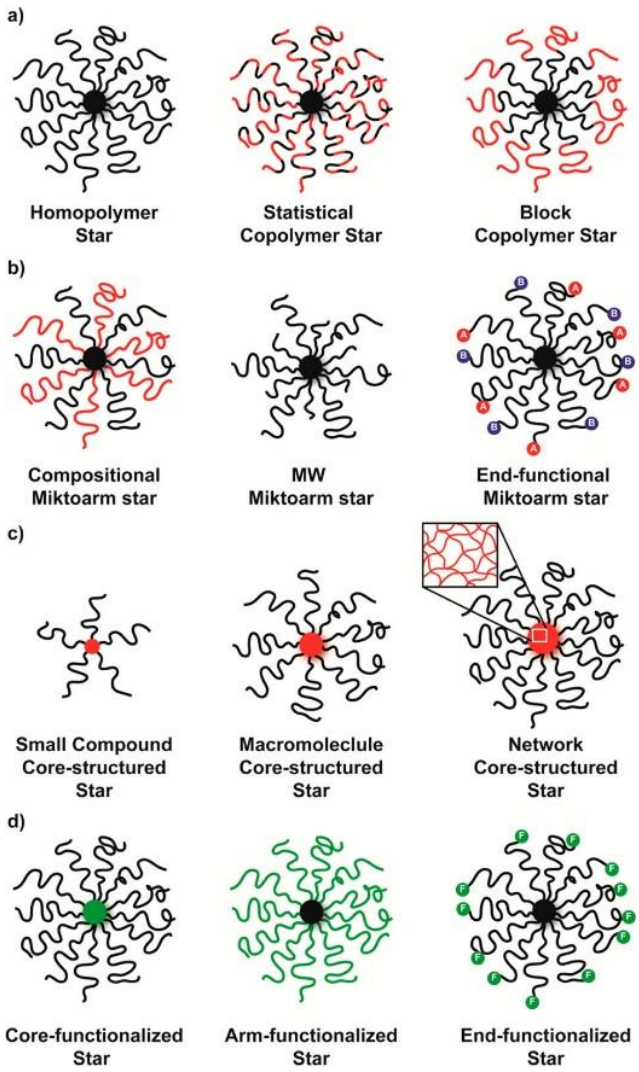

Figure 2.4. Illustration of star polymer types
(Source: Ren et al., 2016)

Nishimura and colleagues have been reported the synthesis of amylose based star polymers which are modified with cationic spermine motif. They have investigated

siRNA complexation of formed polymers, cellular uptake of formed polyplexes and cytotoxicity of both synthesized polymers and polyplexes. First, they have synthesized mono-armed and 8-armed polymers which have positive zeta potentials. The complexation efficiency for 8-armed polymer was found approximately 45 times greater than mono-armed polymers. Even though 8-armed polymer has showed more toxicity than mono-armed polymers, formed polyplexes with 8-armed polymer showed no significant cell death for various N/P ratios. Additionally, cellular uptake of polyplexes and naked-siRNAs was monitored via confocal laser microscopy. Accordingly, naked siRNAs failed to enter and colonized outside of the cell membrane. Besides, 8-armed polymers showed greater internalization when compared to mono-armed polymers. The authors have concluded that this higher internalization can be size-dependent since 8-armed polymer was formed smaller and compact polyplexes than mono-armed polymer as confirmed via DLS (Nishimura et al., 2015).

In different study which was conducted by Liao and colleagues, they have reported poly(2-dimethylamino) ethyl acrylate) (PDMAEA) based star polymers which serve as nucleic acid carrier systems with their protonable moieties. To investigate polyplex formation with DNA and cytotoxicity profiles, they have compared PDMAEA star polymers with their linear counterparts which have equal molecular mass. They observed that PDMAEA star polymers had relatively smaller hydrodynamic radius due to their compactness and the compact structure generated higher cationic density. Hence, complexation was succeeded at lower N/P ratios for star polymers. However, while both star polymer and linear PDMAEA at low molecular weight (10 kDa) showed no toxicity over 3T3 murine cells, both star polymer and linear PDMAEA at high molecular weight (20 kDa) showed enhanced toxicity profiles. They emphasized that even though, star-like architecture bring better complexation with oligonucleic acid therapeutics, cytotoxicity of star polymers without any modification to mask cationic density can be still molecular mass dependent as their linear counterparts (Liao et al., 2017).

The preparation of star polymers can be facilitated by using controlled/living radical polymerization (LRP) techniques such as atom transfer radical polymerization (ATRP), nitroxide mediated radical polymerization (NMP) and reversible addition fragmentation chain transfer (RAFT) polymerization. These LRP techniques are applicable for a wide range of monomers and can be designed to have facile reaction conditions (Huang et al., 2016).

2.4. Synthesis of Star Polymers via LRP techniques

Making use of di-functional (divinyl) cross-linkers via controlled/living radical polymerization (LRP) techniques is a recent methodology to generate branching points in polymers (Boyer et al., 2009b; Bulmus, 2011).

By using controlled radical polymerization techniques, branching points can be introduced with the use of multifunctional initiators, coupling agents or divinyl crosslinkers. Star polymers can be obtained by using wisely-selected monomers, cross-linkers, initiators and polymerization methods and solvent types. Additionally, wise-selection of these parameters contribute wide range of functionalities to synthesized polymers such as biodegradability and biocompatibility.

Copolymerization of a selected monomer and a cross-linker by conventional polymerization techniques can lead to undesired random gel formation. However, in LRP, retarded gelation profiles can be seen due to fast reversible de-activation and a great quantity of dormant reactive species of LRP techniques.

In conventional radical polymerization, four main reactions can take place: initiation, propagation, transfer and termination. Vinyl monomers can polymerize fast when there is no mediating reagent and this quick propagation is followed by termination with radical-radical coupling or disproportionation reactions. Additionally, terminated chains are called as “dead” chains unable to extend through further reactions and there is no control over molecular weight distribution. Hence, by using conventional radical polymerization, it is impossible to form well-designed architectural polymers with pre-determined molecular weights and uniform size (Gao and Matyjaszewski, 2009).

In LRPs, almost constant number of chains grow throughout polymerization. There is a dynamic equilibrium between low concentration of propagating radicals and a considerable amount of dormant species. Hence, reversible activation occurs and life-time of growing chains can be extended and also possible termination reactions can be reduced when compared to conventional radical polymerization (Braunecker and Matyjaszewski, 2007; Odian, 2004).

There are three activation mechanisms that are utilized during LRPs. Firstly, active radicals can be exposed to reversible activation and deactivation (ATRP and NMP). In the ATRP process, activation mechanism includes catalyst based activator (metal complex with lower oxidation state) and dormant species. In activation

mechanism, metal complex with higher oxidation state is formed and used as deactivator. In the NMP process, dormant species cleaved by making use of photochemical or thermal stimulus, hence stable radicals and active propagating radicals can be formed. In both of these LRP processes, every radical-to-radical termination cause accumulation of deactivator and this irreversible accumulation can lead to shifting of equilibrium to the dormant species and prevent reaction from undesired termination (Moad et al., 2003; Gao and Matyjaszewski, 2009).

Active radicals can be also exposed to degenerative transfer reactions as present in RAFT polymerization. RAFT technique does not obey persistent radical effect like NMP or ATRP. In RAFT polymerization, chain transfer agents (CTAs) play important role to provide control over polymerization (Gao and Matyjaszewski, 2009).

RAFT polymerization requires the use of chain transfer agents i.e. RAFT agents. RAFT agents (Figure 2.5) are organic compounds that have thiocarbonylthio moiety.

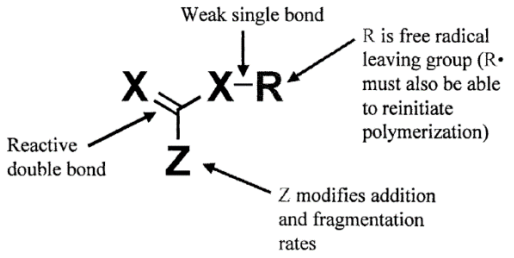

Figure 2.5. General structure of RAFT agent where X= Sulfur (S)
(Source: Moad et al., 2003)

The first step of accepted mechanism of RAFT polymerization is the initiation. In this step, a radical is formed, most commonly via thermal decomposition, as in the case of a conventional free radical polymerization. After the formation of radicals, oligomeric radicals are formed and react with properly-selected RAFT agent molecules, where highly reactive thiocarbonylthio is present, instead of double bonds on the monomer. Hence, formed radical intermediates can be fragmentized backward and creates original RAFT agent and can be fragmentized to create oligomeric RAFT agents along with initiating R radicals. After the re-initiation of R radicals, addition of monomer takes place and polymeric chains begin to grow. The addition of growing polymeric radicals to polymeric RAFT agent creates stabilized radical intermediates. The rapid chain transfer interchange between growing chains and polymeric RAFT agent continues. The lower concentration

of propagating radical chains than stabilized radical intermediates can minimize undesired termination reactions (Figure 2.6) (Boyer et al., 2009b; Bulmus, 2011).

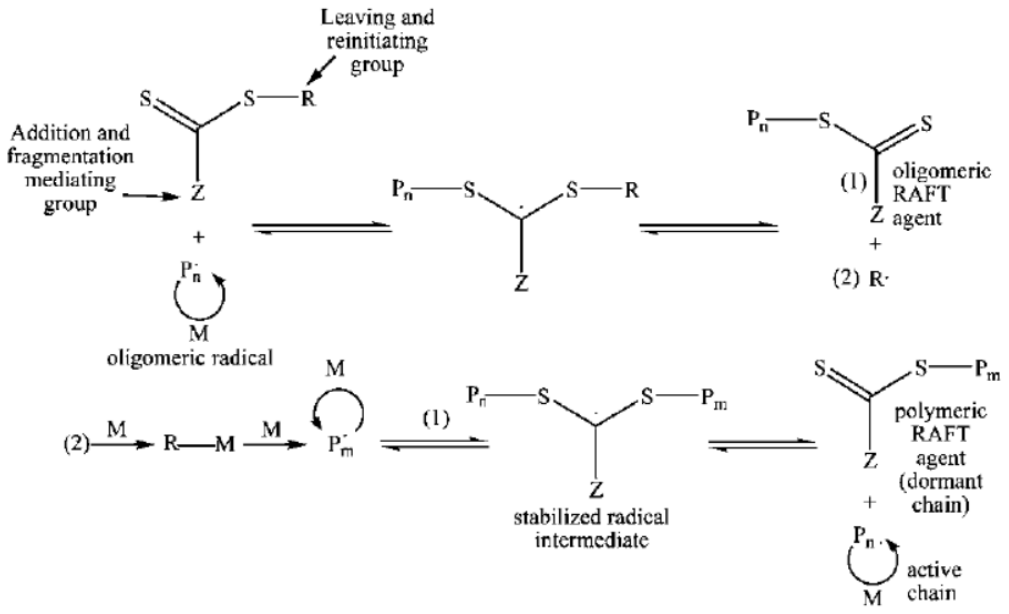

Figure 2.6. Accepted mechanism of RAFT polymerization
(Source: Bulmus, 2011)

There are basically two different ways to synthesize star polymers which are core-first and arm-first approach. The core-first strategy includes the incorporation of pre-designed multifunctional initiator which will be further core structure of star polymer. However, since the pre-designed multifunctional initiator is employed, limited number of arms created certainly depending on the number of functional group that already present in initiator. Moreover, due to small molecular sizes of synthesized multifunctional initiator, core dimensions can be smaller. Another disadvantage of core-first approach is difficulty in preparation of mikto-arm stars in which heterogeneous arms growing out. The preparation of mikto-arm star polymers is tedious procedure. Even in LRP techniques, potential termination reactions are most likely to occur and this termination can lead to star coupling.

Star polymers can also be synthesized using arm-first methodology. This strategy includes the use of functional linear polymers. Linear polymers can be joined each other from a central point and create star-like structures. There are two most common approaches used in arm-first methodology: The first is to employ a multifunctional core reacting with functional end-group of polymer chains. The second approach is to employ

a co-monomer with a cross-linker in the presence of linear macro-initiators/-RAFT agents (Gregory and Stenzel, 2012).

2.4.1. Synthesis of Star Polymers via ATRP and NMP Polymerization Techniques

The core-crosslinked star polymer synthesis via ATRP was first reported in 1999. In this study, polystyrene (polySt)macro-initiators were synthesized and then reacted with several crosslinkers (X) and resulted in $(polySt)_n$-polyX structures where n is arm number per core and polyX is the core of the star polymer formed. It was observed that incorporation of divinylbenzene (DVB) yielded the best non-degradable star polymer structures when compared to ethylene glycol diacrylate and ethylene glycol dimethacrylate crosslinkers, since DVB has a more rigid structure due to its benzene ring structure. However, formed star polymers were contaminated with unreacted residual arms and broad molecular weights were observed because of star-star coupling (Xia et al., 1999).

In a different study, an arm-first star synthesis experiment was carried out in one-pot reaction rather than isolating arms first and adding crosslinker in an another pot of reaction. The authors have used tert-butyl acrylate (t-BA) to form arm polymers. During the reaction for arm synthesis, at a predetermined time and conversion, crosslinker was added to polymerization mixture. However, this led to shorter arms with broader core since a higher quantity of unconverted tBA monomer was left for copolymerization with crosslinker (Gao and Matyjaszewski, 2006).

The core was also used for introducing functional groups into star polymers. Synthesis of functionalized core-crosslinked star polymers involved the sensible selection of functional divinyl crosslinker and a co-monomer. For example, core degradability could be provided using degradable linkers containing disulfides, acetal or siloxane groups (Gao et al., 2005, Themistou and Patrickios, 2004, Kafouris et al., 2006, Themistou and Patrickios, 2006).

Additionally, star polymer arms could be also functionalized for further application of polymers. Particularly, polyester polymers have been widely used since they can be easily degraded by hydrolysis due to their ester bonds. In this aspect, in order

for tuning star polymers as biocompatible and biodegradable poly(∈-caprolactone) (PCL) was used since PCL can be absorbed by the body minimizing severe host response (Krononthal, 1975).

Gao and Matyjaszewski also highlighted that employing a mono-functional linear macro-initiator led to core-crosslinked star polymers, while employing a di-functional macro-initiator led to dumbbell-like structures. One of the drawbacks of using macro-initiators was the star-star coupling reaction which was because of radical-radical or radical-pendant vinyl groups of two different star molecules. This type of star-star coupling reactions could also cause macroscopic gelation. In order for decreasing the probability of coupling reactions, concentration of divinyl crosslinker can be reduced or crosslinker to arm precursor ratio can be adjusted for more dilute reaction conditions. However, such manipulations can also cause the production of star polymers with lower yield and molecular weight. Because of lower yield, star polymers are contaminated by unconverted residual arms and there will be need for extra purification steps to form star polymers with low dispersity and high purity. In an another study of Gao and Matyjaszewski, the authors have formed star polymers with hydrophilic PEO arms and hydrophobic core using PEO methyl ether methacrylate, a di-functional crosslinker EGDMA and pyrene-containing ATRP initiator, they. These stars showed good solubility in water and strong UV absorption because of incorporation of PEO arms and pyrene groups, respectively (Gao and Matyjaszewski, 2007).

Abrol et al. first reported the star production via NMP. They have employed persistent stable radical piperidyl-N-oxly (TEMPO) to mediate polymerization of 4-ter-butylstyrene and DVB cross-linker. In early studies utilizing NMP for production of star polymers, generally polystyrene-based star polymers were synthesized because of the lack of suitable nitroxide radical for acrylates and methacrylates (Abrol et al., 1997).

2.4.2. Synthesis of Star Polymers via RAFT Polymerization Technique

RAFT polymerization can take place under mild conditions and can be applicable for a wide range of monomers (almost all monomer types that can be polymerizable via conventional free radical polymerization.) with proper RAFT agents and radical initiators without the need of any extra metal catalysis. Still, termination reactions are unavoidable,

yet compared to conventional free radical polymerization techniques, they are minimized. Hence, obtaining polymers with narrow polydispersities and targeted molecular weight is possible. Moreover, it is also possible to generate complex polymeric architectures such as block, hyperbranched and star polymers. All these properties make RAFT polymerization technique convenient for bio-applications (Boyer et al., 2009b; Bulmus, 2011).

RAFT technique appears to be the most versatile technique to synthesize functional polymers with complex architectures. RAFT technique can be utilized to synthesize star polymers via both core-first and arm-first approaches.

The core-first synthesis approach starts with the formation of the core structure having multiple RAFT agent functionalities (Ren et al., 2016). This approach can be subdivided into two methods: The R-group method and the Z-group method approach. In the core-first method, there is incorporation of multiple chain-transfer sites. This sites are equivalent to the number of arms. The binding of the RAFT agent can be obtained by covalent attachment of RAFT agent to a multifunctional group either via the R-group or Z-group of the RAFT agent (Figure 2.7) (Gregory and Stenzel, 2012).

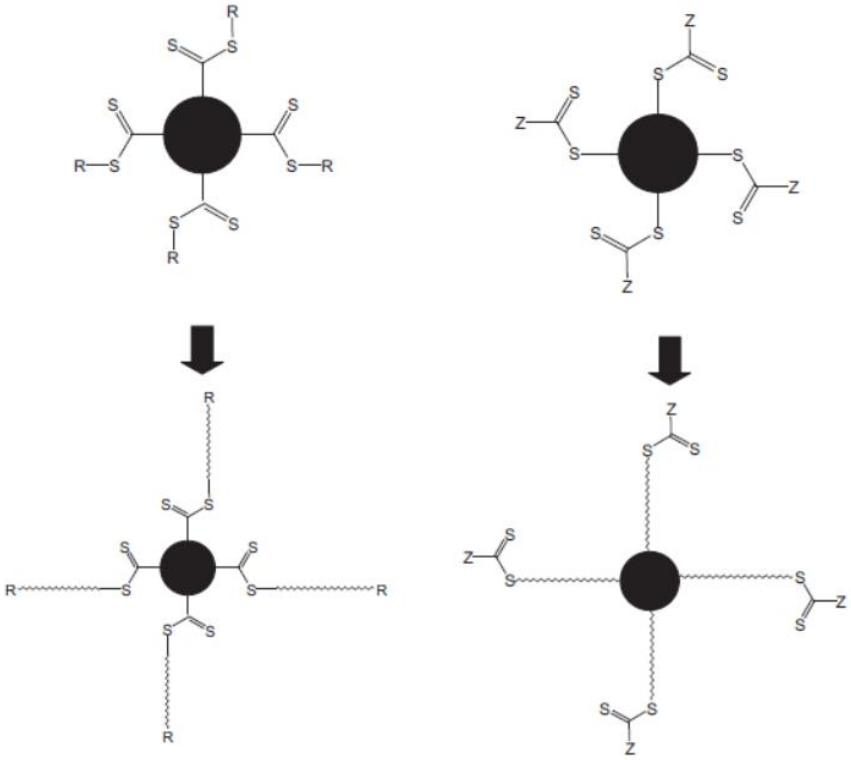

Figure 2.7. Comparison of core-first star synthesis strategy via Z-group (left) and R-group (right) approach (Source: Gregory and Stenzel, 2012)

Chong et al. from CSIRO in 1999 reported the first study on RAFT polymerization synthesis of star polymers via core-first approach. The authors employed tetra-functional and hexa-functional dithioesters for polymerization of styrene and formed well-designed star polymers, but with broad polydispersities (Chong et al., 1999).

Ren and colleagues discussed the criteria for minimizing the quantity of unreacted arms and star-star coupling problem. Accordingly, one of the crucial parameters was to use low initiation rates and a monomer with high propagation rate, since low radical concentration reduces the risk of termination reactions between radicals. Also, these undesired termination reactions can be minimized by using rate-retarded chain transfer agents (RAFT agents) (Ren et al., 2016).

There are several studies on incorporation of dendritic scaffolds as core structures. One of them is 16-armed dendritic chain, which have dithiobenzoate groups at termini. These were used as macroRAFT agents for further polymerization of methyl acrylate to synthesize star polymers with well-defined molecular weights and narrow polydispersities (from ~1.27 to ~1.35) (You et al., 2004).

In literature, biodegradable star polymers were also studied. In one of these studies, the core-first synthesis of novel 4-armed star polymers was reported. These stars were prepared from methyl methacrylate, dimethylacrylamide and styrene (Figure 2.8). The authors investigated the cleavage of disulfide bonds originating from pyridyl containing RAFT-agent within the core under reductive conditions by using tributylphosphine in an organic environment and by using tris(2-carboxyethyl) phosphine (TCEP) or dithiothretiol (DTT) in an aqueous environment. Additionally, degradation of ester core which was also coming from synthesized 4-armed RAFT-agent was also investigated under either acidic conditions by using HCl or enzymatic conditions by using enzyme esterase. Results have shown that synthesized star polymers can be cleaved due to both disulfide and ester bonds. However, degradation profiles have been observed at slower rate for esters compared to disulfides (Rosselgong et al., 2013).

The core-first approach can be subdivided into two categories as R-group and Z-group approaches that are based on position of thiocarbonylthio group with reference to the core in order for the growth of star polymers (Figure 2.9).

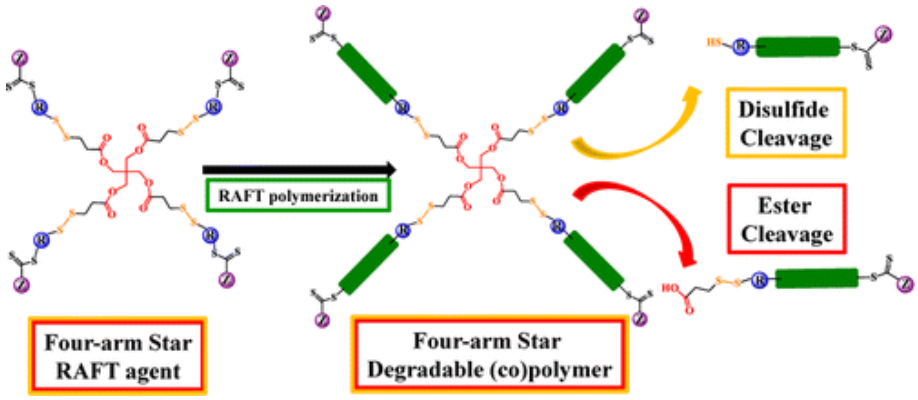

Figure 2.8. 4-armed star polymers via core-first RAFT polymerization route and their degradation profiles (Source: Rosselgong et al., 2013)

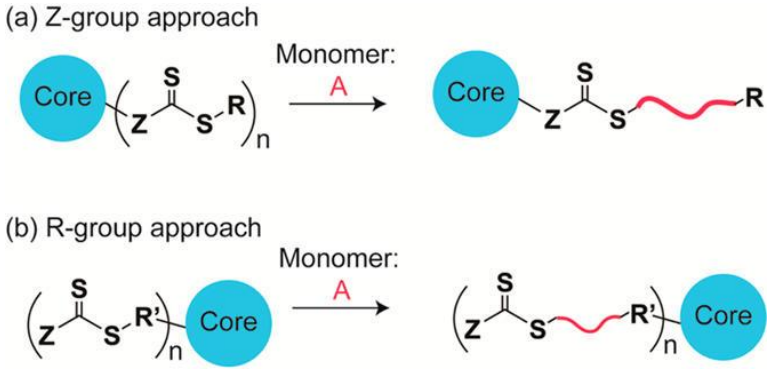

Figure 2.9. Comparison of the Z-group approach and R-group approach for synthesis of star polymers via RAFT polymerization (Source: Ren et al., 2016)

In the Z-group approach, the activating group (referring that non-fragmenting covalent bond) of RAFT agent is attached to the core where arms are radiating from. In the R-group approach, that is just contrary, the leaving group (referring that fragmenting covalent bond) of RAFT agent is attached to core and thiocarbonylthio groups always stays on the exterior surface of star polymers.

However, for R-group approach, star-star coupling termination reaction is more likely to occur since propagating radicals are connected to the core. In the main time, there is one benefit that aminolysis reactions to break the thiocarbonylthio groups may not cause any destruction to the architecture of star polymer.

Conversely, for Z-group approach, star-star coupling termination reaction may not be a complication since reactive sites are not attached to the star. One potential drawback of this approach, aminolysis reaction can be destructive. However, this property can be used as advantage if the aim is to form degradable polymers. Another drawback may be

steric-hindrance, since functional groups can be unreachable for monomers that must penetrate (Figure 2.10) (Ren et al., 2016).

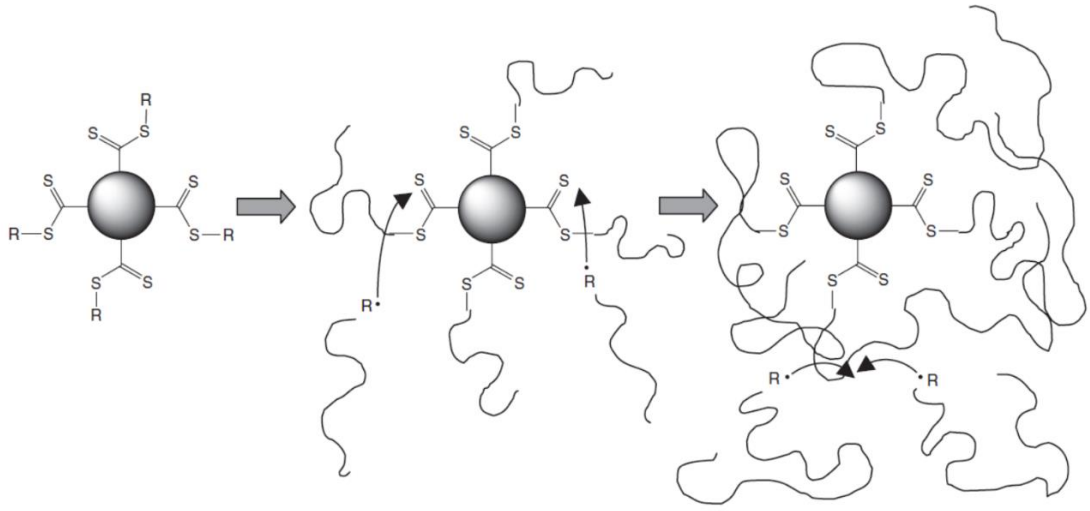

Figure 2.10. Illustration of the shielding effect of growing arms during synthesis of star polymers via Z-group approach (Source: Barner-Kowollik et al., 2006)

Considering all of these, it can be said that taking the advantage of these two approaches is depending on proper selection of the RAFT agent and monomer. Boshmann and Vana states that well-defined star polymers with molecular weights more than $1x10^6$ Da and narrow polydispersities can be obtained by using Z-group approach. The authors have investigated polymerization profiles of acrylate monomers and they have observed that at high monomer conversions there has been unexpected broadening in not only MWs but also MWDs. Additionally, this effect has been increased when acrylate monomer changed from methyl acrylate to butyl- and dodecyl- acrylate. This is the evidence of star-star coupling reactions coming from intermolecular transfer to polymer, transferring radical center from macro-radical to living star polymer (Boshmann and Vana, 2007).

Typically, core-first approach for star polymers causes radical termination reactions. That's why the arm-first approach in which synthesized macroRAFT agents are used for further polymerization of di- or higher vinyl monomers acting as cross-linkers. While the core-first approach where multifunctional RAFT agents are used for polymerization of vinylic monomers requires many preparation steps, the arm-first approach is generally easier (Syrett et al., 2011).

In arm-first route, linear macro-initiators or macroRAFT agents are first created as arm-precursors. These arm-precursors are chain-extended with added co-monomers or

crosslinkers and this leads to formation of core with several incorporated arms radiating from the core (Figure 2.11) (Matyjaszewski et al., 2007).

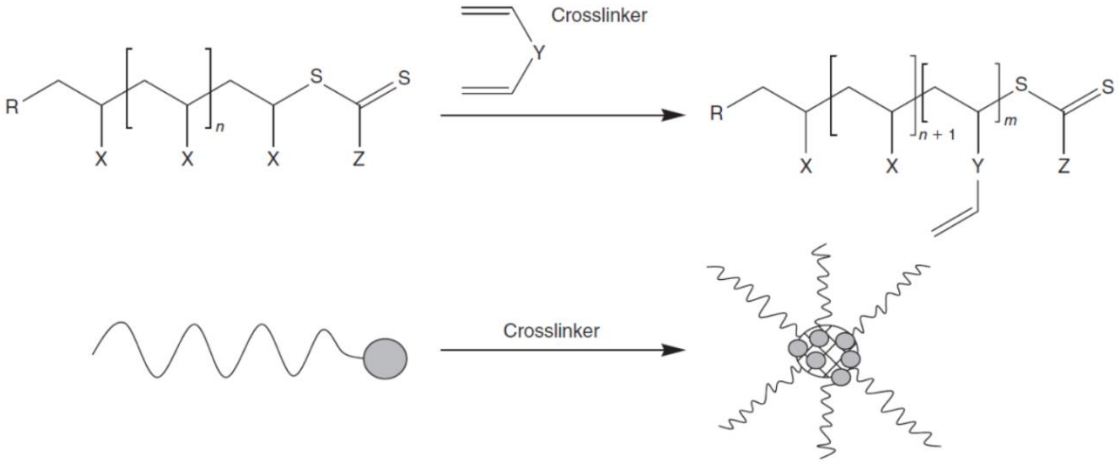

Figure 2.11. Synthesis of star polymers via arm-first methodology
(Source: Barner-Kowollik et al., 2006)

It is known from the literature that arm-first approach can lead to star polymers with high polydispersities (~2). However, broadening in MWD can be limited and controlled by employing crosslinkers having poor solubility in reaction media. Furthermore, molecular weight of synthesized macroRAFT agents which are pre-arm structures can be highly effective to form well-defined star polymers.

Accordingly, Dong et al. have reported that the use of macroRAFT agents with lower molecular weight (meaning that short pre-arms) can lead to star architectures with large core and several arms. On the other hand, the use of macroRAFT agents with higher molecular weight (meaning that long pre-arms) can lead to star architectures with small core and few number of arms emanating from that small core (Figure 2.12) (Dong et al., 2010).

The first one-pot synthesis of star polymers via arm-first approach was reported by Goh et al. In this study, arms were synthesized and crosslinker species were added into the arm synthesis pot to directly form star polymers. Goh et al. revealed that as the molecular weight of arms (length of arms) extended from distinct cross-linked core (typically 10-35% by mass) was higher, to the polymer solution transformed from Newtonian behavior to viscoelastic rheological behavior. Accordingly, increment in molecular weight of arms resulted in increasing relative viscosity. Moreover, the authors have observed that increasing of arm molecular weight decreased branch density which meant reduction in the arm number per core. Hydrodynamic diameter of synthesized star

polymers showed linear increasing trend with increasing molecular weight of stars and arms (Goh et al., 2008).

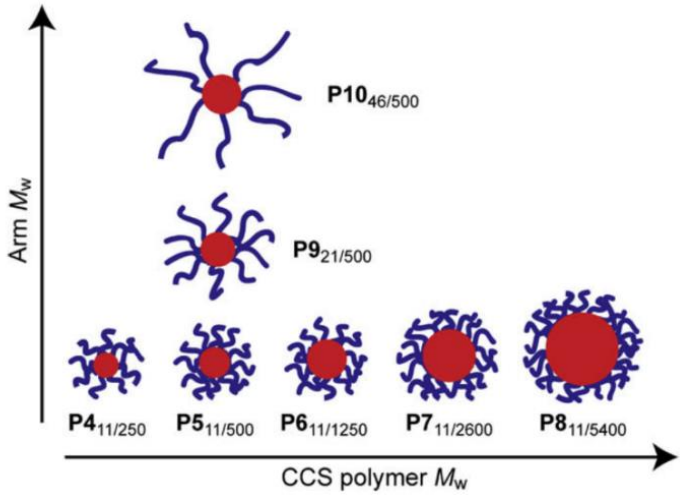

Figure 2.12. Schematic representation of core crosslinked star (CCS) polymers ($P_{x/y}$ where x= M_w of arm in CCS polymer and y=M_w of CCS itself) (Source: Goh et al. 2008)

It was also reported that the number of arms extending from CCS core influence the star-star coupling interactions since high number of arms means high number of end-groups present in the CCS structure (Likos et al., 1998; Watzlawek et al., 1999).

Additionally, Learsch et al. hypothesized that the nature of the crosslinker in terms of flexibility could dictate star production efficiency, and therefore designed three different di-functional crosslinkers with varying flexibility. Type 1 (decane) crosslinker was composed of only nine C-C single bonds which gave more conformational freedom than type 2 (para-xylene) and type 3 (para-phenylene; which was composed of only phenyl ring) crosslinkers. At the end of trials, the authors observed that type 3 crosslinker that was most rigid one gave highest star molecular weight with high conversions. On the other hand, type 1 crosslinker failed to form good star yields, resulting only 10% mass conversion and achieving only to create dimeric species with low molecular weights. However, when low molecular weight arms were reacted with any type of crosslinkers, good incorporation of arms was seen. As a result, the authors have concluded that the increment in crosslinker flexibility (type of crosslinker that can rotate easily) could cause intramolecular cyclization which stopped further star production. Moreover, the increment in molecular weight of arm polymers could cause increasing steric bulk, lower mobility in solution and lots of intramolecular cyclization. In other words, star yield was

decreased as the length of arm polymer increased and as the molar concentration of crosslinker to polymer arm in reaction medium decreased (Learsch et al., 2017).

The arm-first strategy can also be applied using macro-monomers with vinyl end groups instead of macroRAFT agents (Figure 2.13). However, this route is more suitable for monomers, such as polylactides and polypeptides, that are unable to be polymerized via radical polymerization techniques. Via this approach, star polymers that have nearly 10 million Da with broad dispersity were formed using peptide-stabilized nano-particles having poly(benzyl-glutamate) as crosslinking agent (Audouin et al., 2010).

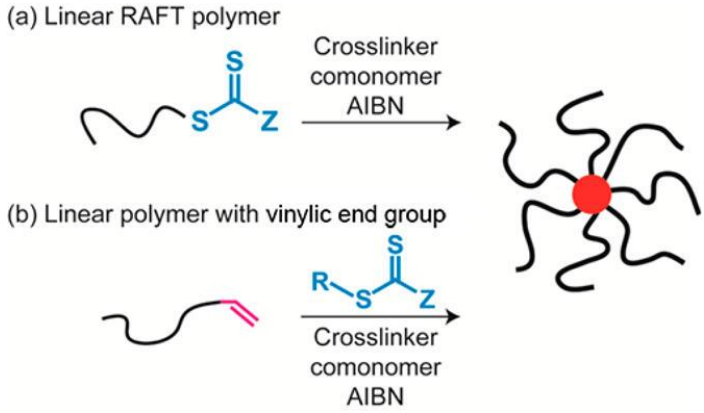

Figure 2.13. Star synthesis via macroRAFT and macromonomer strategies utilizing arm-first approach (Source: Ren et al., 2016)

Even though arm-first approach yields star polymers with broad polydispersity, important improvements lowering polydispersity have been achieved. Ferreria et al. synthesized core-crosslinked star polymers with narrow polydispersity using RAFT polymerization. The authors minimized the star-star coupling reactions that occur due to the radical intermediates terminations by optimizing reaction conditions. For synthesizing star polymers, an arm-first approach was used since termination reactions are more likely to occur in the core-first approach. In the study, poly(oligoethylene glycol methyl ether acrylate) [poly(OEG-A)], poly(tert-butylacrylate) [poly(tert-BuA)], and poly(N-isopropyl acrylamide) [poly(NIPAAm)] with three different molecular weights (5 to 50 kDa) were first synthesized as arm forming macroRAFT agents . For the synthesis of core-crosslinked stars, different cross-linkers N,N'-bis(acryloyl)cystamine, N,N methylene bisacrylamide, 1,2-dihydroxyethylene-bis-acrylamide and 1,6-hexanediol diacrylate] at varying concentrations were used. Additionally, as a solvent for star formation reaction, DMF, acetonitrile and toluene were used to see the influence on star polymerization reaction. N,N'-bis(acryloyl)cystamine is perfectly soluble in DMF and

acetonitrile but not in toluene. Therefore, the authors found that star polymers with low polydispersity could be obtained in toluene using N,N'-bis(acryloyl)cystamine as a crosslinker and poly(OEG-A)] as arm polymer with (Mn=7 kDa) and attributed this result to the fact that the low solubility of the crosslinker led to the incorporation of high number of arms and formation of well-defined star polymers.

Ferreria et al. also analyzed the effect of crosslinker concentration on star polymer formation. After the trial of different sets of crosslinker: MacroRAFT agent ratio between 2 and 32, they observed macro-gel formation above a ratio of 16 and shoulders at lower retention times in GPC chromatograms indicating that star-star coupling. Still, at lower ratios (2 and 4), low arm incorporation was demonstrated.

These authors also studied the effect of molecular weight of macroRAFT agents on star polymer formation. The results showed that there was no distinct difference on star molecular weights and polydispersities but there was difference on solubility profile of synthesized star polymers. Star polymers with short arms were partially-soluble due to their larger hydrophobic core. However, stars with long arms yielded water-soluble nanostructures which were around 20 nm in hydrodynamic diameter. As conclusion, this study showed that well-defined star polymers with narrow polydispersity could be synthesized using poorly soluble crosslinker and that crosslinker ratio to macroRAFT agent is a process that needs optimization for well-incorporation of arms and avoiding from macro-gel formation (Ferreria et al., 2011).

Additionally, the importance of hydrophilicity/hydrophobicity of linear arms chains covering exterior surface of star polymers was also investigated. Wei and colleagues made use of hydrophobic butyl methacrylate (BMA), cationizable dimethylaminoethyl methacrylate (DMAEMA) and hydrophilic OEGMA as arm forming chains. Broadening in polydispersity of star polymers was observed as dimethacrylate crosslinker to total macroRAFT agent ratio and the hydrophobic PBMA macroRAFT agent proportion were increased. The increment in crosslinker ratio caused increase in molecular weight from 80 kDa to 180 kDa. They synthesized star polymer presented only PDMAEMA and POEGMA without PBMA homopolymers and star polymer with only PBMA homopolymer, well-defined star polymers were obtained in both circumstances. This can be because of joining of pre-arms that have different hydrophilicity profiles (in which hydrophobic PBMA presented with hydrophilic POEGMA arm forming chains) can ruin the morphology of mikto-arm star polymers due to aggregation of hydrophobic chains (Wei et al., 2014).

In literature, there are also studies reporting the use of ionic RAFT polymerization for star polymer synthesis. However, using ionic polymerization methods such as cationic or anionic polymerization, it is hard to make copolymerization with a wide range of olefinic monomers due to irreconcilability of growing chains (Gao and Matyjaszewski, 2009).

For instance, in 2017, Uchiyama et al. reported the synthesis of star polymers via arm-first strategy using cationic RAFT polymerization. After the production of the macroRAFT agents as arm polymers, block copolymerization of divinyl monomers was carried out to obtain core-crosslinked star polymers with controlled molecular weights (within the range of 200-600 kDa), controlled arm number per core (15-40), narrow polydispersity (from 1.1 to 1.4) and hydrodynamic sizes between 15 and 30 nm. The authors have used three different synthetic methodologies:

The first method was one-pot RAFT block copolymerization of divinyl ethers in the presence of cationogen (triflic acid) instead of a radical initiator. Accordingly, linear polymers of isobutyl vinyl ether as arms were first synthesized. When the most of isobutyl vinyl ether converted to polymers (conversion up to 99%), crosslinking reactions were carried out in-situ with the addition of divinyl ethers which have butyl- and cyclohexyl-spacers. As a result, slightly higher yield of star polymers was obtained via divinyl ether with cyclohexyl spacer (star yield: 93%) than divinyl ether with flexible butyl spacer (star yield: 88%) because of lower probability of intramolecular addition for rigid cyclohexyl structure.

In order to understand the effect of added divinyl ethers, divinyl ether/macroRAFT agent ratios were changed from 5 to 20. From these experiments the authors concluded that at the highest ratio (20) star-star merging occurred because of the formation of large cross-linked core compared to arms since star polymers with higher polydispersity were produced.

The second methodology was to prepare first macroRAFT agents via cationic RAFT polymerization, followed by simultaneous crosslinking reaction via radical RAFT polymerization of various divinyl compounds. Because of slow fragmentation of macroRAFT agent into vinyl ether radicals when compared with acrylate radicals of added divinyl compounds, it was observed that most of the macroRAFT agent remained unreacted. The yield of star polymers was improved by using hetero-divinyl compounds which had acrylate and vinyl ether groups. This was attributed to the reaction of acrylate radicals with vinyl ether group, creating vinyl ether radicals eventually.

In the third methodology, block copolymers as macroRAFT agents were first via cationic RAFT polymerization by using hetero divinyl monomers, afterwards the crosslinking reaction via radicals was performed separately. The authors observed that as block copolymer macroRAFT agent concentration got higher, the molecular weights of star polymers increased but resulting in broader and nonsymmetrical traces of SEC. Further increase in concentration of block copolymer macroRAFT agent caused insoluble gel formation during reaction (Uchiyama et al., 2017).

Optimization of reaction conditions and well-selection of polymerization type and monomers are key factors for synthesis of star polymers as desired vehicles for gene or drug delivery. However, in order to create star polymers with desired properties such as biocompatibility and biodegradability, some modifications on core and arm structures may be required.

Disulfide, ketal and acetal based crosslinkers can be used to obtain biodegradable star structures. Such star polymers are potential nanocarriers for both gene and drug delivery and can be also be advantageous for further release of loaded drug or gene into the target cells. For instance, star polymers with hydrophilic arms and with degradable, protonable core moiety offer water-soluble potential carrier systems for gene delivery throughout and can be degraded in response to external-stimuli after the entry of target cells (Syrett et al., 2011).

Wei et al. have designed redox-cleavable mikto-arm stars via arm-first approach. Since core structure contained disulfide bonds, degradation of the core was observed upon addition of a reducing agent (Bu_3P), Molecular weight of cleaved star structures was different from that of macroRAFT agents because of the employment of spacer monomers and residual crosslinker (Wei et al., 2014). A similar result was obtained in another study where core-crosslinked by bis(acryloyl)cystamine star polymers have been subjected to glutathione (100 mM) which is a natural reducing agent found in cytoplasm and degradation was seen after 14 h with slightly higher molecular weights of linear arm polymers (Liu et al., 2012). In a different study, it has been demonstrated that disulfide-incorporated star polymers with polydispersity of 1.3-1.4 and diameter of approx. 20 nm have been degraded within 48 h in the presence of 100 mM GSH and under physiological conditions of GSH (4 mM) degradation has been observed after 4-7 days depending on core composition (Cho et al., 2011).

In literature, there are several examples on synthesis of functionalized cores for loading of specific drugs or nucleic acids. For instance, Liu et al. have synthesized star

polymers (molecular weights up to 132 kDa with narrow polydispersities and diameters around 20 nm) via arm-first approach. They have chain-extended preformed PEG macroRAFT agents (10 kDa and 20 kDa) using a disulfide crosslinker, N,N'-bis(acryloyl)cystamine, and a co-monomer, vinylbenzaldahyde (VBA). This led to the incorporation of degradable disulfide bonds and aldehyde groups to the core structure. The presence of aldehyde groups in the core provided attachment of doxorubicin via imine linkages. Since these linkages are pH-sensitive, they can be unstable at acidic environment and can provide release and endosomal escape of loaded drug (Liu et al., 2012).

Alternatively, cationic star polymers for loading negatively charged oligonucleic acids via electrostatic attractions can be produced. It is known that compared to linear polymers, star polymers provide higher charge density. However, having highly charged cationic cores can be problematic, since such cores can interact with serum proteins and also be toxic. Non-specific interactions with serum proteins can cause the formation of large aggregates. This problem can be fixed by employment of poly(oligo(ethylene glycol) methyl ether methacrylate (POEGMA) or polyethylene glycol (PEG) as non-immunogenic, non-toxic and neutral arms. POEGMA and PEG can shield the cationic charge on the core of star polymers. Moreover, employment of PEG can decrease barriers for non-specific adhesion onto cationic polymers. However, it has also its own drawbacks. Non-optimized PEGylation can retard the complexation of negatively charged genes with star polymers because of steric-effects. Optimized PEGylation can reduce the strength of polyplex and accelerate more effective and easy release of nucleic acids inside cells. (Cho et al., 2011; Teo et al., 2016).

In another study that was conducted by Teo et al., the design of cationic and degradable mikto-arm (heterogeneous) star polymers was reported. The authors have incorporated cationic dimethylaminoethyl methacrylate (DMAEMA) monomer and disulfide crosslinker for chain extension of POEGMA and PDMAEMA macroRAFT agents. They changed the arm lengths of star polymers (long POEGMA with short PDMAEMA (star 1), long POEGMA with long PDMAEMA (star 2), short POEGMA with long PDMAEMA (star 3) and non-POEGMA with PDMAEMA) and formed structures up to 145 kDa with low dispersity (approximately 1.35). They showed that while non-POEGMA star polymer had a zeta-potential of +50 mV, POEGMA containing stars shifted to +18 mV (for star 1) and +25 mV (for star 2 and 3, respectively). This was attributed to the steric hindrance effect of long-POEGMA chains around the star polymer.

However, complexation with siRNA was achieved for all three of POEGMA star polymers. Additionally, it was reported that after complexation, POEGMA containing star polymers showed outstanding cytotoxicity profiles when compared to non-POEGMA star polymers. The authors concluded that POEGMA which has same low-fouling property with PEG is vital for star polymers to deliver and release siRNA to the cytosol of target cell (Teo et al., 2016).

CHAPTER 3

MATERIALS AND METHODS

3.1. Materials

3.1.1. Chemicals

N-(2-hydroxyethyl) ethylenediamine (Aldrich, %99), di-tert-butyl dicarbonate (Aldrich, %99), triethylamine (Merck, %99), chloroform (Aldrich, %99.5), methacryloyl chloride (Sigma, %99.3), ethanol (Tekkim, %96) were used as supplied. Oligo(ethylene glycol)methyl ether acrylate (OEGMA) (Mn= 475 g/mol) was passed through an alumina column before use. 2,2-azobisisobutyronitrile (AIBN) was recrystallized twice in methanol before use. Tetrahydrofuran (THF) (Carlo-Erba, HPLC grade), hexane (Aldrich>%99), dichloromethane (DCM, Sigma Aldrich), toluene (Sigma-Aldrich >%99,7), acetonitrile (Sigma >%99,9), diethylether (Sigma >%99,5) were used as supplied. (4-Cyano-4-(phenylcarbonothioylthio) pentanoic acid (CPADB) (Sigma-Aldrich) was used as supplied as a chain transfer agent (CTA) for RAFT polymerizations. Silica gel (with pore size 60 Å, 70-230 mesh) was purchased from Fluka. Bis(2-methacryloyl) oxyethyl disulfide (contains <6000 ppm hydroquinone as stabilizer) crosslinker was purchased from Aldrich. Deuterium oxide (D_2O) (deuteration degree min 99.9% for NMR), deuterium chloroform ($CDCl_3$) (0.03 vol. % TMS, deuteration degree min. 99.8% for NMR and stabilized with silver) were purchased from Merck for Nuclear Magnetic Resonance (NMR) spectroscopy analysis. Dialysis membrane (MWCO=3.5, 10 and 100 kDa) was purchased from Spectrum® Laboratories. Standard desalted siRNA (sense: 5′-GCUAUGGGCUGAAUACAAAUU-3′; antisense: 5′-UUUGUAUUCAGCCCAUAGCUU-3′) (21 bp) was purchased from IDT DNA. Agarose and ethidium bromide were purchased from Sigma. 6x loading dye solution and DNA markers were purchased from Fermantas. Trypsin, Dulbecco's Modified Eagle's medium (DMEM) and Thiazoyl blue tetrazolium bromide (MTT) reagent were purchased from

Sigma and Dimethyl sulfoxide (DMSO) was obtained from Carlo-Erba. Trypan Blue Stain was supplied from Gibco. Human breast cancer cell line (MDA-MB-231-luc2-GFP) was kindly provided from Dr. Özgür Şahin's laboratory at Bilkent University.

3.1.2. Instruments

3.1.2.1. Nuclear Magnetic Resonance (NMR)

Throughout this study, ^{1}H NMR spectroscopy (Varian, VNMRJ 400 spectrometer) were used to investigate conversion of monomers after polymerization reactions, chemical composition of compounds, purification and deprotection yield of polymers. In order to carry out NMR analyses, polymer samples (10-15 mg/mL) were dissolved in $CDCl_3$ or D_2O depending on their solubility.

3.1.2.2. Gel Permeation Chromatography (GPC)

Gel permeation chromatography (GPC) was used to determine the molecular weight and molecular weight distribution of polymers synthesized in the study. A Shimadzu modular system connected to a WAYYT^{TM} multi-angle light scattering detector (MALLS) was used. A Shimadzu modular system included an auto injector (SIL-10AD), Waters Styragel guard and HR4 (molecular weight range 5 kDa-600 kDa) and HR3 (molecular weight range 500 Da-30 kDa) columns, refractive-index detector (RID-10A). The system was calibrated with low polydispersity poly(styrene) standards. The mobile phase was tetrahydrofuran (THF) containing 250 mg/kg 2,6-di-tert-butyl-4-methylphenol as stabilizer. Flow rate of mobile phase was 0.3 mL/min. All synthesized polymers were prepared at 4 mg/mL concentration and filtered with PTFE 0.22 μm syringe filters before analyses.

3.1.2.3. UV-Visible Spectrophotometer

In this study, UV-visible spectrophotometer was used to determine the RAFT-end group functionality of synthesized macroRAFT agents, show the activity of reducing agents for degradation of disulfide bonds and the aminolysis kinetics of RAFT end-groups of synthesized star polymers. UV-visible light absorbance of the samples was analyzed using a Thermo Scientific Evolution^{TM} 201 UV-visible spectrophotometer in the range between 190 nm and 600 nm.

3.1.2.4. Dynamic Light Scattering

Hydrodynamic size of polymers was determined using a Nanoplus zeta/particle size analyzer system. After preparation of samples, polymers were filtered using PTFE 0.22 μm syringe filters and the number average hydrodynamic size of samples was measured.

3.1.2.5. Agarose Gel Electrophoresis

The electrostatic complexation of siRNA with polymers was investigated via agarose gel electrophoresis using a Thermo Scientific Owl^{TM} B1 Midi Gel system connected to power source (Thermo EC250-90).

3.2. Methods

3.2.1. Synthesis of 2- ((tert-butoxycarbonyl) (2-((tert-butoxycarbonyl) amino) ethyl) amino) ethyl methacrylate (BocAEAEMA)

The monomer which have protected primary and secondary amine groups was synthesized according to the procedure reported by Kurtulus et al. (Kurtulus et al., 2014). The reaction scheme for synthesis of BocAEAEMA is shown in Figure 3.1.

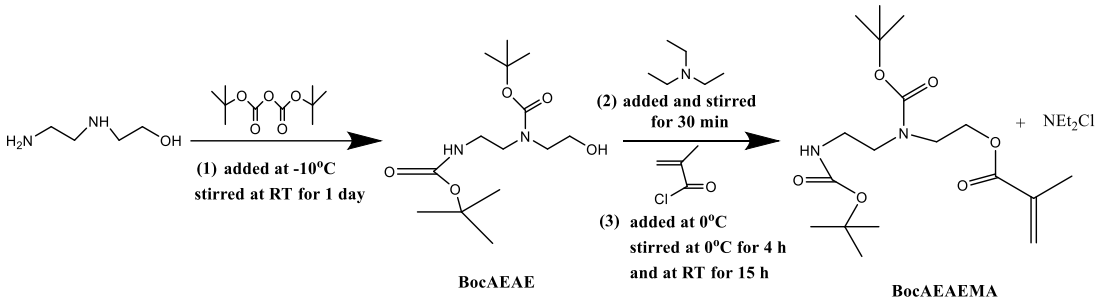

Figure 3.1. Reaction scheme for synthesis of BocAEAEMA monomer

Briefly, N-(2-hydroxyethyl) ethylenediamine (2.5 g, 0.025 mol) was first dissolved in dry DCM (40 mL) at -10°C [Solution 1]. Separately, di-tert-butyl dicarbonate (10.5 g, 0.048 mol) was dissolved in dry DCM (40 mL) [Solution 2]. Afterwards, solution 2 was added drop by drop into solution 1 at -10°C and final solution was stirred under N_2 for 3 h and then stirred without N_2 for 24 h at ambient temperature. After reaction completed, formed precipitate (tert-butyl hydrogen carbonate) was removed from reaction medium by filtration. Unreacted N-(2-hydroxyethyl) ethylenediamine was removed by water-DCM extraction performed at least three times. After the organic phase was gathered, the solvent was discharged using a rotary evaporator (Buchi® Rotavapor® RII). As the final product, tert-butyl-2- (((tert-butoxycarbonyl) amino) ethyl) (2-hydroxyethyl) carbamate (BocAEAE) (**1**) was obtained and analyzed via ^{1}H-NMR spectroscopy.

At the second step, methacryloylation was performed. Briefly, **(1)** (BocAEAE) (4 g, 0.015 mol) was dissolved in dry DCM (40 mL) at 0°C. Triethylamine (0.04 mol) was added drop by drop to the solution under nitrogen and the solution was stirred for about 30 minutes. Afterwards, methacryloyl chloride (0.03 mol) was added dropwise into the solution and continued to stir for 4 h at 0°C under nitrogen and for further 15 h at ambient

temperature. After reaction completed, formed salts were removed from reaction medium by filtration. Remaining reaction solution was extracted first with brine solution for three times, and then with water for three times. The product was dried under vacuum. As a final step, the product was purified via silica gel column chromatography using hexane and ethylacetate at varying volume ratios (1/0, 10/1, 8/1, 6/1, 4/1, 2/1, 0/1) as mobile phase. The final pure product, 2-((tert-butoxycarbonyl) (2-((tert-butoxycarbonyl) amino) ethyl) amino) ethylmethacrylate (BocAEAEMA), was obtained and characterized via ^{1}H-NMR spectroscopy (Kurtulus et al., 2014).

3.2.2. Synthesis of Poly(oligo(ethylene glycol)methylether Methacrylate P(OEGMA) MacroRAFT Agent

For the synthesis of poly(oligo(ethylene glycol) methyl ether methacrylate P(OEGMA) macroRAFT agents, 2,2–azobisisobutyronitrile (AIBN) as an initiator, 4-cyano-4-(phenylcarbonothioylthio) pentanoic acid (CPADB) as a RAFT agent, oligo(ethylene glycol)methylether methacrylate (OEGMA) (Mn= 475 g/mol) as monomer and acetonitrile (ACN) as solvent were used. Briefly, OEGMA monomer, CPADB and AIBN were dissolved in ACN (where OEGMA/CPADB/AIBN mole ratio = 50/1/0.25 and $[OEGMA]_o$= 1 M). The resultant solution was purged with nitrogen in order to remove oxygen in reaction flask for about 30 minutes. After purging with N_2, the reaction flasks were immersed into an oil bath at 65°C. The polymerization reaction was carried out for 2 h or 5 h. The polymerization reaction scheme for the synthesis of p(OEG-MA) macroRAFT agents are given in Figure 3.2.

After the polymerization stopped, the ACN was evaporated using vacuum oven. In order to remove unreacted monomer, RAFT agent and initiator, purification procedure was performed. Polymers with higher molecular weights (> 5,000 Da) were precipitated into cold diethyl ether (DEE) and the supernatant was removed by centrifugation. Precipitation and centrifugation cycle was repeated for more than three times. Polymers with lower molecular weights (< 5,000 Da) were dialyzed against distilled water for 1 week by using a dialysis membrane (MWCO= 3,500 Da) and finally freeze-dried. Final polymers were analyzed by using GPC, ^{1}H-NMR and UV-visible spectroscopies.

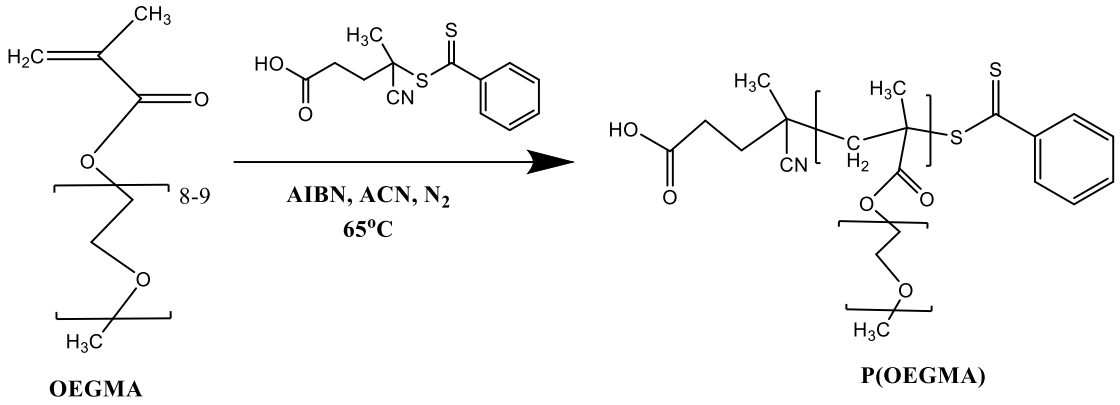

Figure 3.2. Polymerization reaction scheme for the synthesis of P(OEGMA) macroRAFT agents

3.2.3. Synthesis of Star Polymers via RAFT Polymerization

For the synthesis of star polymers, "arm-first" approach was followed using P(OEGMA) linear homopolymers as macroRAFT agents. Various star polymers were synthesized using P(OEGMA) macroRAFT agents with molecular weights varying between 5 kDa and 10 kDa in the presence of a biodegradable crosslinker (bis (2-methacryloyl) oxyethyl disulfide) and BocAEAEMA co-monomer. The reaction time, crosslinker/macroRAFT agent ratio and BocAEAEMA co-monomer/macroRAFT agent ratio were also varied in experiments to investigate their effects on star formation. As an initial condition; MacroRAFT agent/Crosslinker/Initiator/BocAEAEMA comonomer mole ratio of 1/Crosslinker/0.1/BocAEAEMA was selected. The crosslinker to MacroRAFT agent ratio (X) was changed from 2 to 8 and BocAEAEMA comonomer ratio to MacroRAFT agent ratio (Y) was changed from 1.5 to 8. As a solvent for polymerization, toluene, a poor solvent for bis(2-methacryloyl) oxyethyl disulfide crosslinker was used. After purging reaction vials with N_2 for 20 minutes, vials were sealed and immersed into an oil bath at 70°C for different periods of time. The reaction conditions used for synthesis of star polymers throughout the study are shown in Table 3.1. The polymerization scheme is also shown in Figure 3.3. After reaction completed, polymers were dialyzed against ethanol/water mixture for one week using a dialysis membrane (MWCO=10 or 100 kDa). Purified products were analyzed using ^{1}H-NMR spectroscopy and GPC.

Table 3.1. Polymerization conditions used to synthesize star polymers where [MacroRAFT agent]$_0$= 0.03 M)

MacroRAFT M_n (kDa)	MacroRAFT/**Crosslinker**/AIBN/**BocAEAEMA** mole ratio	Time (h)
10	1/**8**/0.1/**1.5**	2
10	1/**8**/0.1/**1.5**	8
10	1/**8**/0.1/**1.5**	16
10	1/**8**/0.1/**1.5**	24
10	1/**8**/0.1/**1.5**	24
10	1/**6**/0.1/**1.5**	24
10	1/**2**/0.1/**1.5**	24
10	1/**8**/0.1/**8**	24
10	1/**8**/0.1/**6**	24
10	1/**8**/0.1/**1.5**	24
10	1/**8**/0.1/**16**	24
5	1/**8**/0.1/**1.5**	24
5	1/**6**/0.1/**1.5**	24
5	1/**2**/0.1/**1.5**	24
5	1/**8**/0.1/**8**	24
5	1/**8**/0.1/**6**	24
5	1/**8**/0.1/**1.5**	24
5	1/**8**/0.1/**16**	24
10	1/**6**/0.1/**1.5**/0.25*	24
8	1/-/0.1/**1.5**	24
-	1/-/0.1/**1.5**	24
10	1/**8**/0.1/**2º** (OEG-MA as comonomer)	24
8	1/**6**/0.25/**1.5**	2
8	1/**6**/0.25/**3**	2

*: MacroRAFT/**Crosslinker**/AIBN/**BocAEAEMA**/*Excess RAFT agent*

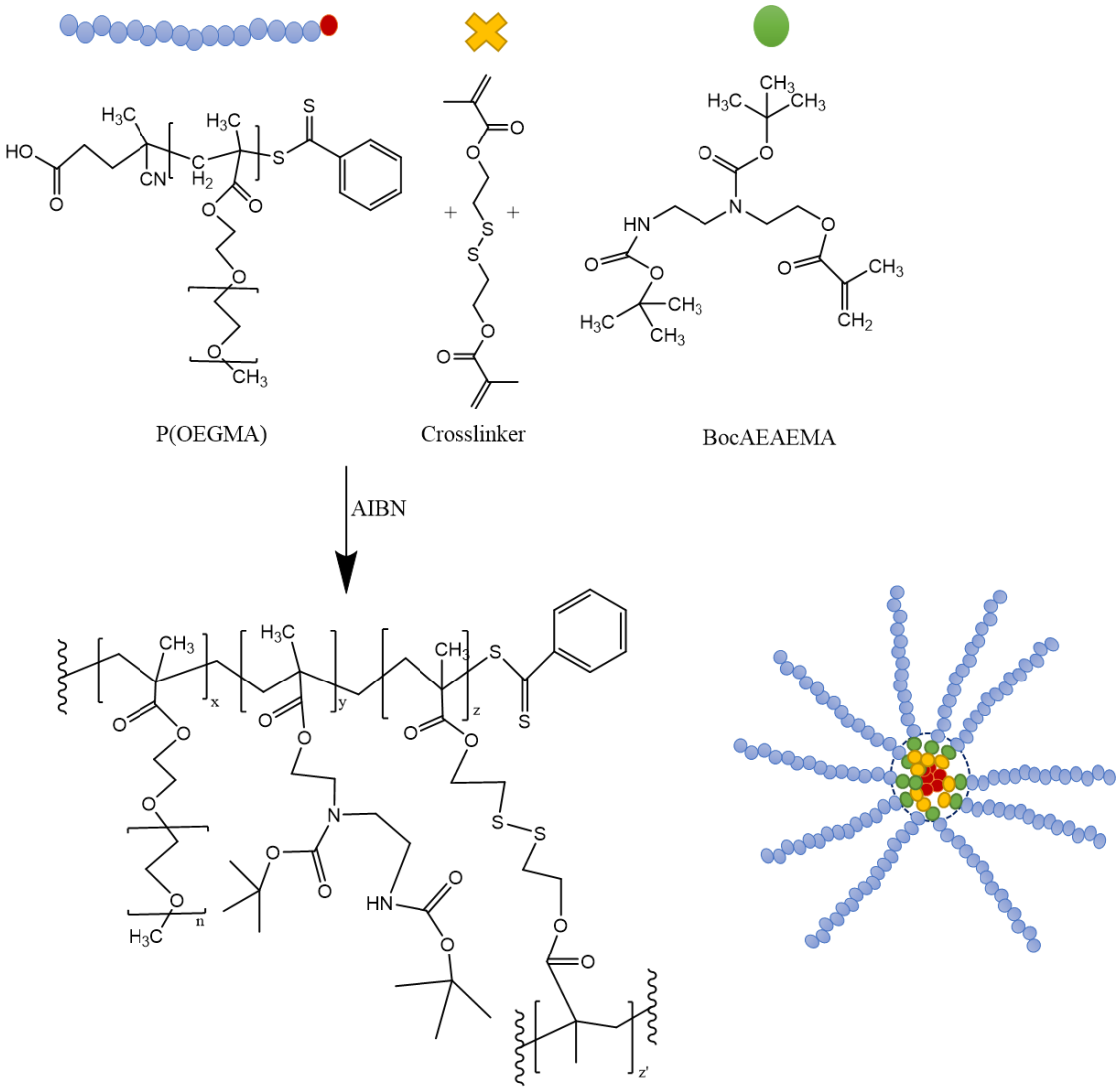

Figure 3.3. The polymerization scheme for synthesis of star polymers

3.2.4. Deprotection of Star Polymers

To deprotect amino groups within P(BocAEAEMA) core of star copolymers, Boc groups were removed (Figure 3.4). Briefly, all synthesized star polymers (4.35 μM) were dissolved in DCM (1 mL). Trifluoroacetic acid (TFA) (500 μL) was then added dropwise at 0°C. The solution was then stirred at ambient temperature for 30 minutes and the solvent was evaporated purging the solution with N_2. In order to purify, the crude polymer was first washed with cold diethyl ether and centrifuged more than three times. Finally, polymers were dissolved in methanol and then precipitated in cold diethyl ether,

centrifuged three times and dried under vacuum. To ensure that Boc- groups were removed after purification, polymers were characterized by ^{1}H-NMR spectroscopy.

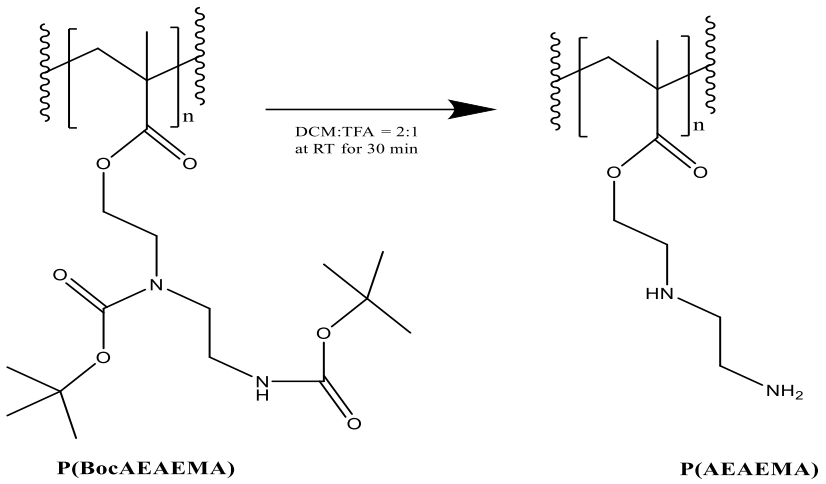

Figure 3.4. Reaction scheme for deprotection of P(BocAEAEMA) within the core of star polymers.

3.2.5. Determination of Degradation Profiles of Star Polymers

Since a degradable crosslinker was introduced into the core structure of star polymers, it was expected that the star polymers could degrade under reductive conditions resulting unimeric polymer chains. The cleavage of star polymers was investigated before and after deprotection of amino groups of star polymers. Since the star polymers before deprotection were not soluble in aqueous solutions, these polymers were treated with an organic-soluble reducing agent, triphenylphosphine. On the other hand, since the star polymers after deprotection became water-soluble, they were treated with a water-soluble reducing agent, tris(2-carboxyethyl) phosphine hydrochloride (TCEP.HCl). However, a control experiment was first performed to test the reducing ability of both reducing agents using a disulfide containing molecule dithiodipyridine (DTP) (Figure 3.5).

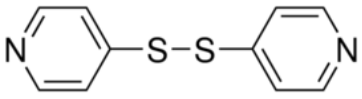

Figure 3.5. Structure of dithiodipyridine (DTP)

It is known from the literature that the disulfide bonds within DTP can be cleaved in a suitable reducing medium to form 2-pyridinethione which specifically absorbs light at 370 nm (Boyer et al., 2009a).

For this control experiment, dithiodipyridine (0.16 mg/mL) was dissolved in THF and triphenylphosphine solution (50 mM) in THF was added. The final solution was then observed via a UV-Visible spectrophotometry at different time points (0, 5 and 30 minutes). Similarly, dithiodipyridine (0.16 mg/mL) was dissolved in THF/water (50/50 by volume) and tris(2-carboxyethyl) phosphine hydrochloride (TCEP.HCl) (50 mM) solution in water was added. The final solution was observed via a UV-Visible spectrophotometry at different time points (0, 5, 30 and 108 minutes).

Star polymers before deprotection, were dissolved in THF at a concentration of 4 mg/mL and then characterized via DLS. 50 mM triphenylphosphine solution was then added and the solution was again characterized via DLS.

Separately, star polymers after deprotection, were dissolved in ultra-pure water at a concentration of 4 mg/mL and then characterized via DLS. 50 mM TCEP.HCl solution was then added and the solution was again characterized via DLS (Figure 3.6).

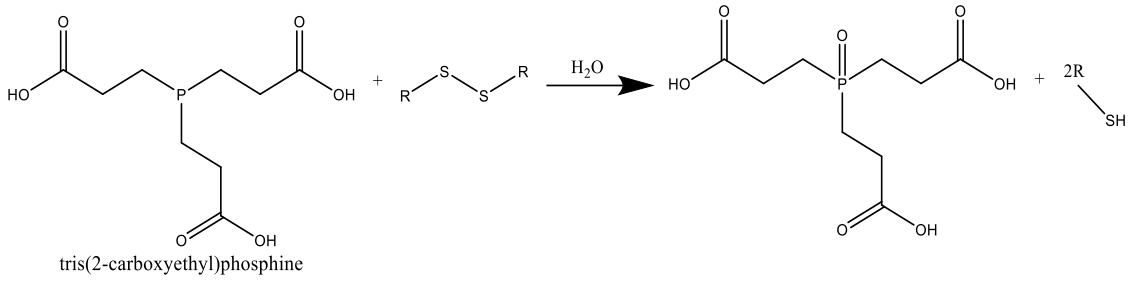

Figure 3.6. Reaction scheme for reduction of disulfide bonds with TCEP

3.2.6. Investigation of Complex Formation of Star Polymers with siRNA

In order to demonstrate the potential of P(OEGMA)-*b*-P(AEAEMA)cationic star polymers as siRNA carriers, selected star polymers were electrostatically complexed with negatively charged siRNA molecules. Table 3.2 shows the properties of star polymers used in these experiments.

Table 3.2. The properties of star polymers used for siRNA complexation

Polymer Code	$M_{w,\ theo\ after\ deprotection}$ (kDa)	Arm Number (N_{arm})	$M_{w,\ theo}$ for P(AEAEMA) (kDa)
Star 1	150	14	42
Star 2	71	7	5
Star 3	70	7	14

To investigate the formation of complexes, agarose gel electrophoresis was used. Briefly, star polymers (dissolved in ultrapure water where pH was 6) (for N/P=200; 13.4 μg/μL for Star 1, 68.3 μg/μL for Star 2, 28.7 μg/μL for Star 3) and siRNA (dissolved in ultrapure water) (0.01 nmol/μL) were used. Star polymers were mixed with siRNA (0.02 nmol for each) at different nitrogen/phosphate (N/P) ratios (1, 25, 100, 200) and incubated at ambient temperature for approx. 45 minutes. After the incubation time, the solutions were mixed with 6x loading dye and then loaded into 3% agarose gel which was stained with ethidium bromide. Together with naked-siRNA and DNA ladder, the gel was run at 100 V for 30 minutes by using 1x TAE buffer.

3.2.7. Investigation of *In Vitro* Cytotoxicity

Thiazoyl blue tetrazolium bromide (MTT) is a colorimetric assay procedure which can be used to investigate cell viability. MTT procedure includes the measurement of cellular enzyme activity which reduce the tetrazolium into insoluble formazan and purple formazan can be measured via microplate reader at 540 nm.

Before MTT assay, polymers were modified via aminolysis reaction to remove thiocarbonylthio RAFT-end group within the polymers in order to suppress any potential toxicity coming from these groups. For aminolysis reaction, briefly polymers were dissolved in methanol and excess triethylamine (10/1 by molar) and hexylamine (10/1 by molar) were added dropwise. Solution was stirred for 3h at ambient temperature after purging with N_2. UV-visible light absorbance of the solutions was analyzed using a UV-visible spectrophotometer at 305 nm to ensure that RAFT-end group successfully removed.

For MTT assay, first of all, human breast cancer (MDA-MB-231-luc2-GFP) cells were seeded in a 96 well-plate in which concentration of cells was 10^4 cells per well. After that, plate was incubated for a day in humidified environment at 37°C and 5% CO_2. Polymers that were used for siRNA complexation experiments (Star 1, Star 2, Star 3) (Table 3.2) were used and compared with bPEI (25 kDa). After incubation, varying concentrations (40 μM, 20 μM, 10 μM, 4 μM, 2 μM and 1 μM) of polymers were prepared in PBS and 5 μL of polymer solutions transferred to wells. Plate was incubated for 24 h and MTT dye (5 mg/mL) was added to each well (where final volume 100 μL) by adjusting %10 (v/v). After addition of dye, plate was incubated for another 4h. Afterwards, supernatants were removed, DMSO (100 μL) was added to each well and pellets were dissolved. The absorbance was recorded at 540 nm by using microplate reader. The percentage of cell viability was calculated by using following equation.

$$\text{Cell Viability (\%)} = \frac{A_{\text{cell with polymer}}}{A_{\text{control}}} \text{x} 100 \qquad (3.1)$$

CHAPTER 4

RESULTS AND DISCUSSION

4.1. Synthesis of 2- ((tert-butoxycarbonyl) (2-((tert-butoxycarbonyl) amino)ethyl)amino)ethyl Methacrylate (BocAEAEMA)

2- ((tert-butoxycarbonyl) (2-((tert-butoxycarbonyl) amino) ethyl) amino) ethyl methacrylate monomer was synthesized according to a procedure that was reported by Kurtulus et al. (Kurtulus et al., 2014). As a first step of synthesis, the primary and secondary amine groups of N-(2-hydroxyethyl) ethylenediamine were protected with di-tert-butyl dicarbonate (Boc-) in order to avoid any undesired side reaction. At the second step of the synthesis, after Boc- protection, the hydroxyl group of the diaminoethane compound was reacted with methacryloyl chloride to prepare a methacrylate monomer. After the silica gel column chromatography, the final product, 2- ((tert-butoxycarbonyl) (2-((tert-butoxycarbonyl) amino) ethyl) amino) ethyl methacrylate (BocAEAEMA) monomer was analyzed via ^{1}H-NMR spectroscopy (Figure 4.1).

As a sign of successful amine-protection reaction, the distinctive proton signals of the Boc- groups were observed between 1.40 ppm and 1.50 ppm (18 H). Besides that, as a sign of successful methacryloylation reaction, the characteristic proton signals of vinyl protons (-CH_2 and -CH_3) appeared at 6.08 ppm (1 H), 5.55 ppm (1 H) and 1.91 ppm (3 H). Additionally, the signal that was located at 4.21 ppm, demonstrated the generation of an ester bond after methacryloylation.

The determination of successful protection of amines groups was important parameter to observe since without any protection of amines, highly reactive amine groups can react with the HCl which was formed during methacryloylation step of monomer synthesis and can reduce the yield of methacrylate monomer formation at the end. Additionally, without any protection of amines with Boc- groups, reactive amines can interfere with incorporated RAFT agents that used for further RAFT polymerization reaction, so polymerization can be failed without any controlled polymer formation.

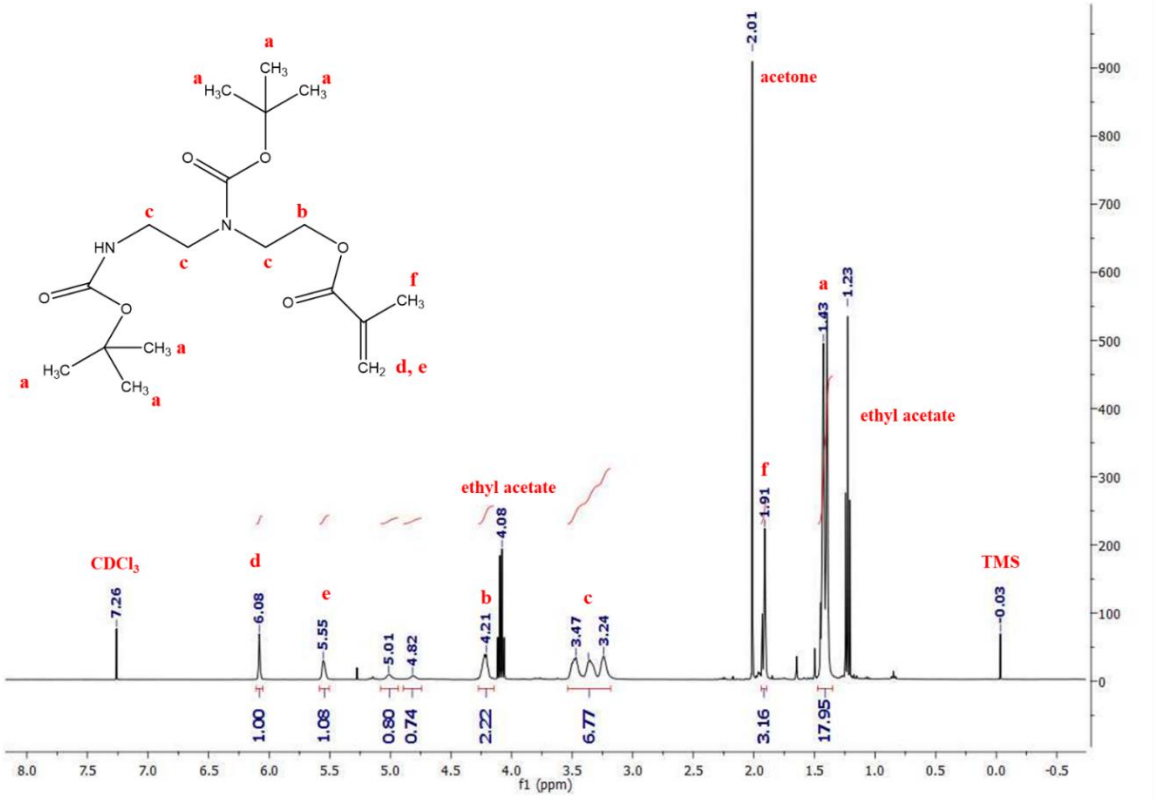

Figure 4.1. ^{1}H-NMR spectrum of 2- ((tert-butoxycarbonyl) (2-((tert-butoxycarbonyl) amino) ethyl) amino) ethyl methacrylate (BocAEAEMA) after purification (M_w= 372.5 g/mol)

4.2. Synthesis of Poly(oligo(ethylene glycol)methylether Methacrylate (P(OEGMA)) as macroRAFT Agent

For synthesizing P(OEGMA) macroRAFT agents which have varying molecular weights (between 5 kDa and 10 kDa) via RAFT polymerization: 2,2–azobisisobutyronitrile (AIBN) as an initiator, 4-cyano-4-(phenylcarbonothioylthio) pentanoic acid (CPADB) as a RAFT agent, oligo (ethylene glycol)methylether methacrylate (OEGMA) (Mn= 475 g/mol) as a monomer and acetonitrile (ACN) as a solvent were used.

Oligo(ethylene glycol)methylether methacrylate (OEGMA) (Mn= 475 g/mol) was passed through the alumina column before use to remove the inhibitors. After column chromatography, the chemical structure of used oligo(ethylene glycol)methylether methacrylate (OEGMA) monomer was investigated via ^{1}H-NMR spectroscopy. The characteristic proton signals of vinyl protons (-CH_2 and -CH_3) appeared at 6.10 ppm (1

H), 5.54 ppm (1 H) and 1.91 ppm (3 H), respectively. Additionally, two protons of methylene group (-CH_2-) of OEGMA monomer can be seen at 4.26 ppm (Figure 4.2).

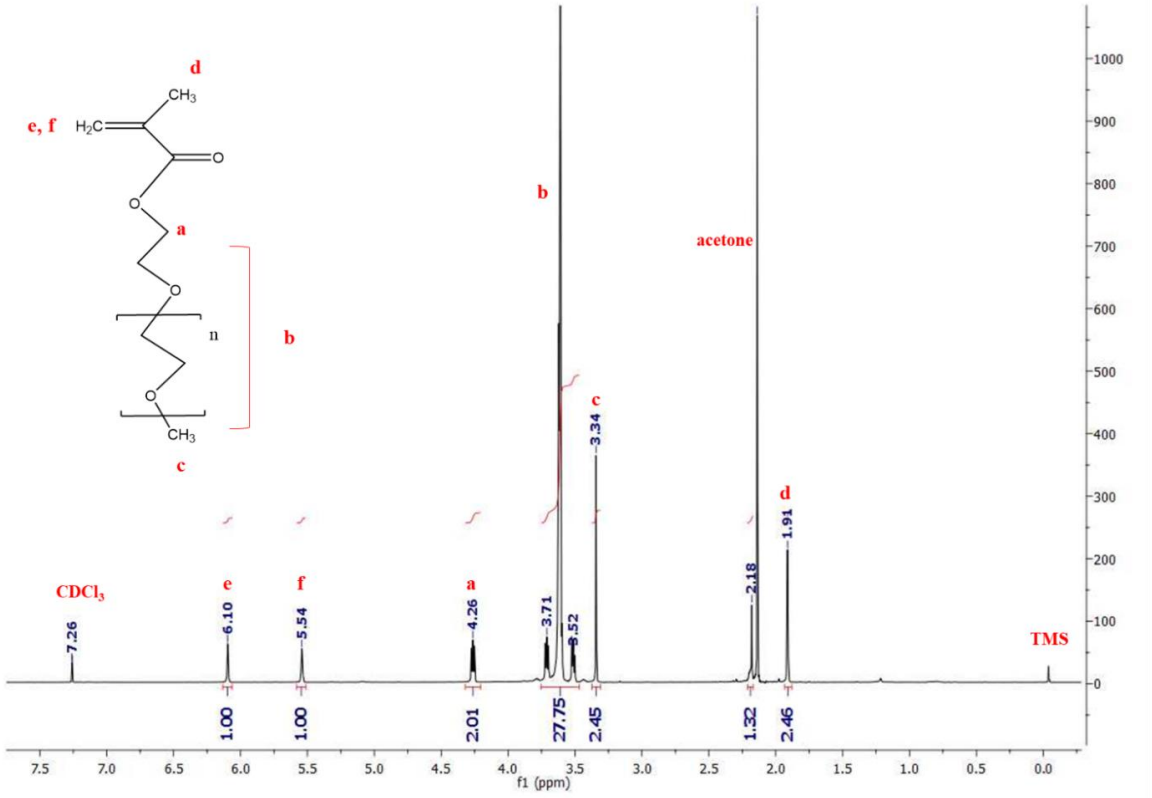

Figure 4.2. ^{1}H-NMR spectrum of oligo(ethylene glycol)methylether methacrylate (OEGMA) (Mn= 475 g/mol)

After RAFT polymerizations of unconverted oligo(ethylene glycol)methylether methacrylate monomer, OEGMA monomer conversion to P(OEGMA) polymers was determined by analyzing crude polymerization reaction mixtures via ^{1}H-NMR spectroscopy (Figure 4.3).

This crude polymerization reaction mixture was expected to contain unconverted oligo(ethylene glycol)methylether methacrylate monomer, remaining 4-cyano-4-(phenylcarbonothioylthio) pentanoic acid (CPADB) RAFT agent and formed linear oligo(ethylene glycol)methylether methacrylate polymer chains. Before analyzing via NMR, reaction medium which was acetonitrile was evaporated and removed from reaction mixture by using vacuum conditions.

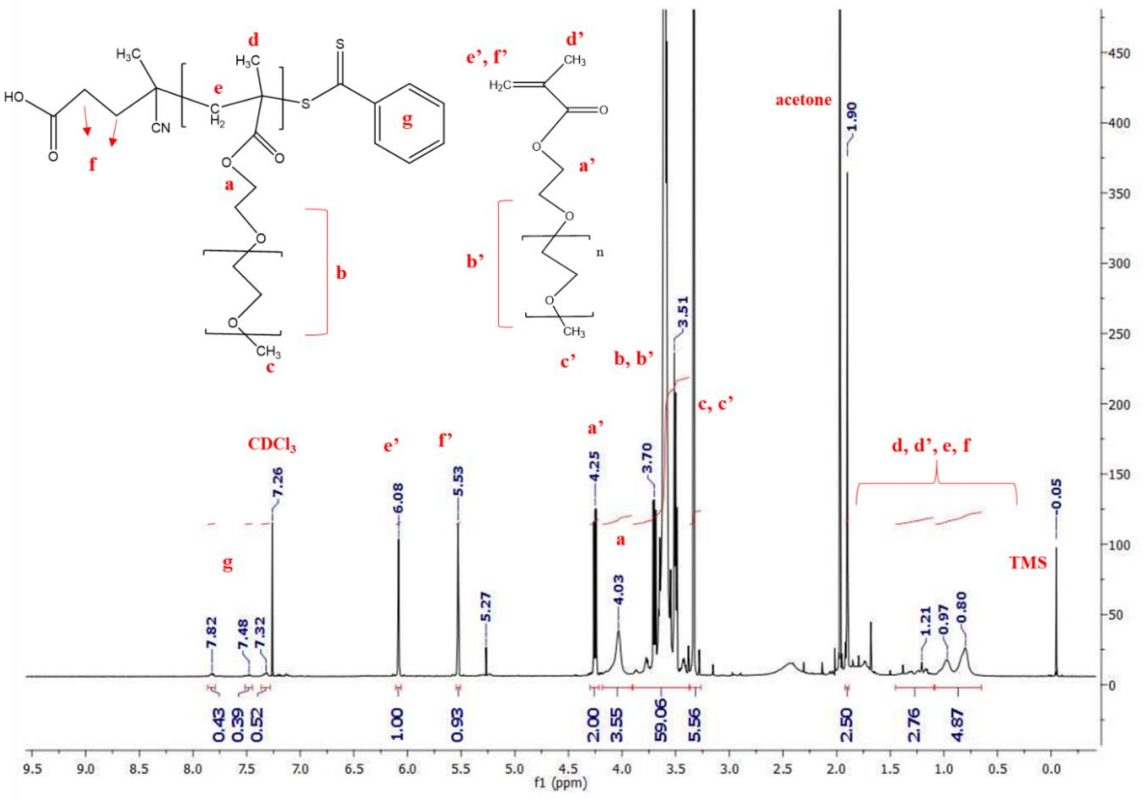

Figure 4.3. A representative ^{1}H-NMR spectrum of P(OEGMA)polymerization mixture before purification ([OEGMA]/[CPADB]/[AIBN] mol ratio of 50/1/0.25; polymerization time= 150 min, conversion= 67%)

Accordingly, the characteristic proton signals of vinyl protons and two protons of methylene group (-CH_2-) of unconverted OEGMA monomer can be seen at 6.08 ppm (1 H), 5.53 ppm (1 H) and 4.25 ppm, respectively. As a sign of polymerization reaction, the proton signals of methylene group of polymerized monomer were shifted from 4.25 ppm to 4.03 ppm. Accordingly, Equation 4.1. was used for calculation of monomer conversion from NMR spectrum of polymerization mixtures before purification.

$$\%\text{Conversion} = \frac{\frac{a,a'}{2} - \frac{f'+e'}{2}}{\frac{a,a'}{2}} \times 100 \qquad (4.1)$$

where e'= $I_{6.08ppm}$ f'= $I_{5.53ppm}$ and a, a'= $I_{4.0\text{-}4.4ppm}$

In order to calculate the molecular weights of linear P(OEGMA) polymers, the polymers after removal of unconverted monomers, CPDAB residues and AIBN, were again analyzed via ^{1}H-NMR (Figure 4.4).

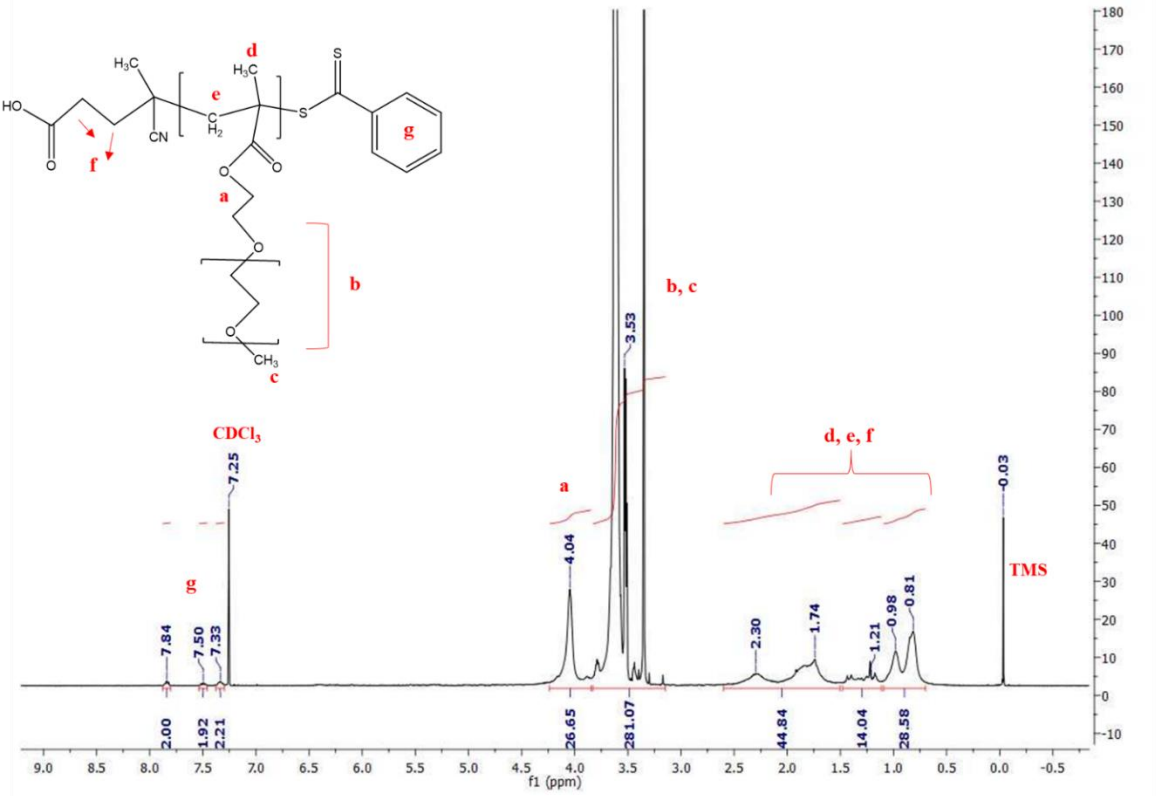

Figure 4.4. A representative ^{1}H-NMR spectrum of P(OEGMA) after purification ([OEGMA]/[CPADB]/[AIBN] mol ratio of 50/1/0.25; polymerization time= 150 min, conversion= 67%)

The disappearance of the characteristic proton signals of vinyl protons (6.08 ppm and 5.53 ppm) coming from OEGMA monomer, indicates the success of the purification method.

Moreover, assuming that all polymer chains have a RAFT end-group, the molecular weight of polymers was calculated via ^{1}H-NMR spectroscopy using Equation 4.2.

$$M_n^{NMR} = \left(\frac{\frac{I_{4\text{-}4.4}}{2}}{\frac{I_{7.9\text{-}7.3}}{5}} \times M_w^{OEGMA} \right) + M_W^{RAFT} \qquad (4.2)$$

where M_w^{OEGMA} and M_W^{RAFT} are the molecular weight of OEGMA monomer and CPADB RAFT agent.

After the synthesis of P(OEGMA) macroRAFT agents, end-group functionality of the polymers was also determined using UV-Visible spectrophotometry (at λ= 305 nm) (Figure 4.5) and Equation 4.3 after establishing a calibration curve of CPADB RAFT agent.

$$\text{RAFT End-group Functionality} = \frac{(Abs_{305} \times M_n)}{(c \times \varepsilon_{305} \times L)} \qquad (4.3)$$

where Abs= absorbance, ε= extinction coefficient at 305 nm (~12 500 M^{-1}. cm^{-1}), L= light path-length (cm), c= polymer concentration (mg/mL) and M_n= molar mass (g/mol).

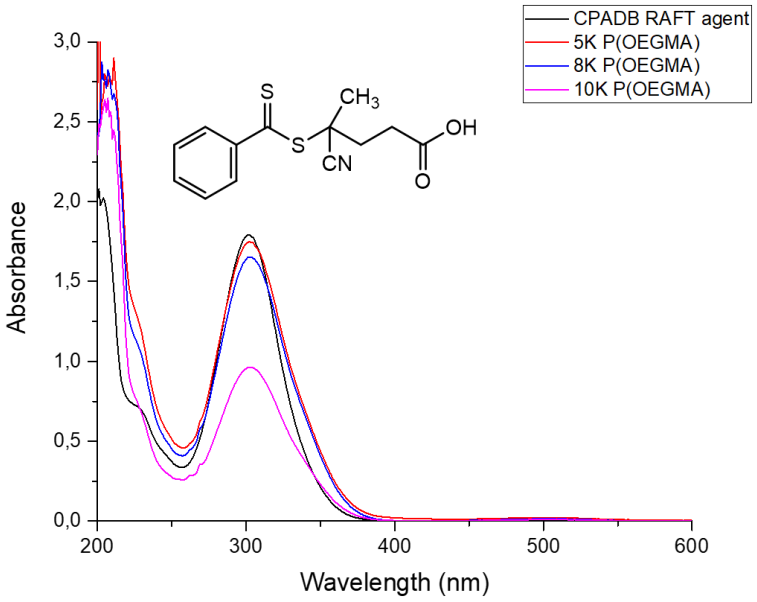

Figure 4.5. UV-Visible Spectra of CPADB RAFT agent (M_w= 279.4 g/mol) and P(OEGMA) polymers with varying molecular weights (5kDa, 8kDa, 10kDa)

The RAFT agent (0.04 mg/mL) and P(OEGMA) polymers (1 mg/mL) were investigated via UV-vis spectroscopy and the absorbance values were determined to calculate the RAFT end-group functionality via Equation 4.3 (Table 4.1). The UV-Visible spectrophotometry results in Figure 4.5. confirmed the presence of RAFT end-group (C=S) of the polymers (at around 305 nm). Since further star synthesis would require the chain extension from macroRAFT agent, the presence of the functional RAFT-end group of P(OEGMA) linear chains was an important criterion for the success of the star synthesis. The end-group functionality of P(OEGMA) macroRAFT agents was found to be 75% and over. Since the experimental molecular weight calculation from ^{1}H-NMR was based on the assumption of a RAFT end-group functionality of 100%, molecular weights were also separately calculated after the determination of the actual number of functional RAFT-end groups in P(OEGMA) polymers (by dividing the Mn values determined from NMR by the end-group functionality, the last column in Table 4.1).

In order to identify the number average molecular weights (M_n) and molecular weight distributions (PDI) of the synthesized polymers, gel permeation chromatography (GPC) was used. The molecular weight characteristics of P(OEGMA) macroRAFT agents used for the further star polymer synthesis can be seen in Table 4.1.

Table 4.1. Summary table for P(OEGMA) homopolymers used throughout the study

Code	M_n[a] (g/mol)	PDI[a]	M_n[b] (g/mol)	Conversion[c] (%)	RAFT end-group functionality[d] (%)	M_n[b]/ RAFT end-group functionality[d]
5K	5360	1.16	4550	41	75	6070
8K	8000	1.13	6800	52	80	8500
10K	11500	1.14	8150	70	79	10300

a: determined via GPC-RI b: calculated via Equation 4.2 using NMR measurements. c: calculated via Equation 4.1. d: calculated via Equation 4.3.

As seen in Table 4.1, the GPC molecular weights were in good agreement with the molecular weights based on NMR and end-group functionality calculations. As an indication of the narrow distribution of molecular weights and controlled mechanism of the RAFT-technique, linear P(OEGMA) homopolymers with low polydispersity index (PDI lower than 1.2) and high RAFT end-group functionality were synthesized and suitably used as macroRAFT agents for synthesis of star polymers.

4.3. Synthesis and Characterization of Star Polymers via RAFT Polymerization

Various star polymers were synthesized using P(OEGMA) linear polymer arms as macroRAFT agents. P(OEGMA) which has low-fouling characteristic (Teo et al., 2016) was copolymerized with BocAEAEMA monomer in the presence of a biodegradable crosslinker (bis (2-methacryloyl) oxyethyl disulfide). The motivation for the use of BocAEAEMA as monomer was to incorporate primary and secondary amines into star core for electrostatically complexing with nucleic acids at nearly neutral pH and for potential proton-sponge activity through endocytic pathway, respectively.

In order to characterize the chemical composition of incorporated difunctional monomer (cross-linker) ^{1}H-NMR spectroscopy was used (Figure 4.6).

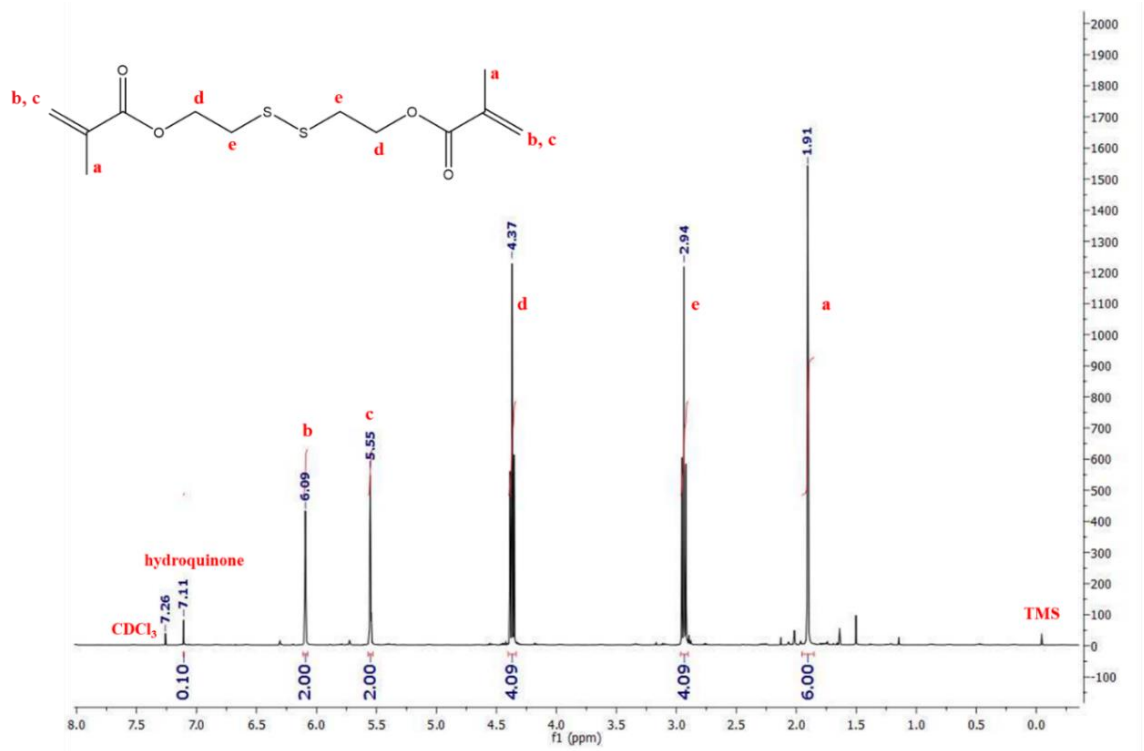

Figure 4.6. H-NMR spectrum of bis(2-methacryloyl) oxyethyl disulfide difunctional monomer (Mw= 290.4 g/mol)

Since the crosslinker contains divinyl group in its structure, four protons and six protons of vinyl groups (=CH_2 and –CH_3) appeared at 6.09 ppm, 5.55 ppm and 1.91 ppm, respectively. The protons of -CH_2- adjacent to disulfide bond appeared at 2.94 ppm, whereas the protons of -CH_2- adjacent to ester bond were observed at 4.37 ppm in the crosslinker structure before polymerization.

The biodegradable crosslinker bis(2-methacryloyl) oxyethyl disulfide and BocAEAEMA comonomer were polymerized via RAFT polymerization technique with the employment of POEGMA macroRAFT agent as a chain transfer agent in toluene which was a poor solvent for the crosslinker.

After the reaction, in order to determine the conversion of bis(2-methacryloyl) oxyethyl disulfide (which is di-functional) crosslinker and BocAEAEMA monomer (which is mono-functional), ^{1}H-NMR spectrum of unpurified polymers was analyzed (Figure 4.7).

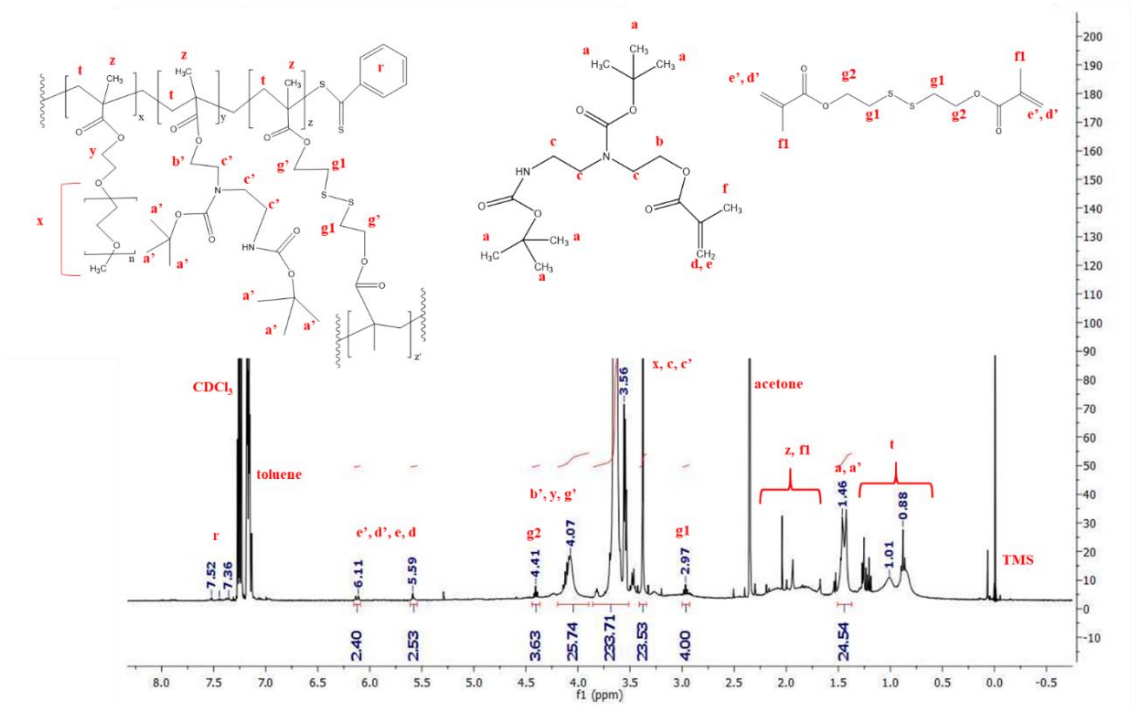

Figure 4.7. Representative 1H-NMR spectrum of star polymers before purification (MacroRAFT/Crosslinker/AIBN/BocAEAEMA= 1/6/0.1/1.5 where t = 24 h, [MacroRAFT agent]0= 0.03 M and Mn of P(OEGMA) MacroRAFT=10 kDa)

The summation of integration values of proton peaks (=CH_2) located at 6.11 ppm and 5.59 ppm represents four protons of unconverted di-functional crosslinker monomer and two protons of BocAEAEMA monomer, remained unreacted. The integral of the peak appeared at 1.46 ppm belongs to eighteen protons of Boc- protection group from both BocAEAEMA monomer and P(BocAEAEMA). The signal at around 4.07 ppm belongs to methylene groups of p(OEGMA) (2H), p(BocAEAEMA) (2H) and polymerized crosslinker (4H) along with BocAEAEMA monomer (2H). Other specific signals have been assigned on the spectrum in Figure 4.7. Accordingly, Equation 4.4 was used to determine BocAEAEMA monomer and crosslinker conversion to polymer via ^{1}H-NMR spectrum.

$$\frac{I_{6.11+5.59}}{2} = \text{2H Crosslinker+1H BocAEAEMA}$$

$$I_{1.46} = \text{18H p(BocAEAEMA)+18H BocAEAEMA}$$

$$\text{BocAEAEMA Conversion (\%)} = \frac{\text{p(BocAEAEMA)}}{\text{BocAEAEMA+p(BocAEAEMA)}} \text{x100}$$

$$I_{4.07} = \text{2H p(OEGMA)+2H BocAEAEMA+2H p(BocAEAEMA)+4H Crosslinker}$$

$$I_{3.63}=28H\ p(OEGMA)$$

$$\text{Crosslinker Conversion (\%)}=\frac{p(\text{Crosslinker})}{\text{Crosslinker}+p(\text{Crosslinker})}x100 \qquad (4.4)$$

Star polymers after purification via dialysis were also investigated via ^{1}H-NMR (Figure 4.8).

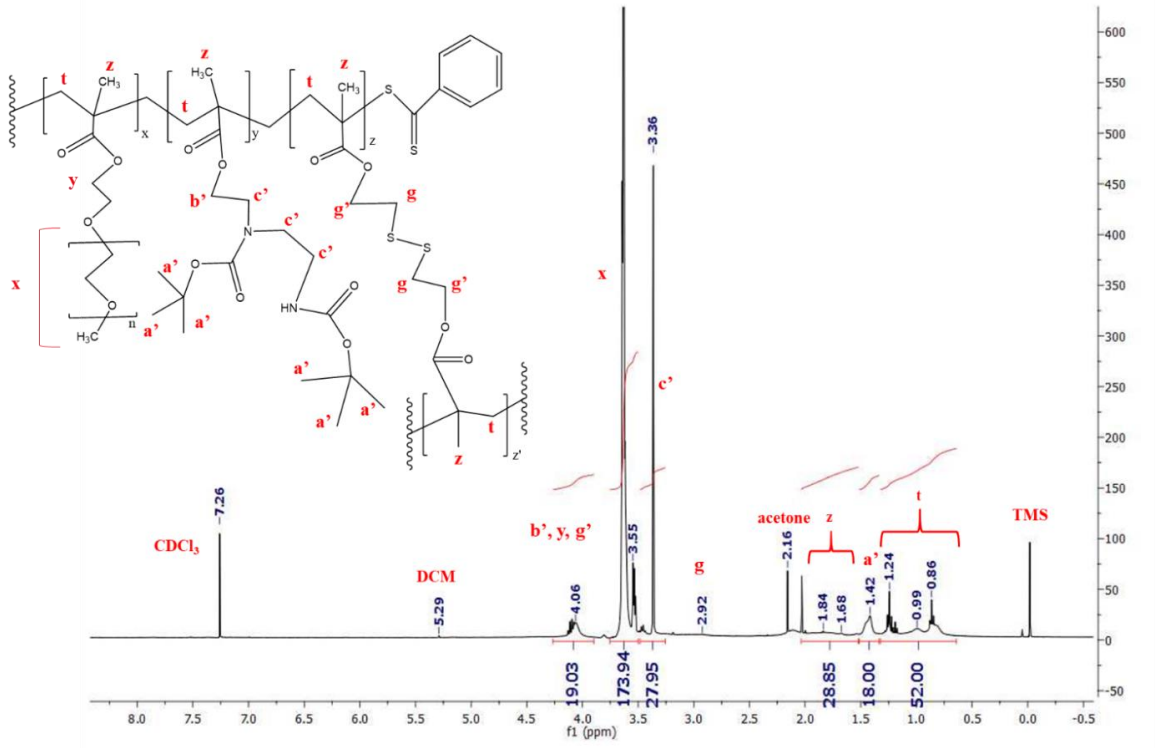

Figure 4.8. ^{1}H-NMR spectrum of star polymers after purification (MacroRAFT/Crosslinker/AIBN/BocAEAEMA= 1/6/0.1/1.5 where t = 24 h, $[\text{MacroRAFT agent}]_0$= 0.03 M and M_n of P(OEGMA) MacroRAFT=10 kDa)

The disappearance of four protons of crosslinker and two protons of monomer at 6.11 ppm and 5.59 ppm was the proof of the successful purification of the star polymers synthesized.

After verification of the successful purification method for polymers, gravimetric analyses were carried out to determine the efficiency of polymerization procedure and the star polymer formation yields (star polymer yields) were calculated as the proportion of the amount of purified polymers to the total amount of initial P(OEGMA) macroRAFT agent ($m^0_{P(OEGMA)}$) and reacted BocAEAEMA monomer ($m^0_{BocAEAEMA}$* BocAEAEMA conversion) and crosslinker ($m^0_{crosslinker}$ x Crosslinker conversion). Additionally, the absolute molecular weight (M_w) and polydispersity (PDI) of the synthesized star polymers

were analyzed via gel permeation chromatography (GPC). The results are presented in below sections.

4.3.1. The Effect of the Polymerization Time on Star Polymer Synthesis

The kinetics of star polymer synthesis via RAFT polymerization were investigated at a fixed macroRAFT agent concentration (0.03 M) and a mole ratio of MacroRAFT agent/Crosslinker/BocAEAEMA of 1/8/0.1/1.5. Polymerization times were varied (t= 2, 8, 16 and 24 h) and conversion of monomer and crosslinker was calculated via ^{1}H-NMR spectroscopy, as described above. The conversions determined via NMR have been presented in Table 4.2. After 2 h of polymerization, the BocAEAEMA and crosslinker conversions reached around 34%. However, when the polymerization time extended, there was a linear increase in both crosslinker and BocAEAEMA conversions ($[M]_0/[M]$) with time (Figure 4.9). The linear increase of monomer and crosslinker conversions with time is the evidence of RAFT controlled polymerization mechanism. After 24 h of polymerization, the BocAEAEMA and crosslinker conversions reached about 71% and 62%, respectively. The gravimetric analysis of the final polymer product after purification via dialysis (using a dialysis membrane with a MWCO of 100 kDa) shows the yield of star polymer formation since dialysis process is expected to remove unreacted P(OEGMA) MacroRAFT arms, crosslinker and BocAEAEMA monomer. Gravimetric analysis results (Figure 4.10) showed that while star polymer yield was only 32% after 2 h of polymerization, the yield at 8, 16 and 24 h of polymerization reached approximately 55% with no significant change with time. This indicates that the incorporation of arms into star structure completed between 2 and 8 h of polymerization. After 8 h of polymerization there was not further arm incorporation into star structure.

The molecular weights and the molecular weight distributions (PDIs) of the star polymers were evaluated via GPC using light scattering (LS) detector (Figure 4.11).

Table 4.2. Summary of the polymerization kinetic study for star polymers (MacroRAFT/Crosslinker/AIBN/BocAEAEMA= 1/8/0.1/1.5 where t = 2, 8, 16, 24 h, $[MacroRAFT\ agent]_0$= 0.03 M and M_n of P(OEGMA) MacroRAFT=10 kDa)

Polymerization Time (h)	M_w (kDa)[a]	PDI[a]	BocAEAEMA Conversion[b]	Crosslinker Conversion[b]
2	116	1.80	0.34	0.34
8	433	1.70	0.53	0.45
16	437	1.61	0.56	0.55
24	620	1.52	0.71	0.62

a: determined via GPC-LS b: calculated via Equation 4.4

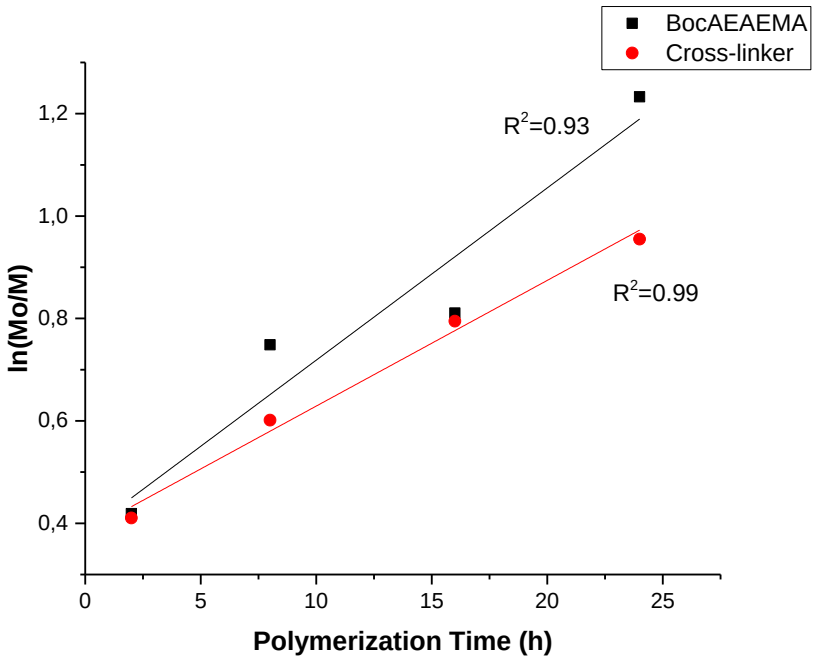

Figure 4.9. ln(Mo/M) plot of star polymers with varying polymerization time (MacroRAFT/Crosslinker/AIBN/BocAEAEMA= 1/8/0.1/1.5, where t = 2, 8, 16, 24 h, [MacroRAFT agent]0= 0.03 M and Mn of MacroRAFT=10 kDa)

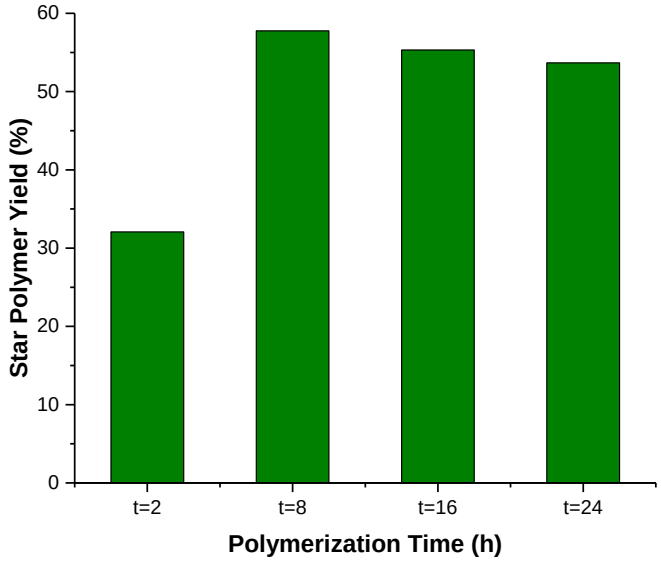

Figure 4.10. Gravimetric analysis of the final star polymers purified by dialysis (MacroRAFT/Crosslinker/AIBN/BocAEAEMA= 1/8/0.1/1.5 where t = 2, 8, 16, 24 h, $[MacroRAFT\ agent]_0$= 0.03 M and M_n of MacroRAFT=10 kDa)

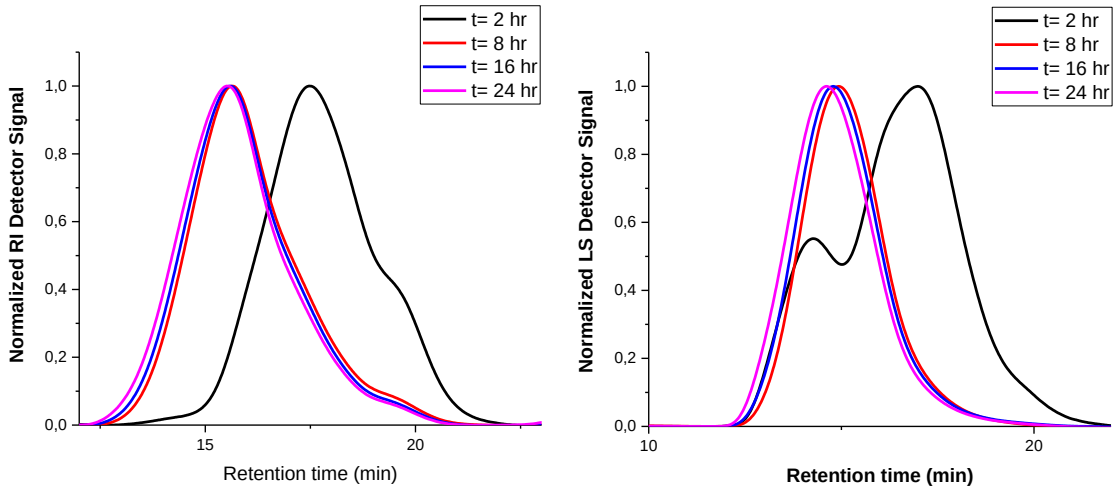

Figure 4.11. GPC-RI and GPC-LS traces of kinetic study for star polymers (MacroRAFT/Crosslinker/AIBN/BocAEAEMA= 1/8/0.1/1.5, polymerization time t = 2, 8, 16, 24 h where $[MacroRAFT]_0$= 0.03 M and M_n of MacroRAFT=10 kDa)

It can be confirmed from GPC traces that during polymerization, the incorporation of P(OEGMA) macroRAFT agent arms into star polymers increased as the polymerization time increased. When the reaction time was 2 h, there was a shoulder at higher retention times which indicates that some arm chains still existed as unimers

without incorporation into star structures. Formation of high molecular weight polymeric structures without any residual arms was the evidence of formation of core-crosslinked star-shaped polymers with extending reaction times (8, 16, 24 h). Moreover, as polymerization time was increased, molecular weight distributions significantly narrowed. The lowest PDI of star polymers was obtained for 24 h reaction time with the highest final product efficiency, molecular weight and monomer conversions.

The change in molecular weight (M_w) obtained from LS detector with monomer and crosslinker conversions can be seen in Figure 4.12. As the reaction times increased, higher BocAEAEMA and crosslinker conversions led to higher molecular weights with lower polydispersities. Linear increase in M_w with monomer conversion was indicative of RAFT-controlled polymerization mechanism.

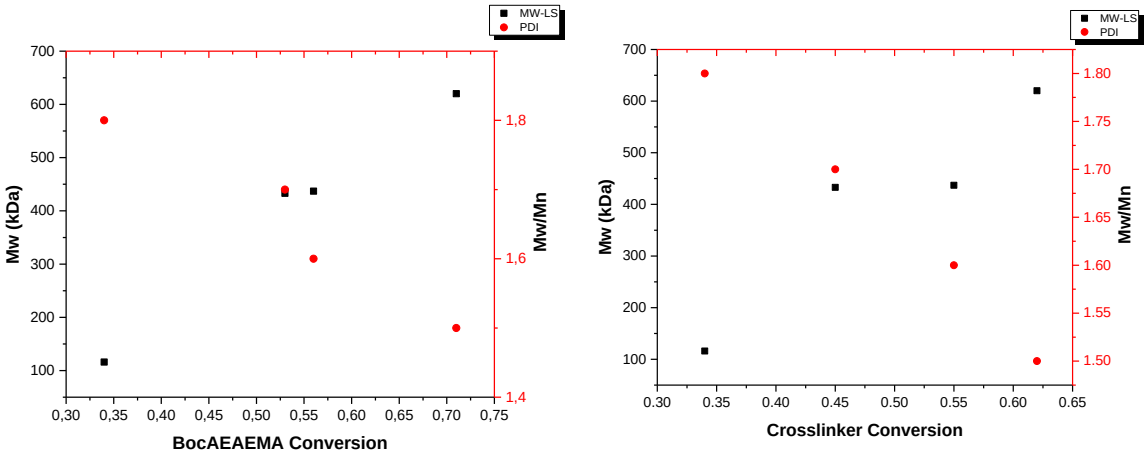

Figure 4.12. Plots of Mw (determined by GPC-LS) of star polymers with monomer and crosslinker conversions (MacroRAFT/Crosslinker/AIBN/BocAEAEMA= 1/8/0.1/1.5, where t = 2, 8, 16, 24 h, [MacroRAFT agent]0= 0.03 M and Mn of P(OEGMA) MacroRAFT = 10 kDa)

4.3.2. The Effect of Excess RAFT-Agent on Star Polymer Synthesis

In a typical star polymer synthesis, chain extension copolymerization of P(OEGMA) macroRAFT agents was carried out using BocAEAEMA monomer and disulfide crosslinker without adding excess RAFT agent. To investigate the effect of the addition of excess CPADB RAFT agent on star polymer synthesis two different polymerizations were performed using a [MacroRAFT Agent]:[Crosslinker]:[AIBN]:

[BocAEAEMA] mole ratio of 1:6:0.1:1.5 at a fixed P(OEGMA) macroRAFT agent concentration of 0.03 M, crosslinker concentration of 0.18 M, BocAEAEMA concentration of 0.045 M and a polymerization time of 24 h. While one of the polymerization mixtures did not contain any CPADB RAFT agent, the other contained CPADB RAFT agent at a CPADB RAFT agent to P(OEGMA) macroRAFT agent ratio of 0.25.

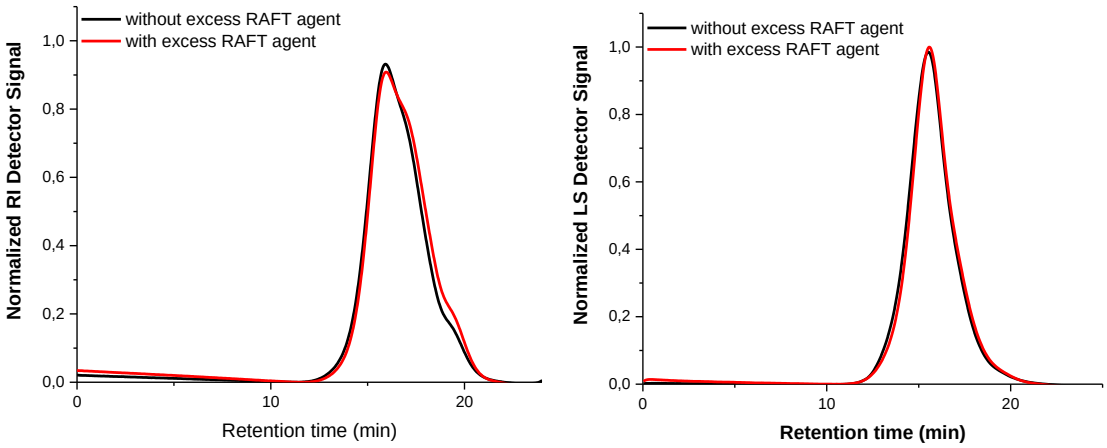

Figure 4.13. GPC-RI and GPC-LS traces of star polymers (MacroRAFT/Crosslinker/AIBN/BocAEAEMA= 1/6/0.1/1.5, where t = 24 h, $[\text{MacroRAFT Agent}]_0$= 0.03 M, M_n of MacroRAFT = 10 kDa. Excess CPADB RAFT agent was used at a RAFT Agent to MacroRAFT agent ratio of 0.25.)

After the reaction, the synthesized polymers were characterized by GPC and ^{1}H-NMR. The calculated conversions for both crosslinker and BocAEAEMA monomer were similar (Conversion of BocAEAEMA (%) = ~63 and Conversion of Crosslinker (%) = ~60). Also the gravimetric analysis demonstrated that the yield of the final product was nearly the same for both samples (~45 %) (Table 4.3).

The GPC traces (Figure 4.13) of both polymers revealed that while the molecular weight of both polymers were similar, the molecular weight distributions were slightly different. For the star polymer synthesized with no excess CPADB chain transfer agent, the polydispersity was 1.4, whereas for the star polymer synthesized with excess CPADB chain transfer agent, the polydispersity was higher (1.6). This result supports that the synthesis of star polymers via arm-first approach was indeed controlled by P(OEGMA) macroRAFT agents and the addition of the excess CPADB RAFT agents distorted the control over polymerization mechanism.

Table 4.3. Summary of the star polymer synthesis with and without excess RAFT agent (MacroRAFT/Crosslinker/AIBN/BocAEAEMA= 1/6/0.1/1.5, where t = 24 h, $[MacroRAFT\ Agent]_0$= 0.03 M, M_n of P(OEGMA) MacroRAFT = 10 kDa)

Excess CPADB RAFT agent to MacroRAFT agent Mole Ratio	Mw (kDa)[a]	PDI[a]	BocAEAEMA Conversion[b]	Crosslinker Conversion[b]	Final Polymer Yield[c] (%)
0.00	208	1.40	0.63	0.60	46.1
0.25	190	1.60	0.63	0.57	45.6

a: determined via GPC-LS b: calculated via Equation 4.4. c: Gravimetric Analysis

4.3.3. The Effect of Crosslinker/Monomer Ratio and Arm Length on Star Polymer Synthesis

The core-crosslinked star polymers were prepared using P(OEGMA) macroRAFT agents (i.e. arms) having two different molecular weights (M_n of 5 kDa and 10 kDa). In addition, in order to investigate the effect of crosslinker to monomer ratio on star polymer formation, crosslinker to MacroRAFT agent ratio (which was called as **X** throughout the study) were changed from 2 to 8 and monomer to MacroRAFT agent ratio (which was called as **Y** throughout the study) were changed from 1.5 to 8 , while the other conditions were kept constant (MacroRAFT/Crosslinker/AIBN/Monomer = 1/Crosslinker/0.1/ Monomer) in which $[MacroRAFT\ Agent]_0$= 0.03 M and the reaction time was 24 h. Branching points can be introduced into linear polymer chains with the employment of divinyl crosslinkers, but higher concentrations of divinyl crosslinkers can end up with the formation of macro-gels during polymerization reactions (Gao and Matyjaszewski, 2009; Ferreira et al., 2011). Therefore, crosslinker/monomer ratio was tried to be optimized using pre-arms having two different lengths.

First, the star polymers having P(OEGMA) pre-arms with a M_n of 10 kDa were prepared by varying crosslinker to monomer ratio. All polymers were characterized via GPC and ^{1}H-NMR. After purification, it can be seen from gravimetric analysis results (Figure 4.14) that as the ratio of crosslinker to MacroRAFT agent ratio (X) was decreased from 8 to 2 while Y was fixed at 1.5, the polymer yield dropped. As the ratio of

BocAEAEMA monomer to MacroRAFT agent (Y) was decreased from 8 to 1.5 while X was kept at 8, no significant change was observed in terms of the polymer yield.

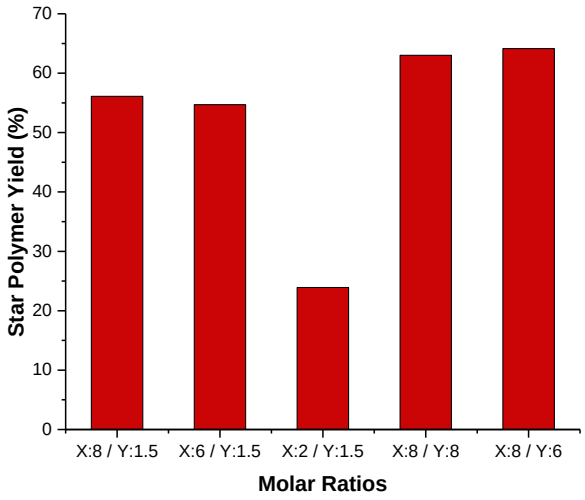

Figure 4.14. Gravimetric analysis for star polymers synthesized with a P(OEGMA) macroRAFT agent M_n of 10 kDa and varying X and Y where MacroRAFT/Crosslinker/AIBN/BocAEAEMA= 1/Crosslinker/0.1/BocAEAEMA, where X= Crosslinker/MacroRAFT agent, Y=BocAEAEMA/MacroRAFT agent and $[\text{MacroRAFT agent}]_0$= 0.03 M, polymerization time = 24 h

Conversions for BocAEAEMA monomer and crosslinker were also evaluated via ^{1}H-NMR spectroscopy (Figure 4.15). Increasing crosslinker conversion, but decreasing BocAEAEMA conversion was observed with increasing crosslinker to macroRAFT agent (X) ratio while BocAEAEMA monomer to macroRAFT agent ratio (Y) was kept fixed. In case of increasing BocAEAEMA monomer to macroRAFT agent ratio (Y) the exact opposite profiles were observed. In the RAFT polymerization, when good solvent is selected for polymerization of divinyl monomers, star polymer formation with broad PDI is more likely to occur since unreacted linear arms can be present (Zheng and Pan, 2005; Lord et al., 2003). In star polymerization, any propagating reaction will create linear chain radical or linear chain that have RAFT-end group. Hence, if poor solvent was chosen for divinyl crosslinker monomer, released polymer chains can remain in the core because of their aggregation within the selected solvent (Zheng et al. 2006). In this study, toluene was chosen as poor solvent for crosslinker which can be incompatible with medium and nanophase separation can occur. Hence, increasing crosslinker ratio can form self-organized, stable and rigid core that fragmentation reaction for BocAEAEMA can be competitive. Increasing BocAEAEMA ratio can overcome this issue but decreasing crosslinker conversions can reduce the probability to form stable core-crosslinked star

structures. Also, amphiphilic property can be weakening with perturbing the hierarchical morphology.

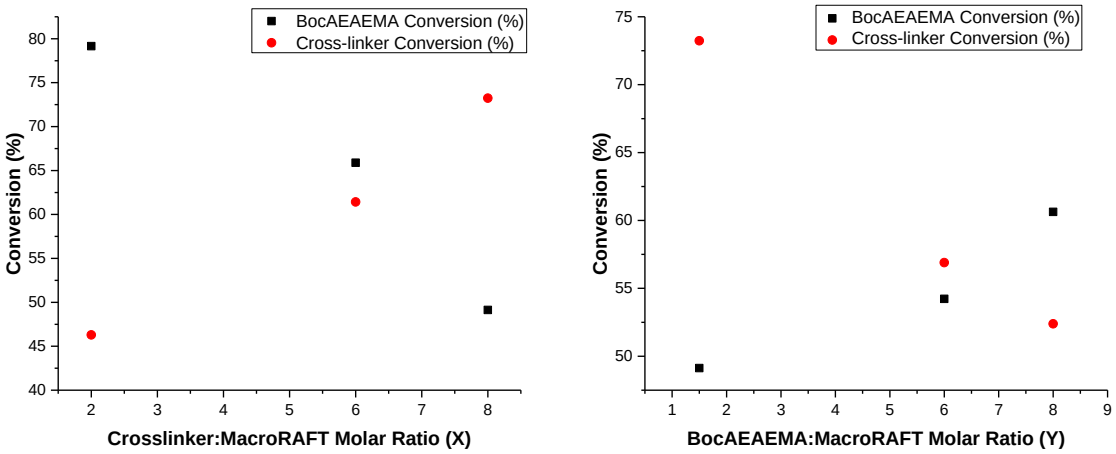

Figure 4.15. Crosslinker and BocAEAEMA conversions with respect to varying crosslinker to macroRAFT agent and BocAEAEMA to macroRAFT agent. The M_n of P(OEGMA) macroRAFT agent was 10 kDa.

In order to confirm proposed mechanism, GPC measurements were also used (Figure 4.16). It can be understood that increasing crosslinker to macroRAFT agent ratio caused increment in molecular weight and molecular weight distributions. In literature, similar results demonstrated that as the crosslinker ratios were increased, molecular weights and polydispersities were increased (Wei et al., 2014). In the star synthesis, random block polymerization occurred first and produced nano-sized micelles. Because of high crosslinker conversion, the diffusion of BocAEAEMA monomer - into that nano-sized structures can be restricted. This leads to compact core-crosslinked star polymers with high molecular weight and high polydispersity. As the crosslinker to macroRAFT agent ratio was decreased, optimal molecular weight distributions were obtained. Increasing BocAEAEMA monomer to macroRAFT agent ratio also caused increment in molecular weight distributions. In case of the highest BocAEAEMA to macroRAFT agent ratio (8/1) (X=8, Y=8), the shoulder at the lower retention times of GPC-RI traces was a proof that higher molecular weight polymeric chains were obtained. Also, GPC-LS traces of the same polymer evidenced that the molecular mass of polymer was beyond the separation range of GPC columns. Additionally, further increase in BocAEAEMA to macroRAFT agent ratio caused macro-gel formation. In the case of BocAEAEMA to macroRAFT agent ratio of 16/1, gelation was observed during polymerization.

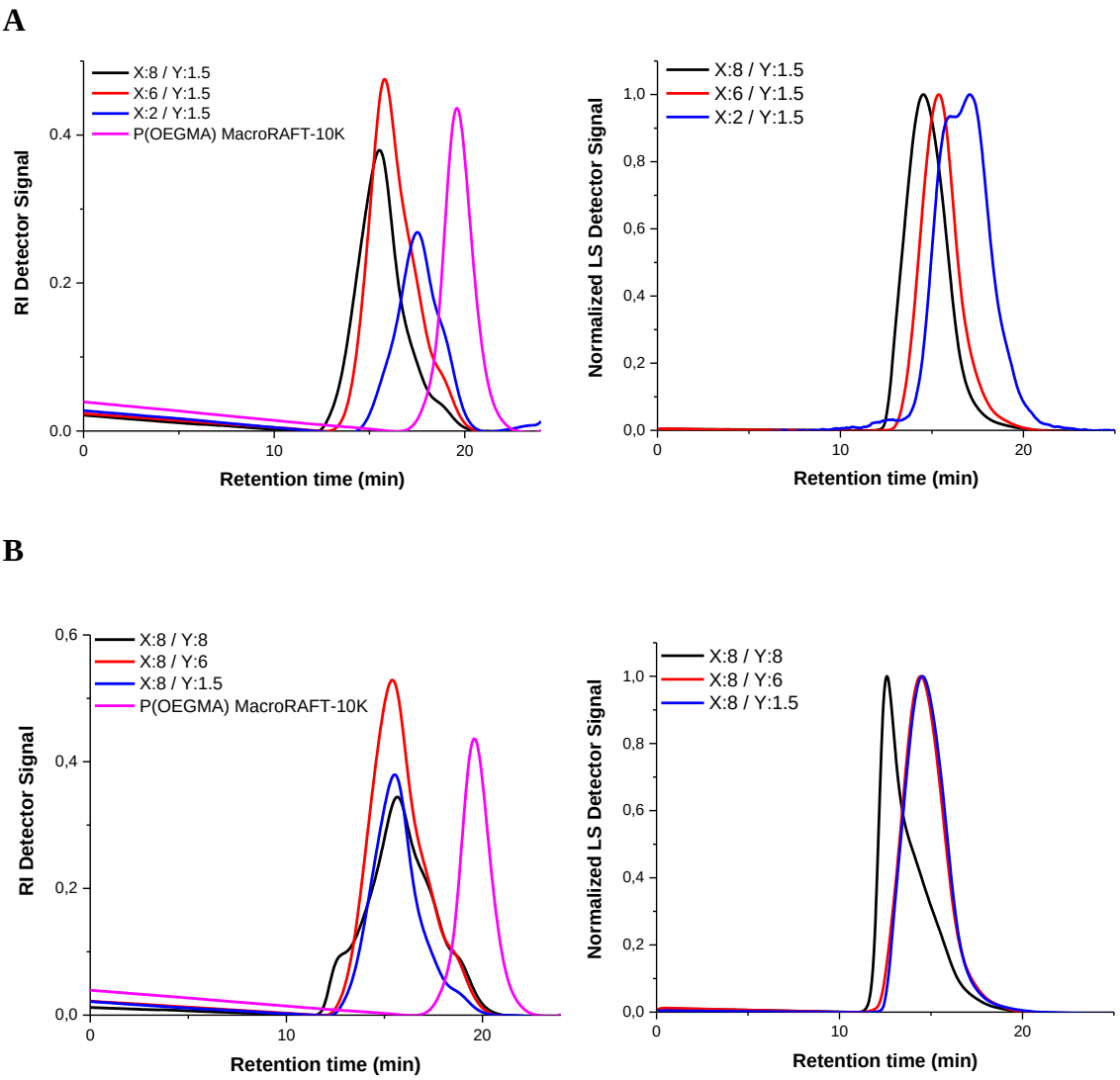

Figure 4.16. GPC-RI and GPC-LS traces for star polymers synthesized with varying crosslinker/MacroRAFT agent ratio (X) (A) and BocAEAEMA /MacroRAFT agent ratio (Y) (B) (MacroRAFT/Crosslinker/AIBN/BocAEAEMA = 1/Crosslinker/0.1/BocAEAEMA, where polymerization time= 24 h and $[\text{MacroRAFT agent}]_0$= 0.03 M. P(OEGMA) MacroRAFT agent with a M_n of 10 kDa was used.

Moreover, in literature, it was demonstrated that when the crosslinker to macroRAFT agent ratio was too low, amphiphilic block became too short that driving force to assemble into compact and stable star polymers cannot be provided. Hence, only branched polymers appeared without proper crosslinking. Also, when the crosslinker to macroRAFT agent ratio was too high, crosslinking reaction between separate star polymers was more likely to occur and this can cause broadening in molecular weights leading to higher polydispersities (Zhang et al., 2012). Similar trends can be seen in Table 4.4. When crosslinker to macroRAFT ratio (X) was 8:1 at a fixed BocAEAEMA to

macroRAFT ratio (Y) of 1.5:1, higher molecular weights with higher molecular weight distributions were observed. Also, when crosslinker ratio (X) was decreased to 2, polymers with decreasing molecular weight were obtained with lower polymer yields indicating that a high quantity of low molecular weight polymeric chains were removed during purification.

Table 4.4. Summary table for star polymers synthesized using P(OEGMA) macroRAFT agent with M_n of 10 kDa and varying X and Y

MacroRAFT/Crosslinker/AIBN/ BocAEAEMA mole ratio	Mw[a] (kDa)	PDI[a]	BocAEAEMA Conversion[b]	Crosslinker Conversion[b]
1/8/0.1/1.5	595	1.66	0.49	0.73
1/6/0.1/1.5	262	1.51	0.66	0.61
1/2/0.1/1.5	129	1.36	0.79	0.46
1/8/0.1/8	1193	5.00	0.60	0.52
1/8/0.1/6	385	2.04	0.54	0.57
1/8/0.1/1.5	595	1.66	0.49	0.73
1/8/0.1/16	*Gel formation was observed.*			

a: determined via GPC-LS b: calculated via Equation 4.4.

The molecular weight change with monomer and crosslinker conversion can be seen in Figure 4.17. To summarize, at a fixed monomer concentration, increasing crosslinker ratio can reduce the monomer conversion and lead to polymers with higher molecular weights and PDI. At a fixed crosslinker concentration, increasing BocAEAEMA ratio can increase BocAEAEMA conversion but leads to polymers with higher molecular mass and PDI, because of the fact that there is no controlled production of stable core-crosslinked star structures. Hence, it can be said that stable, low polydispersity star polymers can be prepared by using optimally low concentrations of both BocAEAEMA and crosslinker monomer.

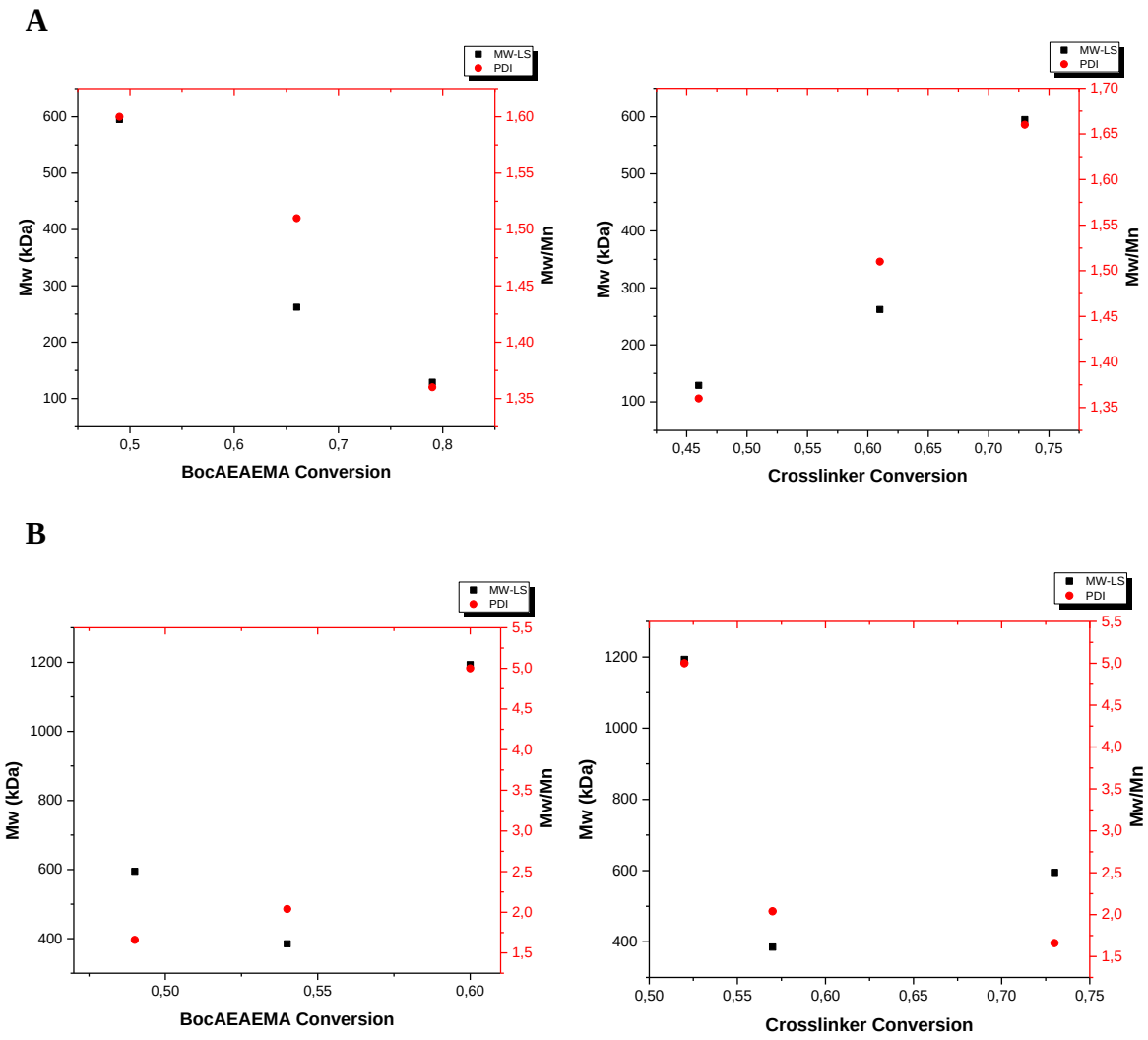

Figure 4.17. Plots of M_w (determined by GPC-LS) of star polymers with BocAEAEMA monomer and crosslinker conversions. P(OEGMA) macroRAFT agent with a M_n of 10 kDa was used by varying X (A) and Y (B) where X= Crosslinker/MacroRAFT agent, Y=BocAEAEMA/MacroRAFT agent mole ratio. $[\text{MacroRAFT agent}]_0$= 0.03 M, polymerization time = 24 h

Secondly, the star polymers having P(OEGMA) pre-arms with M_n of 5 kDa were prepared by varying crosslinker to macroRAFT agent (X) and BocAEAEMA monomer to macroRAFT agent (Y) ratios. The gravimetric analysis for these star polymers showed almost the same trends with the star polymers having P(OEGMA) pre-arms with M_n of 10 kDa arms. As the crosslinker to macroRAFT ratio (X) was decreased, the amount of final product also decreased (Figure 4.18).

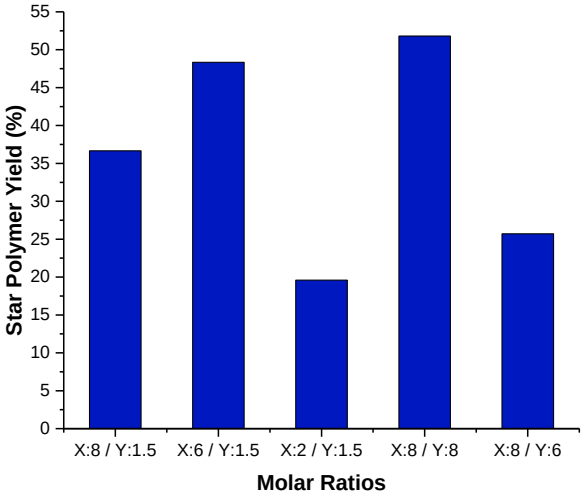

Figure 4.18. Gravimetric analysis for star polymers synthesized using P(OEGMA) macroRAFT agent with M_n of 5 kDa and varying X and Y

BocAEAEMA monomer conversions increased as increasing BocAEAEMA to macroRAFT agent ratio and decreasing crosslinker to macroRAFT agent ratio were used. Besides, crosslinker conversions were increased as increasing crosslinker to macroRAFT agent ratio and decreasing BocAEAEMA monomer ratio similar to star polymers having P(OEGMA) pre-arms with M_n of 10 kDa arms (Figure 4.19).

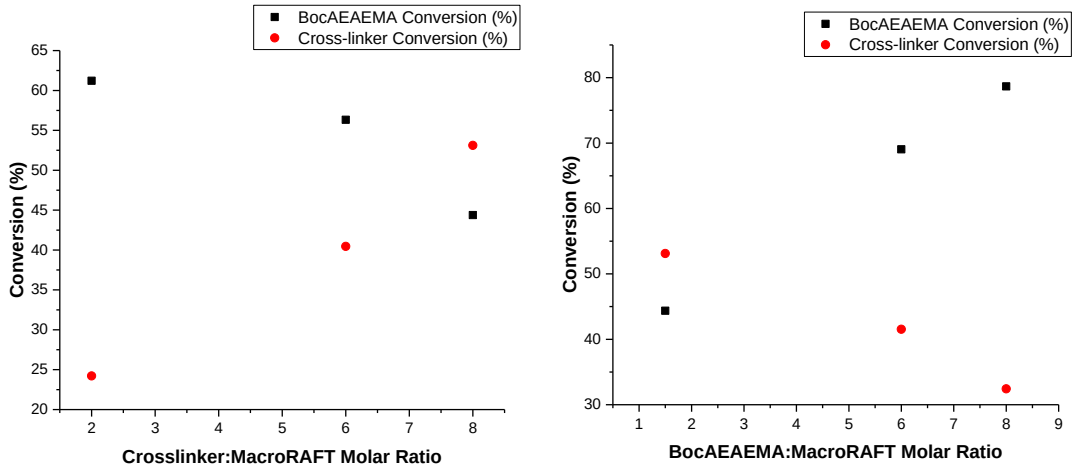

Figure 4.19. Crosslinker and BocAEAEMA conversions with respect to varying crosslinker to macroRAFT agent and BocAEAEMA to macroRAFT agent. The M_n of P(OEGMA) macroRAFT agent was 5 kDa.

When GPC traces of polymers were evaluated (Figure 4.20), it was seen that the increment in crosslinker to macroRAFT agent ratio (X) led to polymer having broad molecular weight distribution. This was attributed to the higher mobility of shorter arm lengths and the less steric hindrance resulting in the incorporation of more arms (Learsh and Miyake, 2018). Decreasing of arm molecular weight (shorter arm length) causes

increased branch density which means increase in arm number per core of star polymer and number of arm chains extending from core influence the star-star coupling interactions since high number of arm means high number of end-group present in the star polymer structure (Goh et al., 2008). This effect was also supported by the GPC traces of polymers in which BocAEAEMA to MacroRAFT agent ratio (Y) was increased from 1.5 to 8. The shoulder at low retention times (GPC-RI) was an indication of some coupling reaction leading to significantly larger molecular weight distribution values.

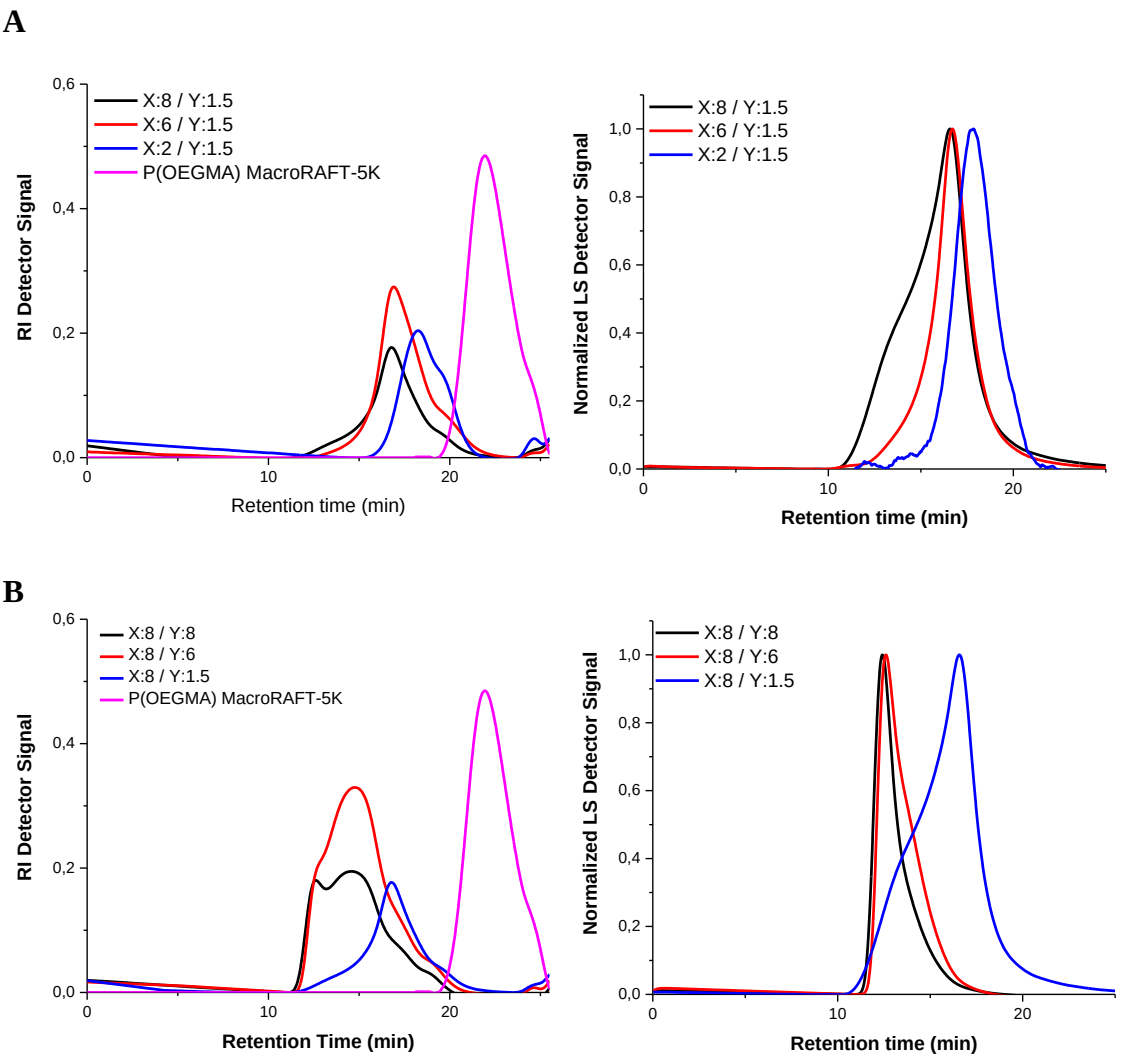

Figure 4.20. GPC-RI and GPC-LS traces for star polymers synthesized with varying crosslinker/MacroRAFT agent ratio (X) (A) and BocAEAEMA /MacroRAFT agent ratio (Y) (B) (MacroRAFT/Crosslinker/AIBN/BocAEAEMA=1/Crosslinker/0.1/BocAEAEMA where polymerization time= 24 h and $[\text{MacroRAFT agent}]_0$= 0.03 M. P(OEGMA) MacroRAFT agent with a M_n of 5 kDa was used.

The use of shorter arms can cause higher arms per star with higher molecular mass because of faster diffusion of short arm chains without steric bulk effect. As can be seen

in Table 4.5. Larger molecular mass of polymers was obtained compared to the star polymers synthesized with P(OEGMA) pre-arms having M_n of 10 kDa arms at the same conditions.

Table 4.5. Summary table for star polymers synthesized using a P(OEGMA) macroRAFT agent with M_n of 5 kDa and X and Y where X= Crosslinker/MacroRAFT agent, Y=BocAEAEMA/MacroRAFT. $[MacroRAFT\ agent]_0$= 0.03 M, polymerization time = 24 h

MacroRAFT/Crosslinker/AIBN/ BocAEAEMA mole ratio	Mw[a] (kDa)	PDI[a]	BocAEAEMA Conversion[b]	Crosslinker Conversion[b]
1/8/0.1/1.5	1186	1.38	0.44	0.53
1/6/0.1/1.5	344	1.35	0.56	0.40
1/2/0.1/1.5	93	1.33	0.61	0.24
1/8/0.1/8	3370	3.44	0.78	0.32
1/8/0.1/6	1868	3.21	0.69	0.41
1/8/0.1/1.5	1186	1.38	0.44	0.53
1/8/0.1/16	*Gel formation was observed.*			

a: determined via GPC-LS b: calculated via Equation 4.4.

The molecular weight (Mw by GPC-LS) versus BocAEAEMA monomer and crosslinker conversion plots can be seen in Figure 4.21. The same results with the star polymers having P(OEGMA) arms with a M_n of 10 kDa were obtained. Briefly, low polydispersity star polymers can be prepared by using optimally lower concentrations of both BocAEAEMA and crosslinker monomer to the macroRAFT agent.

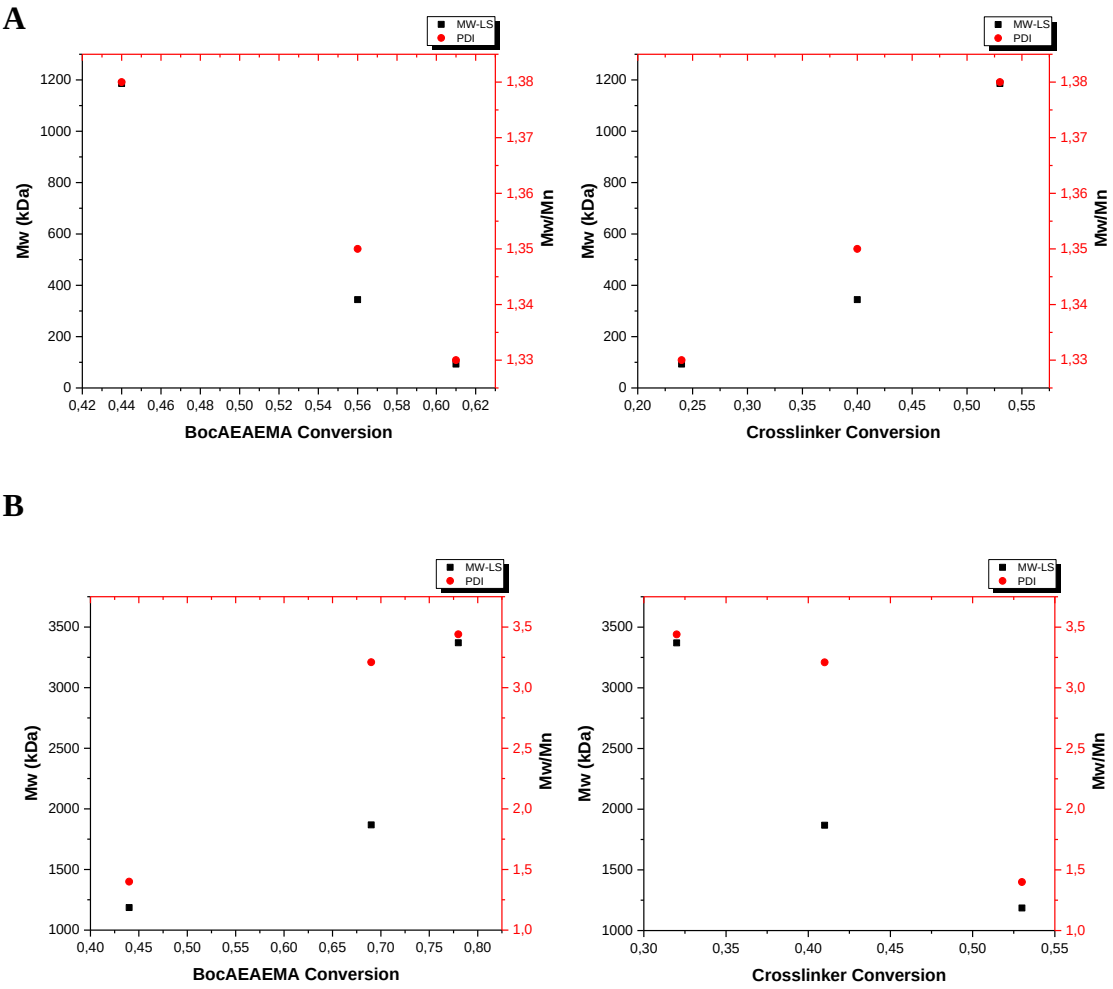

Figure 4.21. Plots of M_w (determined by GPC-LS) of star polymers using a P(OEGMA) macroRAFT agent with a M_n of 5 kDa varying X (A) and Y (B) where X= Crosslinker/MacroRAFT agent, Y=BocAEAEMA/MacroRAFT agent. $[MacroRAFT\ agent]_0$= 0.03 M, polymerization time = 24 h

4.3.4. Deprotection of P(BocAEAEMA) Core of Star Polymers

In order to make the star polymers cationic, BocAEAEMA monomer was used. However, primary and secondary amine containing monomer was protected with Boc-groups and these groups must be removed for further use of amine groups of the star polymers. The star polymers were deprotected by treatment of trifluoroacetic acid for 30 minutes at ambient temperature. After the deprotection reaction, polymers were analyzed via ^{1}H-NMR. It must be emphasized that for the characterization via NMR, polymers were dissolved in D_2O not in $CdCl_3$ because of altered solubility of polymers with

enhanced polarity after removal of Boc- groups. According to ^{1}H-NMR spectrum of star polymers after deprotection (Figure 4.22), the disappearance of the characteristic peak of Boc- groups located at 1.47 ppm was the evidence of complete deprotection and formation of p(AEAEMA) within the star core.

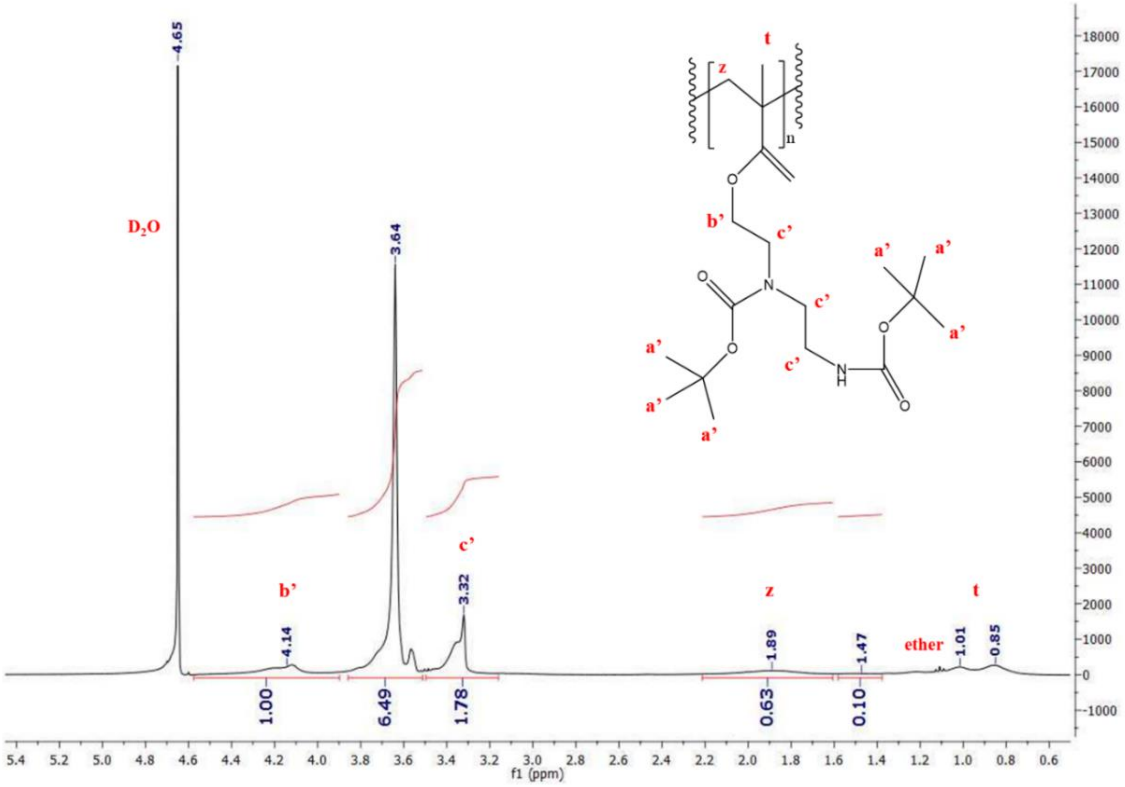

Figure 4.22. Representative ^{1}H-NMR spectrum of star polymers after removal of Boc-groups (MacroRAFT/Crosslinker/AIBN/BocAEAEMA = 1/6/0.1/1.5, where t = 24 h and [MacroRAFT agent]0= 0.03 M, P(OEGMA) MacroRAFT agent with a Mn of 10 kDa was used.

4.3.5. Determination of Hydrodynamic Size and Degradation Profiles of Star Polymers

In the synthesis of star polymers, disulfide containing di-vinyl crosslinker was used for obtaining a bio-cleavable core structure. Hence, DLS experiments were carried out before and after cleavage of disulfide bonds to determine the change in the hydrodynamic size of star polymers as the formation of smaller unimers after the degradation of disulfide bonds were expected. Firstly, control experiments were performed to test the reducing agent activities using an organic solvent-soluble disulfide

compound, dithiodipyridine (DTP) via UV-Visible spectrophotometer. If the reducing agents can break the disulfide bonds in DTP, 2-pyrdinethione can form which results in the UV absorption at 370 nm. Triphenylphospine (3PHEp) as a reducing agent soluble in organics was first used to degrade DTP in THF (Figure 4.23). Accordingly, the formation of 2-pyrdinethione was seen as time passed. Also, visual comparison has shown that DTP solution turned from colorless to yellowish solution with time indicating the formation of 2-pyridinethione.

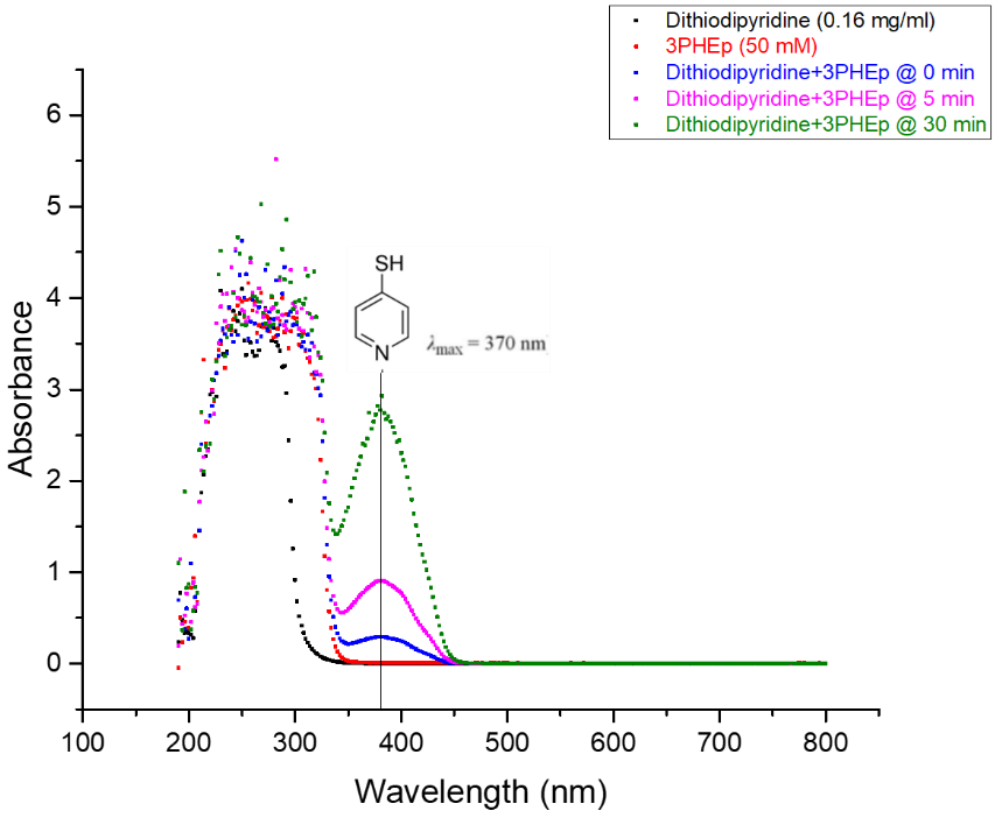

Figure 4.23. UV-visible spectrophotometer result for reducing DTP using triphenylphosphine (solvent: THF)

After that, tris(2-carboxyethyl) phosphine hydrochloride (TCEP) as a reducing agent soluble in water was used to reduce DTP in THF/water (50/50) solution (Figure 4.24). As a visual comparison, the formation of 2-pyrdinethione can be seen just after the addition of TCEP to the solution and this result can be supported by UV-visible spectrophotometer result presented in Figure 4.24.

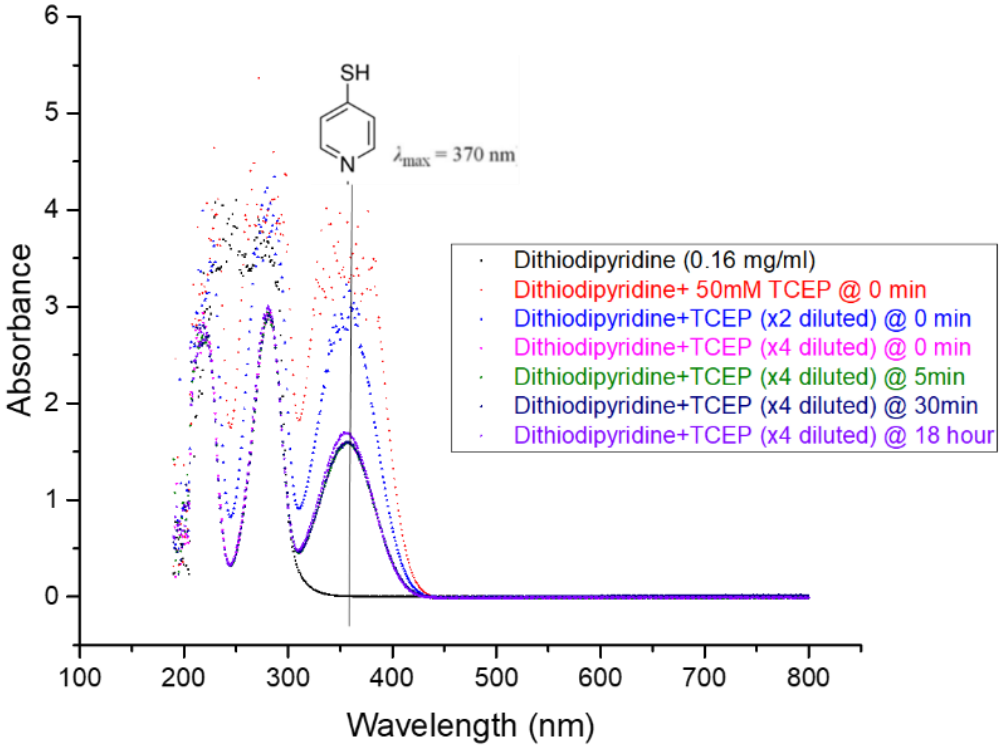

Figure 4.24. UV-visible spectrophotometer result for reducing of DTP with TCEP (Solvent: 50/50 = THF/water)

After ensuring that both reducing agents can actively break disulfide bonds in the structure of DTP, these agents were used for cleaving disulfide containing star polymers. Since polymers before deprotection of amine groups were only soluble in organic such as THF, the Boc-protected star polymers were first dissolved in THF and hydrodynamic sizes were evaluated. The measurements were repeated three times. After the addition of 3PHEp reducing agent into polymer solution and incubation for t=0, 5 min, 30 min and 18 hours, the hydrodynamic sizes were also evaluated for three times (Figure 4.25). Accordingly, the number-average hydrodynamic size of star polymers (which was around 7 nm) was dropped to around 2 nm with time indicating that the degradation of the disulfide bonds in the core of star polymers, resulting in the formation of unimeric arms took place.

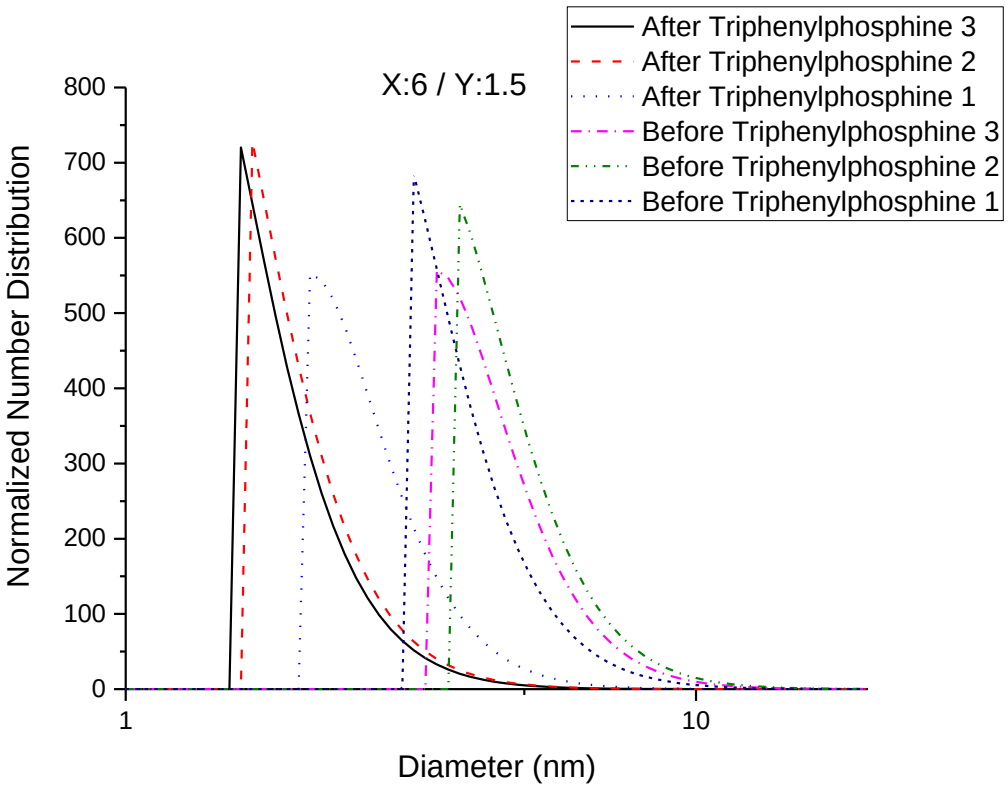

Figure 4.25. Representative DLS results for star polymers (synthesized using a MacroRAFT/Crosslinker/AIBN/BocAEAEMA mole ratio of 1/6/0.1/1.5, t= 24hr and [MacroRAFT agent]$_0$= 0.03 M and M_n of MacroRAFT= 5 kDa) before and after treatments with triphenylphosphine in THF for 1 h

Since the star polymers, after the removal of Boc- deprotection groups, gained water-solubility, the degradation profiles were investigated using water-soluble reducing agent TCEP. Polymers were dissolved in water and the hydrodynamic diameters were evaluated with three replicates before and after the addition of TCEP (Figure 4.26). It can be seen in the figure that while the number-average hydrodynamic diameter of the star polymer before TCEP addition was around 35 nm, after the addition of the reducing agent and reaction for 1 hours, polymer hydrodynamic size dropped to 7-8 nm indicating the cleavage of the core and the release of unimeric chains into solution.

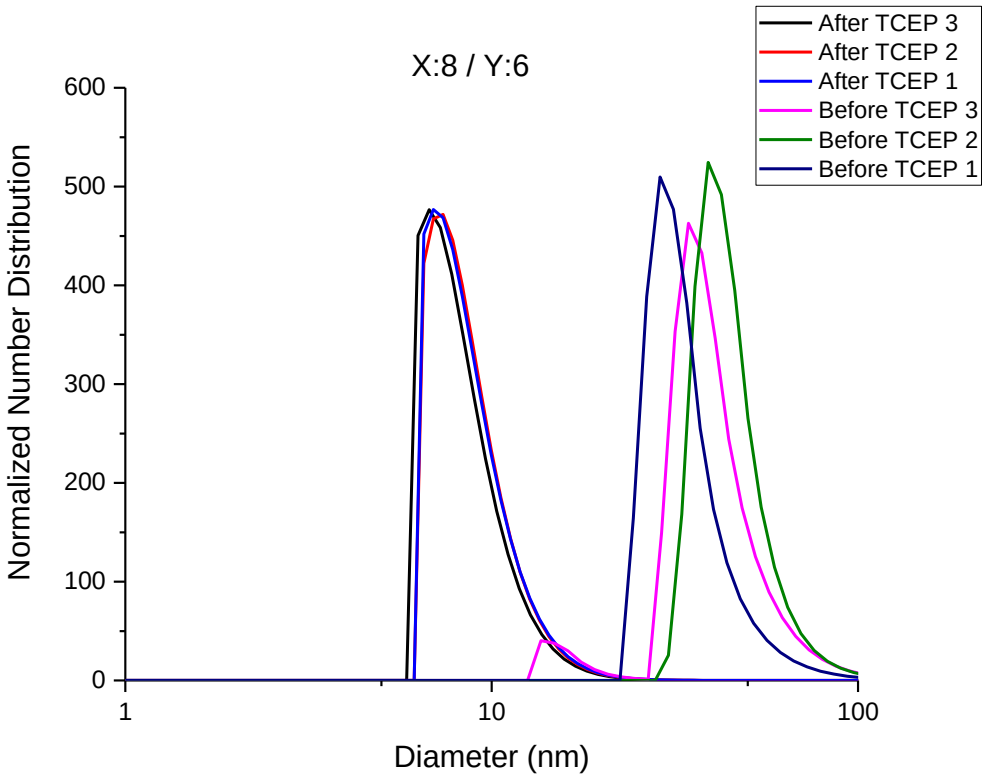

Figure 4.26. Representative DLS results for deprotected star polymers (synthesized using a MacroRAFT/Crosslinker/AIBN/BocAEAEMA mole ratio of 1/8/0.1/6, where t= 24hr, $[\text{MacroRAFT agent}]_0$= 0.03 M and M_n of MacroRAFT=5 kDa) before and 1 h-after treatment with TCEP in water.

A summary table of hydrodynamic sizes of star polymers before and after reducing agent addition was presented in Table 4.6. In this table, the hydrodynamic sizes of certain polymers were not determined due to solubility problems in water. The polymers with solubility problems were the ones synthesized with P(OEGMA) pre-arms of 5 kDa and a BocAEAEMA: macroRAFT agent mole ratio of 1.5/1 or 8/1 at a crosslinker/macroRAFT agent mole ratio of 8/1. it is expected that the star polymers with shorter hydrophilic arm-lengths can ended up with larger agglomerates and weaker polarity. Nevertheless, all other polymers showed degradation with decreasing sizes of polymers after reducing agent (TCEP) addition. The formation of broad molecular weight star polymers was also supported by increment in hydrodynamic sizes. Also, several studies in which the same degradation profiles were observed after the addition of suitable reducing agent reported in the literature (Ferreira et al., 2011; Rosselgong et al., 2013; Wei et al., 2014).

Table 4.6. Number-based average hydrodynamic diameter values (D_{avg}) of different star polymers before and after treatment with TCEP in water. The polymers (4 mg/ml) were treated with TCEP (50 mM) for one hours.

MacroRAFT/Crosslinker/ AIBN/BocAEAEMA mole ratio used for polymer synthesis	MacroRAFT M_n[a] (kDa)	M_w[b] (kDa)	PDI[b]	D_{avg}[c] (nm)	D_{avg}[d] (nm)
1/8/0.1/1.5	10	595	1.66	27 ± 5	18 ± 0.95
1/6/0.1/1.5	10	262	1.51	7 ± 0.87	1.2 ± 0.07
1/2/0.1/1.5	10	129	1.36	2 ± 0.05	1.35 ± 0.35
1/8/0.1/8	10	1193	5.00	21 ± 9	17.5 ± 6
1/8/0.1/6	10	385	2.04	3.4 ± 0.66	1.7 ± 1
1/8/0.1/1.5	5	1186	1.38	nd	nd
1/6/0.1/1.5	5	344	1.35	26.3 ± 8	4.2 ± 3
1/2/0.1/1.5	5	93	1.33	1.7 ± 0.9	nd
1/8/0.1/8	5	3370	3.44	nd	nd
1/8/0.1/6	5	1868	3.21	35.8 ± 5	7.8 ± 0.17

a: determined via GPC-RI b: determined via GPC-LS c: determined via DLS in water before degradation d: determined via DLS in water after degradation

4.3.6. Determination of Arm Number of Star Polymers

The arm number of star polymers is also an important parameter for both synthesis and function of star polymers. The number of arms incorporated to the star structure is important in terms of star synthesis as it directly affects the star polymer yield. In this study, the main aim of using P(OEGMA) arms was to shield the cationic charge of the core and potentially make the surface of polymer-siRNA complex nanoparticles neutral and hydrophilic considering the possible use of cationic star polymers as siRNA carriers However, while incorporation of P(OEGMA) arms can be beneficial in terms of charge shielding and providing stealth charactered, incorporation of large number and/or longer P(OEGMA) arms into star structure can be disadvantageous for complexation of siRNA, lowering or even completely hindering the interaction between the cationic core and siRNA molecules. Hence, it was necessary to investigate the number of arms incorporated

into star polymers synthesized. The average number of arms incorporated into the star polymers (N_{arm}) was calculated by using Equation 4.5 (McKenzie et al., 2015; Uchiyama et al., 2017).

$$N_{arm}=\frac{WF_{arm} \times M_w^{CCS}}{M_n^{arm}} \quad (4.5)$$

where $M_{w,\,CCS}$= core-crosslinked star polymer molecular weight determined via GPC-LS and $M_{n,arm}$= P(OEGMA) molecular weight determined via GPC-RI, WF_{arms}= weight fraction of arms in the star polymer, calculated from Equation 4.6.

$$WF_{arm}=\frac{m_{CCS}-(m_{cross\text{-}linker}\times X_c + m_{BocAEAEMA}\times X_b)}{(m_{cross\text{-}linker}\times X_c + m_{BocAEAEMA}\times X_b)+m_{arm}} \quad (4.6)$$

where the conversion of cross-linker and BocAEAEMA, X_c and X_b respectively, were determined by ^{1}H NMR spectroscopic analysis, m_{CCS} was determined via gravimetric analysis. m_{arm}, $m_{cross\text{-}linker}$ and $m_{BocAEAEMA}$ are the amount (in mg) of the arm, cross-linker and BocAEAEMA monomer employed in the star synthesis. The calculated arm numbers of synthesized star polymers can be seen in Table 4.7.

Table 4.7. The arm numbers of star polymers synthesized in this study. The arm numbers were calculated using Equation 4.5

MacroRAFT/Crosslinker/AIBN/BocAEAEMA mole ratio used to synthesize star polymer	MacroRAFT M_n (kDa)[a]	M_w[b] (kDa)	PDI[b]	**N_{arm}[c]**	**D_{avg}[d] (nm)**
1/8/0.1/1.5	10	595	1.66	25	27 ± 5
1/6/0.1/1.5	10	262	1.51	12	7 ± 0.87
1/2/0.1/1.5	10	129	1.36	5	2 ± 0.05
1/8/0.1/8	10	1193	5.00	43	21 ± 9
1/8/0.1/6	10	385	2.04	15	3.4 ± 0.6
1/8/0.1/1.5	5	1186	1.38	nd	nd
1/6/0.1/1.5	5	344	1.35	47	26.3 ± 8
1/2/0.1/1.5	5	93	1.33	12	1.7 ± 0.9
1/8/0.1/8	5	3370	3.44	nd	nd
1/8/0.1/6	5	1868	3.21	nd	nd

a: determined via GPC-RI b: determined via GPC-LS c: calculated via Equation 4.5. d: determined via DLS in water before degradation

As can be seen in Table 4.7, as the crosslinker: macroRAFT agent ratio increased when both P(OEGMA)s having Mn of 5kDa and 10kDa were used, the number of arms incorporated into star structure increased. This is expected since the pre-arms are joined through crosslinking to form star structures and increased number of crosslinker molecules increases the crosslinking reactions. On the other hand, the effect of increasing the BocAEAEMA monomer/macroRAFT agent ratio could not be determined clearly. In the case of P(OEGMA) 5 kDa pre-arms were used, the polymers could not be analysed as they had solubility issues. In the case of P(OEGMA) 10 kDa pre-arms were used, the number of arms seemed to decrease from 43 to 15 with a decrease of BocAEAEMA monomer/macroRAFT agent ratio from 8 to 6. However, when the ratio was further decreased to 1.5, the number of arms incorporated increased to 25. This may be attributed to the crosslinker/macroRAFT agent ratio of 8, which might be high enough to cause star-star coupling reactions in the absence of sufficient amount of BocAEAEMA monomer, leading to an increase in the apparent number of arms of star polymers. The highest arm number of arms (N_{arm} = 47) was obtained for star polymers of P(OEGMA) 5 kDa macroRAFT agent using a macroRAFT agent/crosslinker/BocAEAEMA mole ratio of 1:6:1.5. This might be due to the effect of several parameters including the higher mobility and less steric hindrance of shorter chain pre-arms, star-star coupling reactions due to the formation of larger cores. As it can be seen further in Table 4.7, as the arm number of star polymers increased, the hydrodynamic radius in water also increased as expected.

4.3.7. Investigation of Complex Formation of Star Polymers with siRNA

Electrostatic complexes of star polymers with siRNA were prepared using selected star polymers as presented in Table 4.8. To investigate the formation of complexes, agarose gel electrophoresis was used. Briefly, star polymers (dissolved in ultrapure water where pH was 6) (for N/P=200; 13.4 μg/μL for Star 1, 68.3 μg/μL for Star 2, 28.7 μg/μL for Star 3) and siRNA (dissolved in ultrapure water) (0.01 nmol/μL) were used. Star polymers were mixed with siRNA (0.02 nmol for each) at different nitrogen/phosphate (N/P) ratios (1, 25, 100, 200) and incubated at ambient temperature for approx. 45 minutes.

Table 4.8. The properties of star polymers used for siRNA complexation

Polymer Code	MacroRAFT/Crosslinker/AIBN/BocAEAEMA	MacroRAFT M_n[a] (kDa)	M_w[b] (kDa)	PDI[b]	$M_{w,after\ deprotection}$ (kDa)[c]	N_{arm}[d]	M_w for P(AEAEMA) (kDa)[e]	DP[f]
Star 1	1/6/0.1/1.5	10	190	1.60	150	14	42	244
Star 2	1/6/0.25/1.5	10	77	1.65	71	7	5	30
Star 3	1/6/0.25/3	10	81	1.70	70	7	14	70

a: determined via GPC-RI b: determined via GPC-LS c: calculated theoretically considering 100% removal of Boc-protection groups d: calculated via Equation 4.5. e: $M_{w\ for\ P(AEAEMA)} = M_{w,after\ deprotection} \times WF_{core} \times Conversion_{BocAEAEMA}$ (%) f: Degree of polymerization (DP) = $M_{w\ for\ P(AEAEMA)} / M_{w\ for\ AEAEMA}$ (where $M_{w\ for\ AEAEMA}$ = 172 g/mol)

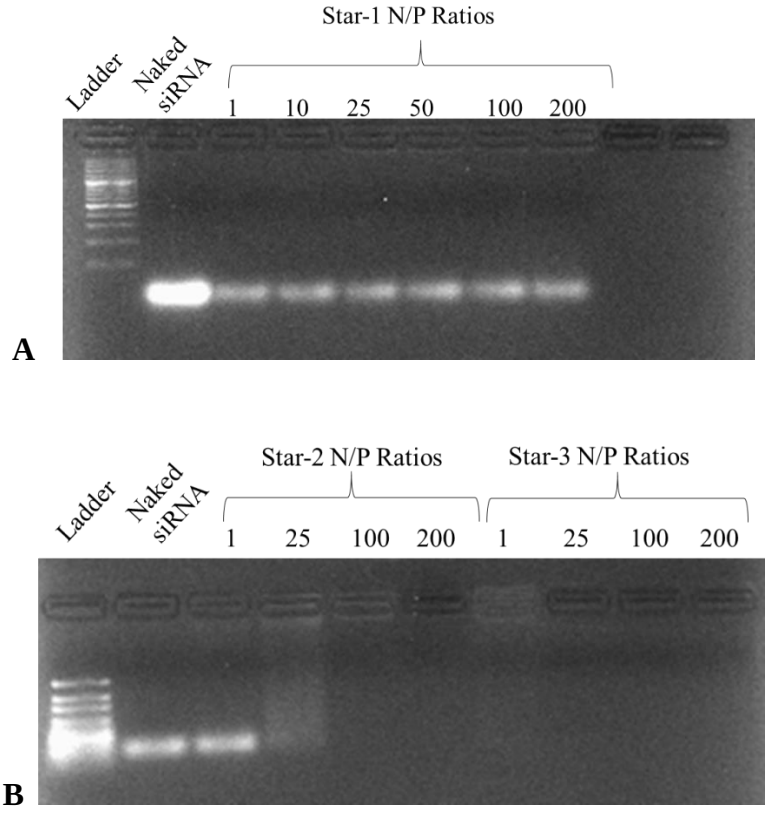

Figure 4.27. Agarose gel electropherogram of Star 1-siRNA complexes (A), Star 2-siRNA and Star 3-siRNA complexes (B), comparison of all complexes (C) at varying nitrogen/phosphate (N/P) ratios.

(Cont. on next page)

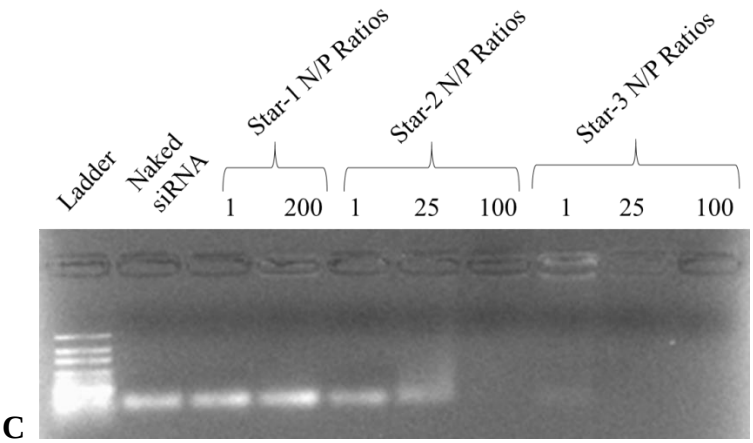

C

Figure 4.27. (Cont.)

According to Figure 4.27, for Star-1 which has the highest number of arms (14) and the largest cationic core showed no siRNA binding efficiency. This can be because of steric hindrance effect of POEGMA, preventing negatively charged siRNA molecules to reach into the cationic core of star molecules. Interestingly, Star 2 having 7 arms and the smallest cationic core (5 kDa AEAEMA) showed efficient complexation when N/P ratios were higher than 25 (at N/P=25, there was still a smear indicating insufficient complexation) with a complete disappearance of siRNA bands on the gel. On the other hand, Star 3 with the same number of arms (N_{arms}= 7) but with larger cationic core showed complexation at an N/P ratio of 1 with almost complete disappearance of siRNA band on gel. siRNA band appeared to stay in the well at N/P ratio of 1. Hence, it can be proposed that with decreasing number of arms, there was a high probability for complexation and this effect can be reinforced with the effect of larger cationic core of star molecules. In other words, incorporation of high number of arms caused negative effect and siRNA binding was hindered. Low number of arms with higher cationic core has led to efficient complexation even at the low ratios of polymer to siRNA. It should also be stated that there is a delicate balance between the number of arms and the quantity of cationic moieties of the star polymers, need to be optimized for efficient complexing with siRNA molecules.

4.3.8. Investigation of *In Vitro* Cytotoxicity

Finally, the effects of star polymers on cell viability was also investigated via MTT assay using human breast cancer cell line (MDA-MB-231-luc2-GFP). Polymers used for siRNA complexation have been used. The properties of these polymers were given in Table 4.8. Polymers at varying concentrations were incubated with the cells for 24 hours and MTT assay was performed to determine the cell viability.

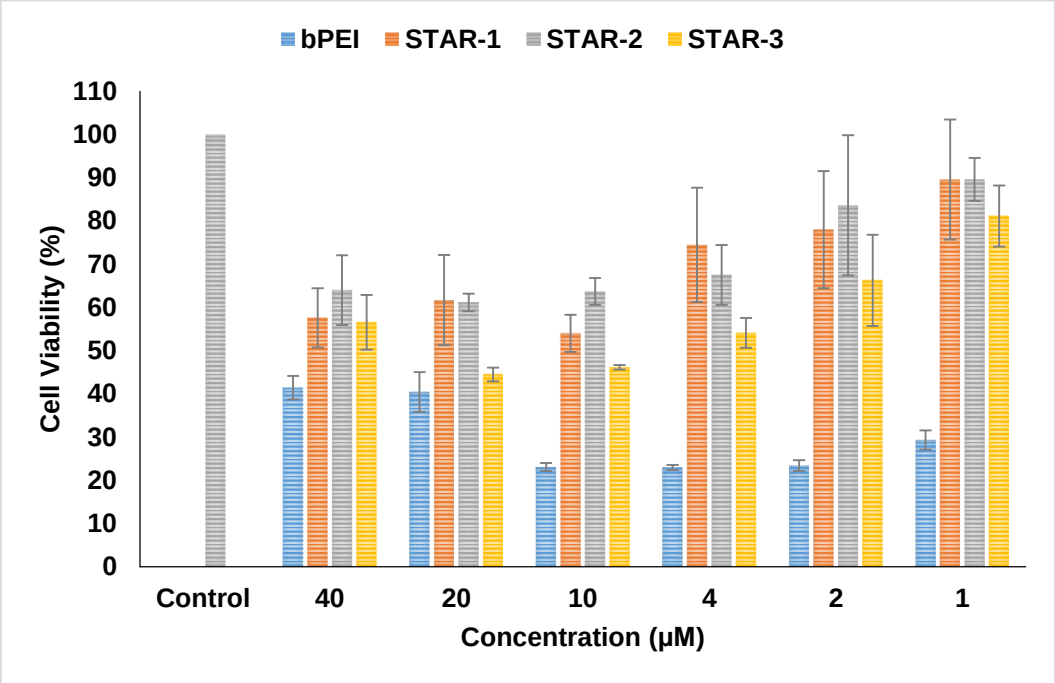

Figure 4.28. Viability of A549 cells after incubation with Star-1, Star-2, Star-3 and bPEI (25 kDa) for 24 h. Control is the cells with no treatment (n=4)

As it can be seen from Figure 4.28. that star polymers showed less toxicity compared to branched PEI at all concentrations tested. This was attributed to the presence of non-toxic P(OEGMA) arms surrounding the cationic core of star polymers. Among all three different star polymers tested, Star 3 which has the arm number of 7 and larger cationic core showed the highest toxicity, probably due to the higher cationic charge density. It is well-known in literature that as cationic charge density increases, cytotoxicity increases. Nevertheless, Star 3 along with other star polymers were significantly less toxic compared to PEI which is a golden standard cationic polymer for siRNA delivery.

CHAPTER 5

CONCLUSION

The aim of this master thesis is to synthesize cleavable, core-crosslinked, cationic, new star polymers via RAFT polymerization as potential siRNA carrier systems. The star polymers were designed to have a protonable and biodegradable central branching point (core) where hydrophilic P(OEGMA) chains (arms) emanating from. Accordingly, linear polymers of oligoethylene glycol methacrylate (M_n: 450 g/mol) P(OEGMA) with varying molecular weights (between 5 kDa and 10 kDa) were first synthesized. Afterwards, the biodegradable crosslinker, bis(2-methacryloyl) oxyethyl disulfide, and BocAEAEMA monomer were polymerized with the employment of P(OEGMA) macroRAFT agents as chain transfer agents. BocAEAEMA was used as a monomer to synthesize cationic star polymers for the first time in the literature as this monomer possess primary and secondary amines which are well-suited for electrostatically complexing with nucleic acids at nearly neutral pH and also protonable over a pH range existing in the endocytic pathway. Toluene was used as a polymerization solvent since it was a poor solvent for the crosslinker, facilitating the formation of star polymers.

The kinetics of star polymer synthesis via RAFT polymerization were first investigated at a macroRAFT agent concentration of 0.03 M and a MacroRAFT agent/Crosslinker/Initiator/BocAEAEMA mole ratio of 1/8/0.1/1.5. Polymerization times were varied (t= 2, 8, 16 and 24 h). After 2 h of polymerization, the BocAEAEMA and crosslinker conversions reached around 34%. However, when the polymerization time extended, there was a linear increase in both crosslinker and BocAEAEMA conversions ($[M]_0/[M]$) with time indicating RAFT controlled polymerization mechanism. Gravimetric analysis results showed that while star polymer yield was only 32% after 2 h of polymerization, the yield at 8, 16 and 24 h of polymerization reached a constant value, approximately 55%. This indicated that the incorporation of arms into star structures completed between 2 and 8 hours of polymerization. Moreover, as polymerization time was increased, molecular weight distributions significantly narrowed (PDI = 1.80 for t = 2 h and PDI = 1.52 for t = 24 h). The lowest PDI (1.52) of star polymers was obtained for 24 h reaction time with the highest final product efficiency, molecular

weight and monomer conversions (yield: 54%, Mw=620 kDa, BocAEAEMA Conversion=0.71 and Crosslinker conversion=0.62).

The effect of the ratio of crosslinker to MacroRAFT agent (X) (which was varied from 2 to 8), the ratio of BocAEAEMA monomer to MacroRAFT agent (Y) (which was varied from 1.5 to 8) and the length of P(OEGMA) macroRAFT agent (5 kDa and 10 kDa) on star polymer formation were investigated using the same initial conditions where $[\text{MacroRAFT Agent}]_0$ and the polymerization time were 0.03 M and 24 h, respectively. The polymerization solvent was toluene which was expected to cause nano-phase separation because of its poor solvation effect on divinyl crosslinker. Accordingly, it was shown that increasing X led to increasing crosslinker conversion with the formation of more self-organized, stable and rigid core in which fragmentation reactions for BocAEAEMA monomer was competitive, hence polymerization resulted with the decreasing BocAEAEMA conversion. Additionally, the highest ratio of X (8) led to the formation of compact core-crosslinked star polymers with higher arm incorporation and molecular weight for both lengths of P(OEGMA) linear arms (595 kDa stars with 10 kDa arms and 1186 kDa stars with 5 kDa arms), when compared with the star polymers synthesized at the lowest X (2) (129 kDa for 10 kDa arms and 93 kDa for 5 kDa arms).

On the other hand, increasing the Y led to increasing BocAEAEMA conversion while decreasing crosslinker conversion. Hence, the polymerization ended up with the formation of branched polymers with broader molecular weights (1193 kDa and PDI of 5.00 for 10 kDa P(OEGMA) arms; and 3370 kDa and PDI of 3.44 for 5 kDa P(OEGMA) arms) without proper crosslinking and controlled synthesis of star polymers. This was attributed to the competition of the crosslinker and BocAEAEMA monomer during polymerization and also loosening amphiphilic block property of the chains because of the decreased conversion of the crosslinker.

Interestingly, the use of shorter linear arms as P(OEGMA) macroRAFT agents (5 kDa) led to a dramatic increase in molecular weights of star polymers (e.g. up to 3370 kDa where $[\text{MacroRAFT agent}]_0$ = 0.03 M, polymerization time was 24 h, macroRAFT/Crosslinker/AIBN/BocAEAEMA ratio= 1/8/0.1/8) when compared to star polymers synthesized with longer arm chains (10 kDa) at the same polymerization conditions. This was probably because of higher mobility of shorter arm lengths and the less steric hindrance resulting in the incorporation of more arms into star structures. This potentially leads to the higher number of end-groups present in the star polymer structure, likely resulting in termination reactions.

Since the star polymers, after the removal of Boc- deprotection groups, gained water-solubility, the degradation profiles were investigated using water-soluble reducing agent TCEP. Polymers were dissolved in water and the hydrodynamic sizes were evaluated via DLS. Star polymers before TCEP addition was around 2-36 nm (depending on the crosslinker/AEAEMA mole ratio), after the treatment with the reducing agent for 1 h, the hydrodynamic sizes dropped to 1-18 nm, indicating the cleavage of the core and the release of unimeric chains into solution. The polymers synthesized with P(OEGMA) pre-arms of 5 kDa displayed solubility problems, as expected, since the star polymers with shorter hydrophilic arms can ended up with weaker polarity and higher tendency to agglomerate.

The main motivation of using P(OEGMA) arms was to shield the cationic charge of the core and potentially make the surface of polymer-siRNA complex nanoparticles neutral and hydrophilic considering the possible use of cationic star polymers as siRNA carriers. However, it was known that while incorporation of P(OEGMA) arms can be beneficial in terms of charge shielding and providing stealth charactered, incorporation of large number P(OEGMA) arms into the star structure can be disadvantageous for complexation of siRNA by lowering or even completely hindering the interaction between the cationic core and siRNA molecules. As expected, incorporation of high number of arms (N_{arm}=14) caused negative effect on the complexation ability of the polymer with siRNA molecules (no complexation with siRNA was observed). The siRNA complexation experiments demonstrated that the star polymers which had the lower number of arms with larger cationic core (N_{arm}=7, DP_{AEAEMA} = 70) led to efficient complexation even at the low ratios of polymer to siRNA (N/P=1).

Additionally, the cell viability experiments demonstrated that the star polymers had less cytotoxicity compared to branched PEI at all concentrations tested. Among all three different star polymers tested, the star polymer with N_{arm}=7 and DP_{AEAEMA} = 70 showed the highest toxicity than the star polymers with N_{arm}=14, DP_{AEAEMA} = 244 and N_{arm}=7, DP_{AEAEMA} = 30, probably due to the combination of the lower number of arms and higher cationic charge density. It is well-known in the literature that as cationic charge density increases, cytotoxicity increases. Nevertheless, the star polymer with N_{arm}=7 and DP_{AEAEMA} = 70 which demonstrated the best complexation ability (even at lower polymer/siRNA (N/P=1) ratios) along with other star polymers tested were significantly less toxic compared to branched PEI which is a golden standard cationic polymer for

siRNA delivery. This was attributed to the presence of non-toxic and non-ionic P(OEGMA) arms surrounding the cationic core of the star polymers.

The following suggestions can be given for further improving this study;

1. Gene silencing activities of siRNA-star polymer complexes may be investigated after determination of hydrodynamic sizes and charge density of formed polyplexes in more detail.
2. Heterogeneous star polymers which have both P(OEGMA) and P(AEAEMA) as macroRAFT agents or homogeneous star polymers which have P(OEGMA)-P(AEAEMA) block copolymers may be synthesized in order to increase complexation efficiency of star polymers with siRNA molecules.
3. Different solvents for polymerization reaction may be tried and compared in order to reduce competitive nature of the disulfide crosslinker and BocAEAEMA monomer.

REFERENCES

Abrol, Simmi, Peter A Kambouris, Mark G Looney, and David H Solomon. "Studies on Microgels, 3. Synthesis Using Living Free Radical Polymerization." *Macromolecular rapid communications* 18, no. 9 (1997): 755-60.

Audouin, Fabrice, Ruther JI Knoop, Jin Huang, and Andreas Heise. "Star Polymers by Cross-Linking of Linear Poly (Benzyl-L-Glutamate) Macromonomers Via Free-Radical and Raft Polymerization. A Simple Route toward Peptide-Stabilized Nanoparticles." *Journal of Polymer Science Part A: Polymer Chemistry* 48, no. 20 (2010): 4602-10.

Azuma, Yusuke, Takaya Terashima, and Mitsuo Sawamoto. "Precision Synthesis of Imine-Functionalized Reversible Microgel Star Polymers Via Dynamic Covalent Cross-Linking of Hydrogen-Bonding Block Copolymer Micelles." *Macromolecules* 50, no. 2 (2017): 587-96.

Bansal, Ruby, Pallavi Kiran, and Pradeep Kumar. "Synthesis, Characterization and Evaluation of Diglycidyl-1, 2-Cyclohexanedicarboxylate Crosslinked Polyethylenimine Nanoparticles as Efficient Carriers of DNA." *New Journal of Chemistry* 40, no. 6 (2016): 5044-52.

Barner-Kowollik, Christopher, Thomas P Davis, and Martina H Stenzel. "Synthesis of Star Polymers Using Raft Polymerization: What Is Possible?". *Australian journal of chemistry* 59, no. 10 (2006): 719-27.

Behr, Jean-Paul. "Synthetic Gene Transfer Vectors Ii: Back to the Future." *Accounts of chemical research* 45, no. 7 (2012): 980-84.

Benjaminsen, Rikke V, Maria A Mattebjerg, Jonas R Henriksen, S Moein Moghimi, and Thomas L Andresen. "The Possible “Proton Sponge” Effect of Polyethylenimine (Pei) Does Not Include Change in Lysosomal Ph." *Molecular Therapy* 21, no. 1 (2013): 149-57.

Boschmann, Daniel, and Philipp Vana. "Z-Raft Star Polymerizations of Acrylates: Star Coupling Via Intermolecular Chain Transfer to Polymer." *Macromolecules* 40, no. 8 (2007): 2683-93.

Bowen, Sharon, Nadine Tare, Tomoaki Inoue, Motoo Yamasaki, Masami Okabe, Ikuo Horii, and James F Eliason. "Relationship between Molecular Mass and Duration

of Activity of Polyethylene Glycol Conjugated Granulocyte Colony-Stimulating Factor Mutein." *Experimental hematology* 27, no. 3 (1999): 425-32.

Boyer, Cyrille, Volga Bulmus, Thomas P Davis, Vincent Ladmiral, Jingquan Liu, and Sébastien Perrier. "Bioapplications of Raft Polymerization." *Chemical reviews* 109, no. 11 (2009): 5402-36.

Boyer, Cyrille, Jingquan Liu, Volga Bulmus, and Thomas P Davis. "Raft Polymer End-Group Modification and Chain Coupling/Conjugation Via Disulfide Bonds." *Australian journal of chemistry* 62, no. 8 (2009): 830-47.

Braunecker, Wade A, and Krzysztof Matyjaszewski. "Controlled/Living Radical Polymerization: Features, Developments, and Perspectives." *Progress in Polymer Science* 32, no. 1 (2007): 93-146.

Bulmus, Volga. "Raft Polymerization Mediated Bioconjugation Strategies." *Polymer Chemistry* 2, no. 7 (2011): 1463-72.

Cavallaro, Gennara, Carla Sardo, Emanuela Fabiola Craparo, Barbara Porsio, and Gaetano Giammona. "Polymeric Nanoparticles for Sirna Delivery: Production and Applications." *International journal of pharmaceutics* 525, no. 2 (2017): 313-33.

Chen, Bo, Derek G van der Poll, Katherine Jerger, William C Floyd, Jean MJ Fréchet, and Francis C Szoka. "Synthesis and Properties of Star-Comb Polymers and Their Doxorubicin Conjugates." *Bioconjugate chemistry* 22, no. 4 (2011): 617-24.

Chen, Jinliang, Xiaoyi Sun, Rong Shao, Yichao Xu, Jianqing Gao, and Wenquan Liang. "Vegf Sirna Delivered by Polycation Liposome-Encapsulated Calcium Phosphate Nanoparticles for Tumor Angiogenesis Inhibition in Breast Cancer." *International journal of nanomedicine* 12 (2017): 6075.

Chen, Yongxia, Ziying Yang, Chao Liu, Cuiwei Wang, Shunxin Zhao, Jing Yang, Hongfan Sun, *et al.* "Synthesis, Characterization, and Evaluation of Paclitaxel Loaded in Six-Arm Star-Shaped Poly (Lactic-Co-Glycolic Acid)." *International journal of nanomedicine* 8 (2013): 4315.

Cho, Hong Y, Abiraman Srinivasan, Joanna Hong, Eric Hsu, Shiguang Liu, Arun Shrivats, Dan Kwak, *et al.* "Synthesis of Biocompatible Peg-Based Star Polymers with Cationic and Degradable Core for Sirna Delivery." *Biomacromolecules* 12, no. 10 (2011): 3478-86.

Chong,) YK, Tam PT Le, Graeme Moad, Ezio Rizzardo, and San H Thang. "A More Versatile Route to Block Copolymers and Other Polymers of Complex Architecture by Living Radical Polymerization: The Raft Process." *Macromolecules* 32, no. 6 (1999): 2071-74.

Cooper, Bailey M, and David Putnam. "Polymers for Sirna Delivery: A Critical Assessment of Current Technology Prospects for Clinical Application." *ACS Biomaterials Science & Engineering* 2, no. 11 (2016): 1837-50.

Cosson, Steffen, Maarten Danial, Julien Rosselgong Saint-Amans, and Justin J Cooper-White. "Accelerated Combinatorial High Throughput Star Polymer Synthesis Via a Rapid One-Pot Sequential Aqueous Raft (Rosa-Raft) Polymerization Scheme." *Macromolecular rapid communications* 38, no. 8 (2017).

Dai, Zhuojun, Torben Gjetting, Maria A Mattebjerg, Chi Wu, and Thomas L Andresen. "Elucidating the Interplay between DNA-Condensing and Free Polycations in Gene Transfection through a Mechanistic Study of Linear and Branched Pei." *Biomaterials* 32, no. 33 (2011): 8626-34.

Dong, Zhong-min, Xiao-hui Liu, He-wen Liu, and Yue-sheng Li. "Synthesis of Novel Star Polymers with Vinyl-Functionalized Hyperbranched Core Via “Arm-First” Strategy." *Macromolecules* 43, no. 19 (2010): 7985-92.

Ferreira, Julien, Jay Syrett, Michael Whittaker, David Haddleton, Thomas P Davis, and Cyrille Boyer. "Optimizing the Generation of Narrow Polydispersity ‘Arm-First’star Polymers Made Using Raft Polymerization." *Polymer Chemistry* 2, no. 8 (2011): 1671-77.

Fox, Megan E, Francis C Szoka, and Jean MJ Fréchet. "Soluble Polymer Carriers for the Treatment of Cancer: The Importance of Molecular Architecture." *Accounts of chemical research* 42, no. 8 (2009): 1141-51.

Gao, Haifeng, and Krzysztof Matyjaszewski. "Low-Polydispersity Star Polymers with Core Functionality by Cross-Linking Macromonomers Using Functional Atrp Initiators." *Macromolecules* 40, no. 3 (2007): 399-401.

Gao, Haifeng, and Krzysztof Matyjaszewski. "Structural Control in Atrp Synthesis of Star Polymers Using the Arm-First Method." *Macromolecules* 39, no. 9 (2006): 3154-60.

Gao, Haifeng, and Krzysztof Matyjaszewski. "Synthesis of Functional Polymers with Controlled Architecture by Crp of Monomers in the Presence of Cross-Linkers: From Stars to Gels." *Progress in Polymer Science* 34, no. 4 (2009): 317-50.

Gao, Haifeng, and Krzysztof Matyjaszewski. "Synthesis of Star Polymers by a New "Core-First" Method: Sequential Polymerization of Cross-Linker and Monomer." *Macromolecules* 41, no. 4 (2008): 1118-25.

Gao, Haifeng, Nicolay V Tsarevsky, and Krzysztof Matyjaszewski. "Synthesis of Degradable Miktoarm Star Copolymers Via Atom Transfer Radical Polymerization." *Macromolecules* 38, no. 14 (2005): 5995-6004.

Goh, Tor Kit, Kristopher D Coventry, Anton Blencowe, and Greg G Qiao. "Rheology of Core Cross-Linked Star Polymers." *Polymer* 49, no. 23 (2008): 5095-104.

Gregory, Andrew, and Martina H Stenzel. "Complex Polymer Architectures Via Raft Polymerization: From Fundamental Process to Extending the Scope Using Click Chemistry and Nature's Building Blocks." *Progress in Polymer Science* 37, no. 1 (2012): 38-105.

Harris, J Milton, and Robert B Chess. "Effect of Pegylation on Pharmaceuticals." *Nature reviews Drug discovery* 2, no. 3 (2003): 214.

Hild, Frederic, Nam T Nguyen, Eileen Deng, Juliano Katrib, Georgios Dimitrakis, Phei-Li Lau, and Derek J Irvine. "Facile Determination of Molecular Structure Trends in Amphiphilic Core Corona Star Polymer Synthesis Via Dielectric Property Measurement." *Macromolecular rapid communications* 37, no. 15 (2016): 1295-99.

Huang, Jianbing, Hui Liang, Du Cheng, and Jiang Lu. "Polypeptide–Poly (Ethylene Glycol) Miktoarm Star Copolymers with a Fluorescently Labeled Core: Synthesis, Delivery and Imaging of Sirna." *Polymer Chemistry* 7, no. 9 (2016): 1792-802.

Junquera, Elena, and Emilio Aicart. "Recent Progress in Gene Therapy to Deliver Nucleic Acids with Multivalent Cationic Vectors." *Advances in colloid and interface science* 233 (2016): 161-75.

Kafouris, Demetris, Efrosyni Themistou, and Costas S Patrickios. "Synthesis and Characterization of Star Polymers and Cross-Linked Star Polymer Model Networks with Cores Based on an Asymmetric, Hydrolyzable Dimethacrylate Cross-Linker." *Chemistry of materials* 18, no. 1 (2006): 85-93.

Kamada, Jun, Kaloian Koynov, Cathrin Corten, Azhar Juhari, Jeong Ae Yoon, Marek W Urban, Anna C Balazs, and Krzysztof Matyjaszewski. "Redox Responsive Behavior of Thiol/Disulfide-Functionalized Star Polymers Synthesized Via Atom Transfer Radical Polymerization." *Macromolecules* 43, no. 9 (2010): 4133-39.

Kanayama, Naoki, Shigeto Fukushima, Nobuhiro Nishiyama, Keiji Itaka, Woo-Dong Jang, Kanjiro Miyata, Yuichi Yamasaki, Ung-il Chung, and Kazunori Kataoka. "A Peg-Based Biocompatible Block Catiomer with High Buffering Capacity for the Construction of Polyplex Micelles Showing Efficient Gene Transfer toward Primary Cells." *ChemMedChem* 1, no. 4 (2006): 439-44.

Kronenthal, Richard L. "Biodegradable Polymers in Medicine and Surgery." In *Polymers in Medicine and Surgery*, 119-37: Springer, 1975.

Kunath, Klaus, Anke von Harpe, Dagmar Fischer, Holger Petersen, Ulrich Bickel, Karlheinz Voigt, and Thomas Kissel. "Low-Molecular-Weight Polyethylenimine as a Non-Viral Vector for DNA Delivery: Comparison of Physicochemical Properties, Transfection Efficiency and in Vivo Distribution with High-Molecular-Weight Polyethylenimine." *Journal of Controlled Release* 89, no. 1 (2003): 113-25.

Kurtulus, Isil, Gokhan Yilmaz, Muhammed Ucuncu, Mustafa Emrullahoglu, C Remzi Becer, and Volga Bulmus. "A New Proton Sponge Polymer Synthesized by Raft Polymerization for Intracellular Delivery of Biotherapeutics." *Polymer Chemistry* 5, no. 5 (2014): 1593-604.

Learsch, Robert, and Garret M Miyake. "Arm-First Synthesis of Star Polymers with Polywedge Arms Using Ring-Opening Metathesis Polymerization and Bifunctional Crosslinkers." *Journal of Polymer Science Part A: Polymer Chemistry* (2018).

Li, Junbo, Jianlong Zhao, Jiayu Gao, Ju Liang, Wenlan Wu, and Lijuan Liang. "A Block Copolymer Containing Peg and Histamine-Like Segments: Well-Defined Functions for Gene Delivery." *New Journal of Chemistry* 40, no. 8 (2016): 7222-28.

Liao, Xin, Grace Walden, Noelia D Falcon, Simon Donell, Michael J Raxworthy, Michael Wormstone, Graham P Riley, and Aram Saeed. "A Direct Comparison of Linear and Star-Shaped Poly (Dimethylaminoethyl Acrylate) Polymers for Polyplexation with DNA and Cytotoxicity in Cultured Cell Lines." *European Polymer Journal* 87 (2017): 458-67.

Likos, CN, H Löwen, M Watzlawek, B Abbas, O Jucknischke, J Allgaier, and D Richter. "Star Polymers Viewed as Ultrasoft Colloidal Particles." *Physical review letters* 80, no. 20 (1998): 4450.

Liu, Jinna, Hien Duong, Michael R Whittaker, Thomas P Davis, and Cyrille Boyer. "Synthesis of Functional Core, Star Polymers Via Raft Polymerization for Drug Delivery Applications." *Macromolecular rapid communications* 33, no. 9 (2012): 760-66.

Lord, Helen T, John F Quinn, Simon D Angus, Michael R Whittaker, Martina H Stenzel, and Thomas P Davis. "Microgel Stars Via R Eversible a Ddition F Ragmentation Chain T Ransfer (Raft) Polymerisation—a Facile Route to Macroporous Membranes, Honeycomb Patterned Thin Films and Inverse Opal Substrates." *Journal of Materials Chemistry* 13, no. 11 (2003): 2819-24.

Matsumura, Yasuhiro, and Hiroshi Maeda. "A New Concept for Macromolecular Therapeutics in Cancer Chemotherapy: Mechanism of Tumoritropic Accumulation of Proteins and the Antitumor Agent Smancs." *Cancer research* 46, no. 12 Part 1 (1986): 6387-92.

Matyjaszewski, Krzysztof, Yves Gnanou, and Ludwik Leibler. *Macromolecular Engineering.* Wiley Online Library, 2007.

McKenzie, Thomas G, Jing M Ren, Dave E Dunstan, Edgar HH Wong, and Greg G Qiao. "Synthesis of High-Order Multiblock Core Cross-Linked Star Polymers." *Journal of Polymer Science Part A: Polymer Chemistry* 54, no. 1 (2016): 135-43.

Moad, Graeme, Roshan TA Mayadunne, Ezio Rizzardo, Mellissa Skidmore, and San H Thang. "Synthesis of Novel Architectures by Radical Polymerization with Reversible Addition Fragmentation Chain Transfer (Raft Polymerization)." Paper presented at the Macromolecular Symposia, 2003.

Monnery, Bryn D, Michael Wright, Rachel Cavill, Richard Hoogenboom, Sunil Shaunak, Joachim HG Steinke, and Maya Thanou. "Cytotoxicity of Polycations: Relationship of Molecular Weight and the Hydrolytic Theory of the Mechanism of Toxicity." *International journal of pharmaceutics* 521, no. 1-2 (2017): 249-58.

Nishimura, Tomoki, Kaori Umezaki, Sada-atsu Mukai, Shin-ichi Sawada, and Kazunari Akiyoshi. "Amylose-Based Cationic Star Polymers for Sirna Delivery." *BioMed research international* 2015 (2015).

Odian, George. *Principles of Polymerization.* John Wiley & Sons, 2004.

Oskuee, Reza Kazemi, Maryam Dabbaghi, Leila Gholami, Sajedeh Taheri-Bojd, Mahdi Balali-Mood, Seyyed Hadi Mousavi, and Bizhan Malaekeh-Nikouei. "Investigating the Influence of Polyplex Size on Toxicity Properties of Polyethylenimine Mediated Gene Delivery." *Life sciences* 197 (2018): 101-08.

Pan, Yuanfeng, Pingxiong Cai, Madjid Farmahini-Farahani, Yiduo Li, Xiaobang Hou, and Huining Xiao. "Amino-Functionalized Alkaline Clay with Cationic Star-Shaped Polymer as Adsorbents for Removal of Cr (Vi) in Aqueous Solution." *Applied Surface Science* 385 (2016): 333-40.

Parhamifar, Ladan, Anna K Larsen, A Christy Hunter, Thomas L Andresen, and S Moein Moghimi. "Polycation Cytotoxicity: A Delicate Matter for Nucleic Acid Therapy—Focus on Polyethylenimine." *Soft Matter* 6, no. 17 (2010): 4001-09.

Rafael, Diana, Francesc Martínez, Fernanda Andrade, Joaquim Seras-Franzoso, Natalia Garcia-Aranda, Petra Gener, Joan Sayós, *et al.* "Efficient Efgr Mediated Sirna Delivery to Breast Cancer Cells by Cetuximab Functionalized Pluronic® F127/Gelatin." *Chemical Engineering Journal* (2017).

Ren, Jing M, Thomas G McKenzie, Qiang Fu, Edgar HH Wong, Jiangtao Xu, Zesheng An, Sivaprakash Shanmugam, *et al.* "Star Polymers." *Chemical reviews* 116, no. 12 (2016): 6743-836.

Rosselgong, Julien, Elizabeth GL Williams, Tam P Le, Felix Grusche, Tracey M Hinton, Mark Tizard, Pathiraja Gunatillake, and San H Thang. "Core Degradable Star Raft Polymers: Synthesis, Polymerization, and Degradation Studies." *Macromolecules* 46, no. 23 (2013): 9181-88.

Sigen, A, Qian Xu, Dezhong Zhou, Yongsheng Gao, Jeddah Marie Vasquez, Udo Greiser, Wei Wang, Wenguang Liu, and Wenxin Wang. "Hyperbranched Peg-Based Multi-Nhs Polymer and Bioconjugation with Bsa." *Polymer Chemistry* 8, no. 8 (2017): 1283-87.

Syrett, Jay A, David M Haddleton, Michael R Whittaker, Thomas P Davis, and Cyrille Boyer. "Functional, Star Polymeric Molecular Carriers, Built from Biodegradable Microgel/Nanogel Cores." *Chemical Communications* 47, no. 5 (2011): 1449-51.

Teo, Joann, Joshua A McCarroll, Cyrille Boyer, Janet Youkhana, Sharon M Sagnella, Hien TT Duong, Jie Liu, *et al.* "A Rationally Optimized Nanoparticle System for

the Delivery of Rna Interference Therapeutics into Pancreatic Tumors in Vivo." *Biomacromolecules* 17, no. 7 (2016): 2337-51.

Themistou, Efrosyni, and Costas S Patrickios. "Synthesis and Characterization of Polymer Networks and Star Polymers Containing a Novel, Hydrolyzable Acetal-Based Dimethacrylate Cross-Linker." *Macromolecules* 39, no. 1 (2006): 73-80.

Themistou, Efrosyni, and Costas S Patrickios. "Synthesis and Characterization of Star Polymers and Cross-Linked Star Polymer Model Networks Containing a Novel, Silicon-Based, Hydrolyzable Cross-Linker." *Macromolecules* 37, no. 18 (2004): 6734-43.

Uchiyama, Mineto, Kotaro Satoh, Thomas G McKenzie, Qiang Fu, Greg G Qiao, and Masami Kamigaito. "Diverse Approaches to Star Polymers Via Cationic and Radical Raft Cross-Linking Reactions Using Mechanistic Transformation." *Polymer Chemistry* 8, no. 38 (2017): 5972-81.

Wang, Jie, Ze Lu, M Guillaume Wientjes, and Jessie L-S Au. "Delivery of Sirna Therapeutics: Barriers and Carriers." *The AAPS journal* 12, no. 4 (2010): 492-503.

Watzlawek, Martin, Christos N Likos, and Hartmut Löwen. "Phase Diagram of Star Polymer Solutions." *Physical review letters* 82, no. 26 (1999): 5289.

Wei, Xiaohu, Graeme Moad, Benjamin W Muir, Ezio Rizzardo, Julien Rosselgong, Wantai Yang, and San H Thang. "An Arm-First Approach to Cleavable Mikto-Arm Star Polymers by Raft Polymerization." *Macromolecular rapid communications* 35, no. 8 (2014): 840-45.

Xia, Jianhui, Xuan Zhang, and Krzysztof Matyjaszewski. "Synthesis of Star-Shaped Polystyrene by Atom Transfer Radical Polymerization Using an “Arm First” Approach." *Macromolecules* 32, no. 13 (1999): 4482-84.

Yang, Da-Peng, Ma Nwe Nwe Linn Oo, Gulam Roshan Deen, Zibiao Li, and Xian Jun Loh. "Nano-Star-Shaped Polymers for Drug Delivery Applications." *Macromolecular rapid communications* (2017).

You, Y-Z, C-Y Hong, C-Y Pan, and P-H Wang. "Synthesis of a Dendritic Core–Shell Nanostructure with a Temperature-Sensitive Shell." *Advanced Materials* 16, no. 21 (2004): 1953-57.

Yue, Yanan, Fan Jin, Rui Deng, Jinge Cai, Yangchao Chen, Marie CM Lin, Hsiang-Fu Kung, and Chi Wu. "Revisit Complexation between DNA and Polyethylenimine—Effect of Uncomplexed Chains Free in the Solution Mixture on Gene Transfection." *Journal of controlled release* 155, no. 1 (2011): 67-76.

Zhang, Chunlei, Miao Miao, Xueteng Cao, and Zesheng An. "One-Pot Raft Synthesis of Core Cross-Linked Star Polymers of Polypegma in Water by Sequential Homogeneous and Heterogeneous Polymerizations." *Polymer Chemistry* 3, no. 9 (2012): 2656-64.

Zheng, Genhua, and Caiyuan Pan. "Preparation of Star Polymers Based on Polystyrene or Poly (Styrene-Bn-Isopropyl Acrylamide) and Divinylbenzene Via Reversible Addition-Fragmentation Chain Transfer Polymerization." *Polymer* 46, no. 8 (2005): 2802-10.

Zheng, Quan, Gen-hua Zheng, and Cai-yuan Pan. "Preparation of Nano-Sized Poly (Ethylene Oxide) Star Microgels Via Reversible Addition-Fragmentation Transfer Polymerization in Selective Solvents." *Polymer international* 55, no. 9 (2006): 1114-23.